MAPPING OF THE ROTAVIRUS NONSTRUCTURAL PROTEIN-4-CAVEOLIN-1 BINDING SITE TO THREE HYDROPHOBIC RESIDUES WITHIN THE EXTENDED, C-TERMINAL AMPHIPATHIC ALPHA HELIX

A Dissertation

by

CECELIA VICTORIA WILLIAMS

Submitted to the Office of Graduate Studies of
Texas A&M University
in partial fulfillment of the requirements for the degree of

DOCTOR OF PHILOSOPHY

December 2008

Major Subject: Veterinary Microbiology

MAPPING OF THE ROTAVIRUS NONSTRUCTURAL PROTEIN-4-CAVEOLIN-1 BINDING SITE TO THREE HYDROPHOBIC RESIDUES WITHIN THE EXTENDED, C-TERMINAL AMPHIPATHIC ALPHA HELIX

A Dissertation

by

CECELIA VICTORIA WILLIAMS

Submitted to the Office of Graduate Studies of
Texas A&M University
in partial fulfillment of the requirements for the degree of

DOCTOR OF PHILOSOPHY

Approved by:

Chair of Committee,	Judith M. Ball
Committee Members,	Rebecca D. Parr
	Julian Leibowitz
	Friedhelm Schroeder
Head of Department,	Gerald R. Bratton

December 2008

Major Subject: Veterinary Microbiology

ABSTRACT

Mapping of the Rotavirus Nonstructural Protein-4-Caveolin-1 Binding Site
to Three Hydrophobic Residues Within the Extended, C-Terminal
Amphipathic Alpha Helix. (December 2008)
Cecelia Victoria Williams, B.A., University of New Mexico;
M.S., University of New Mexico; M.S. University of New Mexico
Chair of Advisory Committee: Dr. Judith M. Ball

Rotavirus NSP4, the first described viral enterotoxin, localizes to the plasma membrane of infected cells, possibly through interaction with caveolin-1. A direct interaction between NSP4 and caveolin-1, the structural protein of caveolae, was shown by yeast two-hybrid, peptide binding, and FRET analyses. To dissect the precise NSP4 binding domain to caveolin-1, mutants were prepared by altering either the charged or hydrophobic face of the NSP4 C-terminal amphipathic alpha-helix and examined for binding to caveolin-1. Replacing six charged residues with alanine ($FLNSP4_{Ala}$) disrupted the charged face, while the hydrophobic face was disrupted by replacing selected hydrophobic residues with charged amino acids (aa) ($FLNSP4_{HydroMut}$). In yeast two-hybrid and peptide binding assays, $FLNSP4_{Ala}$ retained its binding capacity, whereas $FLNSP4_{HydroMut}$ failed to bind caveolin-1. Mutants were generated with an N-terminal truncated clone ($NSP4_{46-175}$), which removed the hydrophobic domains and aided in yeast-two hybrid assays. These mutants exhibited the same binding pattern as

FLNSP4 confirming that the N-terminus of NSP4 lacks the caveolin-1 binding site and $NSP4_{46\text{-}175}$ is sufficient for binding.

Seven additional mutants were prepared from $NSP4_{HydroMut}$ in which individually charged residues were reverted to the original hydrophobic aa or were replaced with alanine. Analyses of the interaction of these revertants with caveolin-1 localized the NSP4 binding domain to one critical hydrophobic aa (L116) and one or two additional aa (I113, L127, and/or L134) on the hydrophobic face. Those mutants that bound caveolin-1 bound both the N- and C-terminal caveolin-1 peptides, but lacked binding to a centrally located peptide. These data suggest conformational and hydrophobic constraints play a role in the NSP4-caveolin-1 association.

The mutant NSP4 molecules also were evaluated for transport to the plasma membrane. Mammalian cells were transfected with FLNSP4, $FLNSP4_{1\text{-}175Ala,}$ and $NSP4_{1\text{-}175HydroMut}$ plasmid DNA, surface biotinylated, and examined by IFA or Western blot for NSP4 expression. Epifluorescence revealed FLNSP4 and $FLNSP4_{Ala}$ were exposed on the cell surface in the absence of other viral proteins, whereas $NSP4_{HydroMut}$ remained intracellular. Further, NSP4-transfected cells displayed an intracellular association of with caveolin-1 or the caveolin-1 chaperone complex proteins. These data indicate NSP4 interacts with caveolin-1 in the absence of other viral proteins.

DEDICATION

To my mother, Bebe Navarro Krapcha, who always believes in me; to my sisters, Anna Marie Bowers, Lucy Ann Rubin, Kathryn Bortone, Mary Margaret O'Bannon, Antoinette Ramsey, and sisters-in-law, Dawn Krapcha and Barbara Wilson, who are always there as only sisters can be; to my brothers, Michael E., John Joseph, and Andre' Krapcha, who continually encouraged me; my godsons, Alexander and Daniel O'Bannon, and all my nieces and nephews who cheered me on, and finally to my daughter Jodi Lee Davidson, her husband G. Douglas Davidson, and their sons (my grandsons) Andrew and Geoffrey Wilson, Keegan, Kieran, and Karsen Davidson, who are my biggest fans!

ACKNOWLEDGEMENTS

I would like to thank my committee chair, Dr. Judith Ball, and my committee members, Dr. Rebecca Parr, Dr. Julian Liebowitz, and Dr. Friedland Schroeder, for their time, guidance, and support throughout the course of my studies and research.

Many thanks go to my friends and colleagues and the Department of Pathobiology, CVM faculty, and staff for making my time at Texas A&M University a rewarding experience. I thank everyone in Dr. Ball's laboratory, Dr. Deanne Moore-Smith, Dr. Stephan Storey, Major Thomas F. Gibbons, Ph.D. (USAF), Kiran Mir, and Megan Schroeder, who gave so freely of their time, knowledge, and heart to help me in this endeavor.

I especially thank the "girls"—Megan Schroeder, Lina Covaleda, Gina Lungu, Aline Rodrigues, and Negin Mirhosseini—for the late night talks, the camaraderie, smiles, and the tears—I consider it a real honor to be called your friend. It has been a real pleasure to work and play with you.

This work was supported in part by the USPHS National Institutes of Health GM31651 (FS and AK) and GM62326 (JMB).

I also want to extend my gratitude to the Sandia National Laboratories and the Doctoral Studies Program for providing the support for me to pursue a Ph.D. in veterinary microbiology at Texas A&M University. Also, I wish to thank Margie Tatro and T. Bernadette Montano for keeping me on track over the past several years. Finally, I thank my dear friend and colleague Larry Bustard (deceased) without whom none of this would have been possible.

NOMENCLATURE

aa	amino acid
AAH	amphipathic alpha helical
β-gal	β-galactosidase
BGU	β-galactosidase units
BHK-21	Baby hamster kidney cells
bp	base pairs
BM	basement membrane
$[Ca^{+2}]_i$	intracellular calcium
cav	caveolin
CCC	Caveolin 1 chaperone complex
CCD	coiled coil domain
CHO	clycosylation sites
Cl^-	chloride
CSC	cavitation-sucrose chromatography
CSD	Caveolin scaffolding domain
C-MAD	C-terminal membrane attachment domain
DGE	Aspartate-glycine-glutamate
DLP	Double-layered particle
ds RNA	Double stranded RNA
EGFP	Enhanced green fluorescent protein
eIF	eukaryotic initiation factor

ER	endoplasmic reticulum
endo H	Endo-β-N-acetylglucosaminidase H
ERCIC	Endoplasmic reticulum Golgi intermediate complex
FL	full lengh
FRET	Fluorescent resonance energy transfer
H	Hydrophobic domain
HDL	high density lipoproteins
hpi	hours post infection
hpt	hours post transfection
hsp	Heat shock protein
IDV I	Integrated density value
IFA	Indirect fluorescence antibody
IP3	Inositol 1,4,5-triphosphate
kDa	kilodalton
MOI	Multiplicity of infection
MDCK	Madin-Darby canine kidney cells
Mmol	millimole
mRNA	messenger RNA
NSP, NSP4	Nonstructural protein; Nonstructural protein 4
NA	Neuraminidase
N-MAD	N-terminal membrane attachment domain
OD_{600}	optical density

PAPB	Poly (A)-binding protein
PIP2	Phosphatidylinositol 4,5 bisphosphate
PLC	Phospholipase C
PM	Plasma membrane
PMSF	Phenylmethysulfonyl fluoride
Poly (A)	Polyadenylation
RT	room temperature
RV	Rotavirus
SA	sialic acid
SLP	Single-layered particle
TLP	Triple-layered particle
VP	viral protein
USAF	United States Air Force
Y2H	Yeast two-hybrid

TABLE OF CONTENTS

LIST OF TABLES

LIST OF FIGURES

FIGURE Page

CHAPTER I

INTRODUCTION: ROTAVIRUS, NONSTRUCTURAL PROTEIN-4, CAVEOLIN-1, AND THEIR INTERACTION

Rotavirus Infection

Interest in rotavirus (RV) has grown over the past 30 years, since its first discovery as a major etiologic agent of viral gastroenteritis and diarrhea in young children and mammals (Ball et al., 2005; Dupuis et al., 1995; Estes, 2001; Marrie et al., 1982; Mattion et al., 1994; Parashar et al., 2003; Ramig, 1997). Also, RV has been shown to cause viral gastroenteritis and diarrhea in the elderly and immune-compromised adults (Dupuis et al., 1995; Marrie et al., 1982). RV is the number one, worldwide cause of viral diarrhea in infants and young children under the age of five years (Widdowson et al., 2005) causing severe dehydration that frequently results in death. Annually, 111 million cases of RV infection occur worldwide, with approximately 25 million clinical visits, 2 million hospitalizations and by some estimates, up to 1 million deaths (Parashar et al., 2003). Infant deaths in developing countries account for about 82% of the RVassociated deaths (Ramig, 2004). The occurrence rate of RV infection in developed countries, such as the United States, is about 1% of that of the developing countries with a death rate of 0.02 %. However, the economic impact upon the United States' health care system is upwards to a billion dollars (Glass et al., 1996).

The style of this dissertation follows that of Virology.

RV infects mature enterocytes lining the intestinal villi suggesting these cells have a RV-sensitive receptor as well as a cellular environment favorable to RV infection (Ramig, 2004). The early stage of RV infection is typified by diarrhea prior to the detection of histologic lesions with minimal inflammation (Ramig, 2004). RV-induced gastroenteritis has been shown to cause intestinal damage including flattening of villi and deepening of crypts (Davidson et al., 1977) that results in malabsorption. Early diarrhea results from release of NSP4 by a non-classical pathway that initiates the release of $[Ca^{++}]$ from the endoplasmic reticulum (ER) increasing $[Ca^{++}]_i$. NSP4 disrupts tight junctions allowing paracellular flow of water and electrolytes. Extracellular NSP4 appears to bind a specific receptor on the same or an uninfected cell triggering a signaling cascade via phospholipase C (PLC) and inositol 1,4,5-triphosphate (IP3) that stimulating mobilization of $[Ca^{++}]_I$ and chloride (Cl^-) secretion. The elevated $[Ca^{++}]_I$ levels disrupt the microvilli cytoskeleton network, decrease expression of disaccharides and enzymes at the apical surfaces, and inhibits sodium (Na^+) solute cotransport (Dong et al., 1997). NSP4 also plays a role in the secretory component of RV infection that is characterized by transepithelial Cl^- secretion and paracellular movement of Na^+ and water into the intestinal lumen (Morris et al., 1999).

Serogroup A RV causes the most common type of RV enteric disease. Four other serogroups, B-E, are currently recognized; these are collectively known as the non-group A RV, with groups B and C also infecting humans (Mattion et al., 1994; Ramig, 2004). These non-group A RV have been associated with major epidemics of diarrhea in adults in China and India (Fang et al., 1989; Krishnan et al., 1999), suggesting the possible

emergence of new human pathogens. Many mammal RVs are potentially cross-transmissible between man and mammals. Since RV infection occurs in a large variety of mammal species, it has been suggested that some of the non-group A RV may have been derived from swine and cattle through agriculture ground water cross contamination (Desselberger et al., 2001).

Rotavirus Morphology

RV belong to the *Reoviridae,* Respiratory and Enteric Orphan, family of double stranded RNA (dsRNA) viruses (Ramig, 1997). These virions are non-enveloped with icosahedral capsid symmetry, 75-100 nm in size, and a segmented genome (Estes, 2001; Ramig, 1994). The RV structure is a triple-layered capsid surrounding an inner protein core containing the genome. The genome consists of 11 double-stranded segments. Ten of these gene segments uniquely encode six structural viral proteins (VP) and four nonstructural proteins (NSP), while the eleventh segment encodes two NSP proteins (Estes et al., 2001; Mattion et al., 1994; Ramig, 1994). Each RNA segment contains a 5' cap structure; however, they do not contain polyadenylation (poly A) tails (Jayaram et al., 2004). Figure 1.1A depicts the RV triple-layered particle with cut-aways showing the internal arrangement of the viral proteins and 1.1B shows a Western blot of the structural and nonstructural proteins of a simian RV indicating the relationship to the RNA transcripts.

The inner capsid is made up of VP2 and forms the single layer particle (SLP) that contains the dsRNA genome. The SLP contains the transcription enzymes, VP1 and VP3, required for the synthesis of mRNA transcripts (Chwetzoff and Trugnan, 2006;

Estes et al., 2001) and serves as the metabolically active macromolecular machine from which the mRNAs are transcribed (Coombs, 2006). VP1 is a RNA-dependant RNA polymerase that function in the production of messenger RNAs (mRNAs) from the minus strand genomic templates (Valenzuela et al., 1991), while VP3 possesses guanylyl- and methyltranferase activity which supplies the 5' cap structure to the both the mRNAs and the plus strand genome segments (Pizarro et al., 1991).

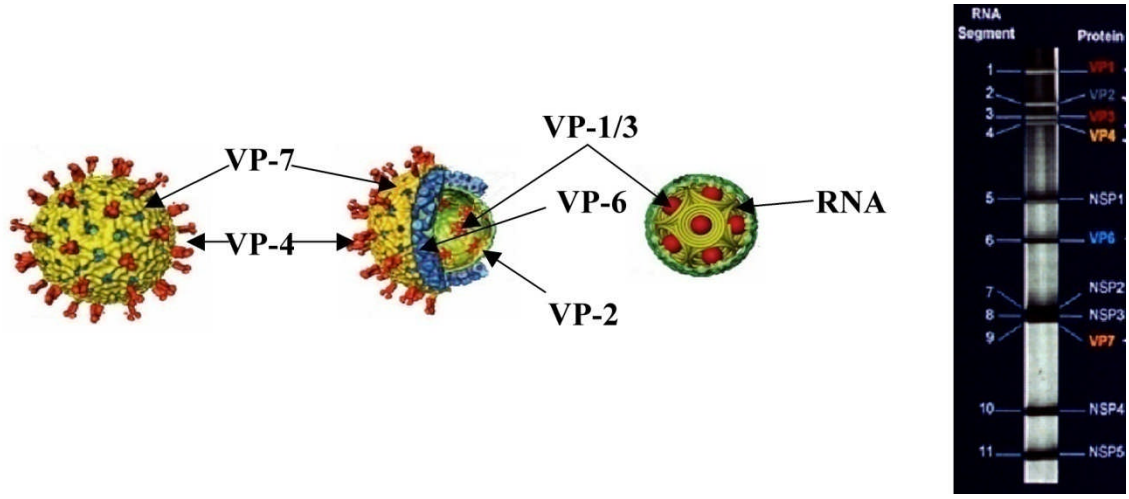

A. B.

Figure 1.1. A. Cryo-EM reconstruction of the rotavirus triple-layer particle. The two outer shells are arranged on a T = 13*l* (levo) icosahedral lattice. VP-7, the major component of outer capsid, is shown in yellow. VP-4 (orange) occurs as 60 surface spikes protruding ~120 Å from the capsid surface. VP-6 is the second shell trimer protein (blue) and VP-2 is the inner core protein (green). VP1/3, the transcription enzymes, are located in the inner core (red). The genome segments (RNA) are shown as inverted conical spirals surrounding the transcription enzymes (Jayaram et al., 2004). **B. Rotavirus western blot**. Western blot showing the structural and nonstructural proteins of a Simian rotavirus indicating relationship to the RNA transcripts (Scott et al., 2005).

Both the intermediate and outer capsid possess T =13 icosahedral symmetry. The intermediate capsid is formed by VP6 trimers located below VP7. VP6 functions in the organization of the RV through interactions with the outer layer protein (VP7) and VP2,

the inner most layer protein, thus integrating the cell entry and endogenous transcription functions (Pesavento et al., 2006). The transcriptionally active DLP has a VP6 coat. The outer capsid of the triple-layered particle (TLP) is composed of VP7, a surface glycoprotein, and VP4, the spike protein, both of which interact with neutralizing antibodies (Estes, 2001; Ramig, 1997). Dimers of VP4 make up the spikes protruding from the outer capsid. VP4 is multi-functional, playing roles in hemagglutination, neutralization, entry into the cell, virulence, and pathogenicity (Delmas et al., 2004). VP4 interacts with not only VP7, but also with VP6, spanning both layers (Estes, 2001).

The RV structure is distinctive in that it possesses 132 large channels that penetrate through the VP6 and VP7 layers that serve to pass aqueous materials and biochemical substances in and out of the inner capsid (Pasavento et al., 2006). Additionally, during transcription RV use the type I channels to discharge the viral mRNA from the subviral particles to the cytosol of the cell (Lawton et al., 2000). The channels are located at the quasi six-fold and five-fold axes of the t = 13 lattice, type I channels (12 each) are located at the five-fold vertices, type II channels (60 each) occur at the pentavalent sites surrounding the type I channels, and type III channels (60 each) are located at the hexavalent positions surrounding the three-fold axes (Pasavento et al., 2006).

The RV non-structural proteins play an important role in genome replication and packaging (Jayaram et al., 2004). NSP1, an RNA-binding protein, appears to be nonessential for virus replication and is the least conserved of the viral proteins (Estes, 2001); however, it may play a role in modulating the innate immune response and

promoting viral cell-to-cell spread (Barro and Patton, 2005). NSP2 and NSP5 are involved in the formation of the viroplasms, electron dense inclusion bodies in which much of the RV replication occurs (Fabbretti et al., 1999; Gallegos and Patton, 1989) and in the synthesis and packaging of the viral RNA (Jayaram et al., 2004; Lopez et al., 2005a). NSP6 interacts with NSP5 and accumulates in the viroplasms. NSP6 is encoded on RV gene 11 with NSP5; however, the function of NSP6 remains unknown and does not appear to be essential for virus replication, at least in cultured cells (Lopez et al., 2005a). NSP3, a functional homolog of cellular poly (A) binding protein (PABP), facilitates the translation of the viral transcripts by binding eIF4G and viral mRNAs, enabling circularizing and delivery to the ribosomes, which represses host protein synthesis (Jayaram et al., 2004; Padilla-Noriega et al., 2002; Varani and Allain, 2002). NSP4 acts as a viral enterotoxin involved in the intracellular signaling pathway (J. M. Ball, personal communication, August 31, 2004) and will be discussed in detail later.

Rotavirus Replication and Morphogenesis

RV infection is initiated with the attachment and entry of the virus via a multi-step process that involves sequential interactions with cell surface molecules (Lopez and Arias, 2004; Mendez et al., 1999). Attachment to the cell is mediated by proteolytic cleavage of VP4 into VP5 and VP8 (Jayaram et al., 2004) which significantly enhances viral infectivity (Arias et al., 1996) and aides in cell entry (Kaljot et al., 1988). VP8 is involved in initial binding to the cell, while VP5 functions in membrane permeabilization, viral entry, and uncoating (Golantsova et al., 2004; Pesavento et al., 2006). The neuraminidase-sensitive (NA) strains interact with sialic acid (SA) through

VP8 with broad specificity followed by more specific viral surface protein interaction with other cell receptors such as integrins or heat shock cognate protein hsc70 (Dormitzer et al., 2002; Lopez and Arias, 2004; Zarate et al., 2000). The NA-insensitive strains, such as the nar3 mutant strain of Rhesus RV, interacts directly with integrin $\alpha 2\beta 1$ through VP5 (Gonzalez et al., 2000; Lopez and Arias, 2006; Zarate et al., 2000). These integrin subunits, $\alpha 2$ and $\beta 3$, and hsp70 have been shown to occur in lipid rafts of MA104 cells (Isa et al., 2004). Additionally, when cholesterol is sequestered from the cell membrane, RV infectivity is reduced by 90% and inhibiting glycoprotein synthesis partially blocks infectivity of both NA-sensitive and NA-insensitive RV strains (Guerrero et al., 2000). These data suggest an important role for lipid rafts in RV cell entry.

Once inside the cell, the low $[Ca^{++}]_I$ promotes uncoating and the activation of VP1, the viral polymerase. The uncoating event involves the loss of the outer capsid VP7 and the VP4 spikes resulting in the Double Layer Particle (DLP) in which transcription occurs. The transcription process requires VPI, VP2, VP3, VP6, NSP1, NSP2, and NSP3. Transcription of the viral genomic minus strands to yield the eleven full length 5'capped plus stranded mRNA takes place in the transcriptionally competent DLP. The nascent (+) mRNAs are extruded through type 1 channels into the cytosol. Although RV mRNAs do not contain Poly (A) tails, the N-terminal region of NSP3 interacts with a 3' consensus sequence in the 11 RV mRNA (Jayaram et al., 2004). The C-terminal region of NSP3 has a strong affinity for the eukaryotic initiation factor (eIF) so that the accumulation of NSP3 in the cytosol results in a decrease in the translation of

cellular proteins by triggering the removal of the cellular poly (A)-binding protein (PABP) from the eukaryotic initiation factor. Viral protein synthesis is instigated by the delivery of the mRNAs to the host translation machinery because the C-terminal region of NSP3 has a strong affinity for the eIF (Jayaram et al., 2004; Padilla-Noriega et al., 2002; Varani and Allain, 2002).

Replication and assembly of the progeny RV occur in electron dense inclusion bodies know as viroplasms. NSP2 and NSP5 form the viroplasm and are required for replication and assembly (Fabbretti et al. 1999; Silvestri et al., 2004). The viroplasm not only forms the DLP from VP1, VP2, VP3, and VP6 that has been concentrated within this inclusion body, but also serves as the site of production of the nascent genomic ds RNA. The DLP is formed when copies of the 11 ds RNAs are packaged with VP1 and VP3 within VP2 (SLP) followed by packaging in VP6. The TLP is formed by an NSP4-mediated process in which the DLP is pulled form the viroplasm into the endoplasmic reticulum (ER), acquiring the outer capsid proteins (VP7 and possibly VP4) and a transient envelope (Lopez et al. 2005b). The VP7 coalesces with the DLPs by an unknown mechanism forming the TLPs. The transient envelope is lost upon exit from the ER and the TLPs are delivered to the apical surface of intestinal cells (Jourdan et al., 1997). In infected cells, VP4 has been shown to traffic to the PM where it probably assembles onto the viral particle via the NSP4-VP4 binding site at amino acids 112-147 of NSP4 (Figure 1.2) (Bergmann et al., 1989; Pesavento et al., 2006; Taylor et al., 1996). Lipid rafts have been implicated as a possible method of delivery of progeny virus,

because infectious particles have been isolated in the raft fractions from *in vitro* and *in vivo* samples (Cuadras and Greenberg, 2003).

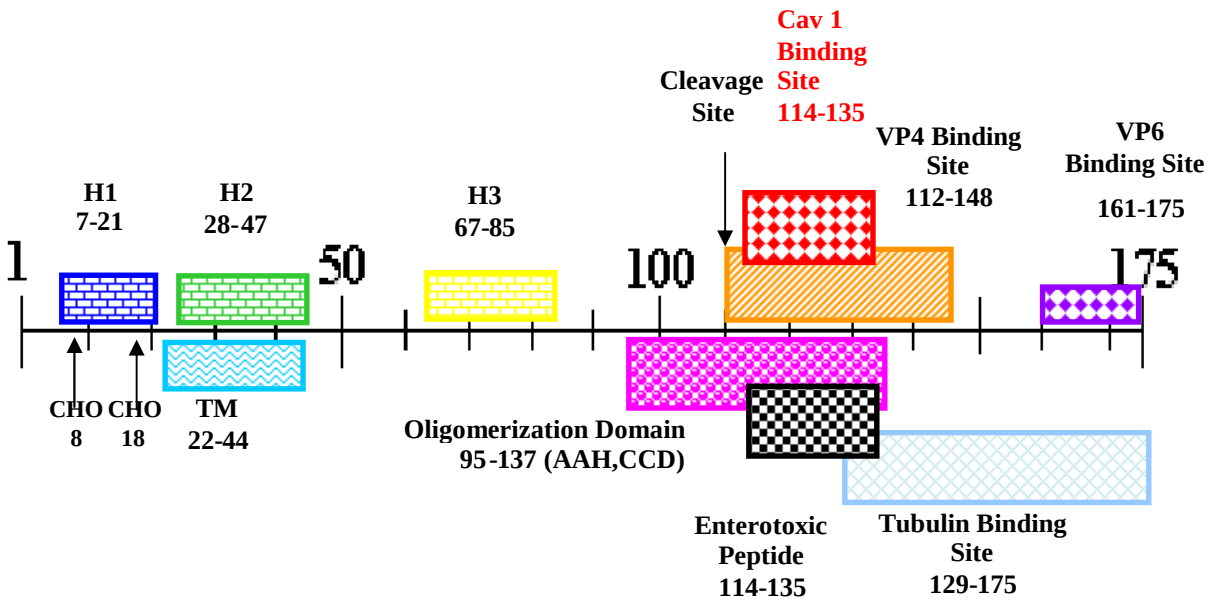

Figure 1.2. Linear schematic of structural and functional domains of NSP4. The 175 aa residues of NSP4 have 3 N-terminal hydrophobic domains H1, H2, and H3 and a single transmembrane domain (TM). AAH, CCD indicates the amphipathic alpha helical region that folds as a coiled coil domain. The C-terminal residues contain the VP6 binding site, the tubulin-binding domain, the VP4 binding site, and a variable domain. The caveolin-1 binding site and enterotoxic peptide coincide (aa 114-135). site at amino acids 112-147 of NSP4 PM (Bergmann et al., 1989; Pesavento et al., 2006; Taylor et al., 1996).

NSP4

As noted above, NSP4 functions as an intracellular receptor essential to RV morphogenesis in which DLPs are pulled from the viroplasms across the ER membrane by NSP4 (Lopez et al., 2005b) through binding to VP6 at amino acid residues 161-175 of NSP4 (Bergmann et al., 1989; Taylor et al., 1996). The NSP4 affinity for VP6 may be the driving force for DLP translocation into the ER through VP7-containing membrane patches and the addition VP7 to the DLP and possibly VP4, although this is

controversial (Au et al., 1989; Pesavento et al., 2006; Taylor et al., 1996). VP4 may assemble onto the viral particle via the NSP4-VP4 binding site at amino acids 112-147 of NSP4 at the PM (Bergmann et al., 1989; Pesavento et al., 2006; Taylor et al., 1996). The infectious viral particle lacking NSP4 is released from the cell.

Also, NSP4 functions in RV pathogenesis as indicated by the induction of a specific, age and dose-dependant diarrhea in neonatal mice as a result of the exogenous addition of either NSP4 or the enterotoxic peptide 114-135 (Ball et al., 1996). This initial diarrheal response occurs in the absence of histologic lesions and is a result of an intracellular calcium $[Ca^{+2}]_i$ –mediated mechanism that results in chloride (Cl^-) secretion and accumulation of fluids in the mouse pup intestinal loops (Ball et al., 1996; Dong et al., 1997). NSP4 mediates $[Ca^{+2}]_i$ mobilization by both exogenous addition and endogenous expression by two distinct mechanisms. Exogenously added NSP4 mobilizes $[Ca^{2+}]_i$ levels through a receptor-mediated, phospholipase C (PLC)-dependent pathway (Brunet et al., 2000; Dong et al., 1997; Tian et al., 1994, 1995, 1996), whereas endogenously expressed NSP4 mobilizes $[Ca^{2+}]_i$ by a phospholipase C (PLC)-independent mechanism (Dong et al., 1997; Tian et al., 1995). The interplay of NSP4 with Ca^{+2} promotes a high $[Ca^{2+}]_i$ required for RV outer capsid structural stability as well as RV maturation (Michelangeli et al., 1995; Ruiz et al., 2000).

NSP4 may contribute to disease by eliciting diarrhea or by disrupting other cellular functions. The viral enterotoxin has been implicated in inducing loss of transepithelial resistance in polarized MDCK cells (Tafazoli et al., 2001) resulting in disruption of tight junctions in the epithelial barrier cells promoting fluid secretion and

diarrhea. Additionally, NSP4 has been shown to disrupt the Na^+ -D-glucose symporter in rabbit brush border membranes causing changes in the intracellular ion concentrations and impairing water re-absorption (Halaihel et al., 2000).

NSP4, the only non-structural protein that does not appear to react with the RNA, acts as a viral enterotoxin involved in the intracellular signaling pathway (J. M. Ball, personal communication, August 31, 2004), functions as a modulator of viral transcription (Silvestri et al. 2005), and plays a role in viral assembly and morphogenesis. When gene 10, which encodes NSP4, is silenced in RV infected cells viral transcription is increased but viroplasm formation is significantly decreased (Lopez et al., 2005b; Silvestri, et al., 2005). The NSP4 viral enterotoxin is implicated in causing the initial diarrhea symptoms prior to detection of histological lesions in the intestine (Ball et al., 1996). NSP4 is synthesized as a primary translation product (Figure 1.1B) containing 175 amino acids (aa) with a molecular weight of 20kDa (J. M. Ball, personal communication, August 31, 2004). This primary translation product is modified by co-translational glycosylation to 29K and oligosaccharide processing to the mature 28kDa glycoprotein (Ericson et al., 1983a), which inserts into the endoplasmic reticulum (ER) bilayer and is anchored by a hydrophobic transmembrane domain (aa 24-44) (Bergmann et al., 1989) such that N-terminal 21 aa reside in the ER lumen and the C-terminal residues 45-175 function as a cytoplasmic tail (Bergmann et al., 1989; Chan et al., 1988).

Figure 1.2 shows a linear schematic of structural and functional domains of NSP4 (Ball et al., 2005). The 175 residues of NSP4 have 3 N-terminal hydrophobic domains H1 (aa 7-21), H2 (aa 28-47), and H3 (aa 67-85) (Chan et al., 1988).

Glycosylation sites (CHO) occur at aa 8 and 18. A single transmembrane domain (TM) localizes to aa 22-44, but varies with the RV strain. Crystallographic analyses of $NSP4_{95-137}$ indicate that it exists as a tetrameric coiled-coil domain (CCD) containing an amphipathic alpha helical (AAH) with distinct polar and hydrophobic faces, and functions in oligomerization (Parr et al. 2006; Bowman et al., 2000; Taylor et al., 1996). This unique AAH has both positively and negatively charged regions within the polar face. The C-terminal residues contain the VP6 binding site at aa 161-175, the tubulin-binding domain (aa 156-175), and the VP4 binding site (aa 112-148). The enterotoxic peptide coincides with the caveolin-1 binding site.

NSP4 is traditionally described as an ER transmembrane glycoprotein because of its role in viral particle morphogenesis at the ER and because of sensitivity of the NSP4 glycosylation sites (CHO) to Endo-β-N acetylglucosaminidase H (endo H) (Bergmann et al., 1989; Ericson et al., 1983a, 1983b). NSP4's high mannose glycosylation indicates a lack of Golgi-specific processing, which supports studies showing NSP4 traffics from the ER by a pathway that bypasses the Golgi (Bergmann et al., 1989; Berkova et al., 2003; Cuadras and Greenberg, 2003).

The C-terminal NSP4 fragment (aa 112-175) has been isolated from culture medium of baculovirus-gene 10 recombinant infected *Spodoptera frugiperda* (SF9) insect cells and RV-infected mammalian cells (Zhang et al., 2000). $NSP4_{114-135}$ has been shown to interact with the extracellular proteins laminin-β3 and fibronectin in yeast-two hybrid assays, which was confirmed by coimmunoprecipitation (Boshuizen et al., 2004). Additionally, Boshuizen et al. found that NSP4 was present in infected enterocytes and

in the basement membrane (BM) of infected neonatal mice and colocalized with laminin-beta3, indicating a physiological interaction at the BM. Similarly, NSP4 colocalizes with Na^+/K^+ ATPase, a PM marker protein, the NSP4 C-terminus is exposed on the exofacial surface of RV-infected mammalian cells, and full-length, high-mannose glycosylated NSP4 is present in the caveolae membrane fraction of RV-infected mammalian cells (Storey et al., 2007).

The NSP4 protein has been shown to localize in other areas of the cell. NSP4 binds microtubules and has been located in the ER-Golgi intermediate compartments (ERGIC) (Xu et al., 2000). In infected cells, vesicular NSP4 tagged with Enhanced Green Fluorescent Protein (NSP4-EGFP) colocalized with the autophagosomal marker LC3 in cap-like structures associated with viroplasms, the site of nascent viral RNA replication (Berkova et al., 2006).

It has been suggested that NSP4 may associate with cellular lipid rafts during infection. Lipid rafts purified from infected cells have been shown to contain infectious RV particles, structural proteins, specifically VP4, and nonstructural proteins including NSP4 (Sapin et al., 2002). Additionally, Cuadras et al. (2006) have shown that silencing VP4 and NSP4 reduced the occurrence of RV particles with lipid rafts. Using circular dichroism and filter binding assays, Huang et al. (2001) report that NSP4 and $NSP4_{114-135}$ preferentially interact with highly-curved lipid vesicles that resemble caveolae, a cholesterol- and sphingomyelin-rich PM microdomain (Huang et al., 2001, 2004). Recent research shows that NSP4 has been isolated with PM caveolae of infected cells from which ER resident proteins have been removed (Storey et al., 2007). NSP4 has

been shown to colocalize with caveolin-1 in reticular structures surrounding the nucleus, in the cytosol, and at the cell periphery in both RV-infected and transfected mammalian cells (Parr et al., 2006). Coimmunoprecipitation of the NSP4-caveolin-1 complexes from RV-infected mammalian cells confirmed this interaction occurs during infection (Gibbons, 2007). Additionally, Parr et al. have demonstrated a direct interaction between NSP4 residues 112-140 of full-length NSP4 and caveolin-1 using the Pro-Quest yeast-two hybrid system and further delineated the binding domain to amino acids 114-135 in peptide binding assays using caveolin-1 from mammalian cell lysates and Sepharose-bound NSP4-specific peptides.

Caveolae and Caveolin-1

Caveolae are invaginations of the plasma membrane containing caveolin proteins (caveolin-1, -2, and -3) and are considered a subset of lipid rafts. These invaginations originally named “plasmalemmal vesicles” (Palade, 1953) are small (50-100 nanometer) and occur in most cell types (Thomas and Smart, 2008) including endothelial cells. Early researchers proposed that “plasmalemmal vesicles” or “caveolae intracellulare” were capable of communicating with the exterior of the cell as well as shuttle molecules within the cell (Simionescu et al., 1983). While the structure is typically flask-shaped, other morphologies such as flat, tubular, and vesicular are noted. Caveolae are considered to be a highly curved subset of lipid rafts that contain the integral membrane protein caveolin-1 and are rich in cholesterol, sphingomyelin, glycosphingolipids, and signaling molecules (Couet et al., 2001). Caveolae differ from other lipid rafts in that they have a striated coat and contain caveolin proteins (Liu et al., 2002; Rothberg et al.,

1992). Caveolae rafts are not functionally the same as non-caveolin containing lipid rafts. Caveolin influences cellular process by forming homo- and hetero-oligomers (Das et al., 1999; Scheiffele et al., 1998; Schlegel and Lisanti, 2000), interact with signaling molecules (Robbins et al., 1995; Shenoy-Scaria et al., 1994), and by regulating cholesterol content in caveolae (Uittenbogaard and Smart, 2000). Caveolae functions include (a) transport, including endocytosis, transcytosis, and cholesterol transport; (b) functioning in Ca^{2+} homeostasis; and (c) signal transduction by regulating a wide variety of signaling pathways.

The family of caveolin proteins includes caveolin-1, -2, and -3, which are referred to as caveolae coat proteins. These proteins serve as identifying markers for caveolae with molecular mass between 18 and 22kD. While the three caveolins are compositionally different, they all contain the caveolin signature sequence of eight aa residues (FEDVIAEP) (Tang et al., 1996).

Caveolin-1 is a protein of 178 aa and occurs as two isoforms, caveolin-1α or full length and caveolin-1β with the beta form being residues 32-178 of the alpha form. Both forms induce caveolae formation *in vitro* (Fujimoto et al., 2000). Caveolin-1 is the main structural protein of caveolae, serving as the caveolae backbone. It regulates the transport of cholesterol to and from caveolae (Kurzchalia et al., 1992; Smart et al., 1994, 1996; Uittenbogaard et al., 1998) and regulates a variety of signal transduction activities of caveolae resident proteins (Chun et al., 1994; Fujimoto, 1993; Li et al., 1996; Song et al., 1996). Stable oligomers of caveolin-1 form filaments along the cytoplasmic face that serve to regulate the formation of caveolae vesicles, known as caveosomes and serve as

a scaffold for these vesicles (Li et al., 1998). Cavesomes, which were first characterized as intermediates in the trafficking of SV40 virus from the cell surface to the ER (Pelkmans et al., 2001), are non-acidic caveolin-1 vesicles lacking both endosomal and lysosomal markers (Nichols, 2002). The oligomers are stabilized by the palmitoylation of three cysteine residues that function in caveolin-cholesterol binding and transport to the PM (Dietzen et al., 1995; Uittenbogaard and Smart, 2000). Both termini of caveolin-1 are exposed in the cytoplasm (Figure 1.3), which results from formation of a hairpin loop in the cytoplasmic leaflet of the PM by a central intermembrane domain (aa 97-131) (Anderson, 1998). The caveolin scaffolding domain (CSD), aa 82-101, functions in membrane attachment resulting in aa residues 82-101 being identified as the N-terminal membrane attachment domain (N-MAD). Similarly, aa residues 135-150 are identified as the C-terminal membrane attachment domain.

Caveolin-2 forms three isoforms, however, the functional significance of the isoforms is not clear (Anderson, 1998). Caveolin-2 is found in the same types of cells as and colocalizes with caveolin-1 and requires it to form caveolae. The caveolin hetero-oligmers found in most cells are made of caveolin-1 and -2 (Thomas and Smart, 2008). Caveolin-3, a muscle specific caveolin, is functionally and structurally similar to caveolin-1, but is 27 aa shorter and can form caveolae independent of caveolin-1 (Tang et al., 1996).

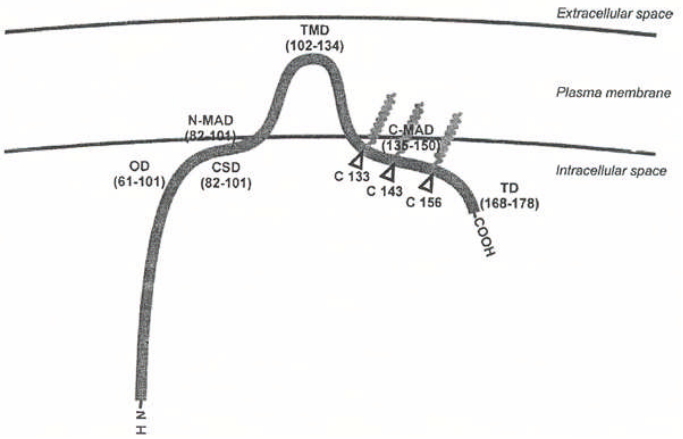

Figure 1.3. Membrane topology and domains of caveolin-1. Caveolin attaches to the plasma membrane (PM) through the centrally located transmembrane domain (TMD) at aa 102-134 forming a putative hairpin within the PM, resulting in both termini of caveolin-1 being exposed in the cytoplasm. Additional attachment to the PM occurs through the caveolin scaffolding domain (CSD, aa102-101), which is known as the N-terminal membrane attachment domain (N-MAD) and the C-terminal membrane attachment domain (C-MAD, aa135-150). Caveolin-1 monomers form stable oligomers through attachment at the oligomerization domain (OD, aa 61-101). Palmitoylation of three cysteine residues (133, 143, and 156) function to stabilize caveolin-1 oligomers.

Cholesterol is a major component of caveolae and stabilizes the caveolae structure at the PM (Simionescu, 1983). Cholesterol levels are in constant flux in and out of caveolae suggesting that caveolae function in cholesterol transport (Smart et al., 1994; Storey et al., 2007). Movement of cholesterol in and out of high density lipoproteins (HDL) is controlled by caveolin-1 (Graf et al., 1999). Additionally, cholesterol has transcriptional control of caveolin-1 through sterol regulatory elements in the caveolin-1 promoter, such that high concentration of intracellular cholesterol stimulate its transcription and low levels decrease it (Bist et al., 1997; Fielding et al., 1997).

NSP4 and Caveolin-1

The multifunctional roles of caveolin-1, including structural protein of caveolae, signal transduction, vesicular, transport, and residence in the PM make it a likely cellular molecule for RV to use to facilitate infection, morphogenesis, and pathogenesis. Caveolin-1 is upregulated in RV-infected Caco-2 cells (Cuadras et al., 2002) suggesting a modulation of its transcription by RV. Full-length, endo-H sensitive NSP4 is present in cavitation-sucrose chromatography caveolae from RV SA11-4F-infected MDCK cells (Storey et al., 2007). NSP4 and caveolin-1 have been shown to colocalize at perinuclear sites, in cytoplasmic structures, and at the cell periphery in RV-infected MDCK cells at both early and late time points (Storey et al., 2007). In NSP4-transfected cells, that is in the absence of all other viral proteins, NSP4 had a similar distribution pattern as the RV-infected cells, i.e., at the cell periphery, in the cytosol, and it colocalized with caveolin-1 at intracellular sites similar to the RV-infected cells (Storey et al., 2007). The colocalization of NSP4 and caveolin-1 during RV infection or NSP4 transfection resolved the proteins to within about 200 nm, while FRET analyses with Cy2- and Cy3-labeled probes resolved the NSP4-caveolin-1 interaction to an area of less than 10 nm in radius. The positive FRET reaction placed at least some portion of the NSP4 and caveolin-1 protein pools within 10 nm of each other, highly indicative of a protein-protein interaction (Storey et al., 2007).

The purpose of this research was to identify the region or regions of the NSP4 C-terminal amphipathic alpha helix (AAH) that are sufficient for binding caveolin-1.

Hypothesis

We hypothesized that hydrophobic face of the NSP4 AAH binds caveolin-1 via a hydrophobic interaction and that a minimum of three hydrophobic residues in the hydrophobic face of the NSP4 AAH are required for binding caveolin-1.

Specific Aims

- Aim 1: Determine if the polar or hydrophobic face of the NSP4 AAH bind caveolin-1 using mutants that disrupt the polar or the hydrophobic face.
- Aim 2: Design and clone NSP4 hydrophobic mutants with contiguous hydrophobic residues in the C-terminal hydrophobic face of the NSP4 AAH. Determine which hydrophobic residues in the C-terminal hydrophobic face of the NSP4 AAH are sufficient for binding caveolin-1 using mutant NSP4 proteins in yeast-two hybrid assays.
- Aim 3: Verify direct interaction between caveolin-1 and yeast two-hybrid positive mutant NSP4 proteins using peptide binding assays.

CHAPTER II

THE HYDROPHOBIC FACE OF THE ROTAVIRUS NSP4 EXTENDED AMPHIPATHIC ALPHA HELIX BINDS CAVEOLIN-1

Overview

A direct interaction between the Rotavirus NSP4 and caveolin-1, the structural protein of caveolae, has been shown by yeast two-hybrid, peptide binding assays, co-immunoprecipitation, and Fluorescence Resonance Energy Transfer (FRET) analyses. Using seven deletion mutants of NSP4, binding to caveolin-1 has been delineated to the enterotoxic domain within the C-terminal amphipathic alpha helix (AAH) of NSP4. Alterations in the charged face or the hydrophobic face of the C-terminal AAH have demonstrated a preferential binding of the hydrophobic face of NSP4 to caveolin-1. In this study, we further explored this finding using mutagenesis, yeast 2-hybrid, and peptide binding assay.

This study localized the NSP4 binding domain for caveolin-1 to one critical hydrophobic aa (L116) and at least one other aa (L127or L134) in the same plane as L116 plus at least one other aa (I113 or Y131) in the other plane of the hydrophobic face. These data provide evidence that conformational and hydrophobic constraints play an important role in the NSP4 to caveolin-1 association.

Introduction

Rotavirus (RV) causes severe diarrhea in young animals and children resulting in the annual hospitalization of nearly 2 million children and the death of over 440,000 children less than five years of age worldwide (Fischer et al, 2007; Pasashar et al. 2003).

RV induces both secretory and maladsorbtive diarrhea, both of which are multifactorial (Estes et al., 2001; Morris and Estes, 2001). One mechanism of secretory diarrhea has been elucidated with the identification of the RV nonstructural protein 4 (NSP4) as the first viral enterotoxin (Ball et al., 1996). In this study NSP4 and the enterotoxic peptide, amino acids (aa) 114-135, induced diarrhea in young mice by promoting Cl^- secretory currents via a calcium-mediated pathway in the absence of histological alterations (Ball et al., 1996).

NSP4, initially identified as an endoplasmic reticulum (ER) resident glycoprotein, is essential to RV morphogenesis (Au et al., 1989). To further define the function(s) of NSP4 in RV morphogenesis, silencing RNA (siRNA) studies were performed on RV-infected cells (Lopez et al., 2005b). These studies demonstrate that in the absence of functional NSP4, there is: (a) an abnormal distribution of viral proteins in the viroplasm, (b) little to no virus particles present, (c) an accumulation of empty virus particles (Lopez et al., 2005a; Silvestri et al., 2005), and (d) an up-regulation of viral transcription (Silvestri et al, 2005). Taken together, these data show the critical role of NSP4 in viral morphogenesis suggesting that NSP4 performs an important regulatory role in the maturation of the transcriptionally active double-layered particles to triple-layered particles.

Increasing evidence has shown NSP4 functions as an enterotoxin by activating a signal transduction pathway initiated at the plasma membrane (PM) (Brunet et al., 2000; Tian et al., 1994, 1995). Exogenously added NSP4 mobilizes $[Ca^{2+}]i$ levels through a receptor-mediated, phospholipase C (PLC)-dependent pathway (Brunet et al., 2000;

Dong et al., 1997; Tian et al., 1994, 1995, 1996), whereas endogenously expressed NSP4 mobilizes $[Ca^{2+}]i$ by a phospholipase C (PLC)-independent mechanism (Dong et al., 1997; Tian et al., 1995).

Identification of a C-terminal fragment of NSP4 (residues 112-175) in RV-infected culture media provide the first experimental evidence that at least a portion of NSP4 leaves the ER (Zhang et al. 2000). Subsequent studies confirm the presence of NSP4 at multiple locations in RV-infected cells (Berkova et al., 2006; Boshuizen et al., 2004; Cuadras and Greenberg, 2003; Parr et al., 2006; Xu et al., 2000). Co-localization studies show NSP4 and caveolin-1 throughout the cell and at the cell periphery (Parr et al, 2006). Interactions between NSP4 and the extracellular matrix proteins, laminin-beta3 and fibronectin have been demonstrated at the basement membrane of rodent intestines and in Yeast-2 Hybrid assays (Boshuizen et al., 2004). Co-localization of NSP4-EGFP with a viroplasm marker, NSP5, and an autophagic vesicle marker, LC3, using confocal imaging indicates NSP4 transport is via a calcium-dependent vesicular pathway that bypasses the Golgi (Berkova et al., 2006). Together, these data clearly support the exit of NSP4 from the ER and the co-localization with caveolin-1 at perinuclear reticular structures, in the cytosol, and at the cell periphery in both RV-infected and transfected mammalian cells. Furthermore, NSP4 associates with cellular proteins that could be implicated in protein trafficking (Berkova et al., 2006; Huang et al., 2004; Silvestri et al., 2005; Storey et al., 2007; Xu et al., 2000).

Data demonstrate preferential binding of NSP4 and $NSP4_{114-135}$ to SUVs that are caveolae-like model membranes, suggesting the caveolae membrane system may serve

as a means of NSP4 transport (Huang et al., 2001, 2004). Caveolin-1 is found in the intestine, interacts with cholesterol, and functions to transport *de novo* synthesized cholesterol to and from the ER and PM caveolae (Devaux and Morris, 2004; Schroeder et al., 2001; Smart et al., 1996; Uittenbogaard et al., 1998. Also, caveolin-1 acts as a scaffolding protein in caveolae for signaling molecules, including those involved in calcium homeostasis (Cheng et al., 2006; Field et al., 1998; Hailstones et al., 1998). In summary, the multi-functional caveolin-1 is likely candidate to facilitate NSP4 movement within the cell as it is involved in cellular activities.

Subsequently, we identified a direct interaction between the structural protein of caveolae, caveolin-1, and NSP4 (Parr et al., 2006). Further analyses have delineated the NSP4 binding site for caveolin-1 to aa 114-135, the enterotoxic domain, using *in vivo* yeast two-hybrid, *in vitro* binding, and co-immunoprecipitation assays (Parr et al., 2006). The goal of the current study was to extend these findings and determine if the secondary structure of the $NSP4_{95-137}$ amphipathic alpha helix interacts with caveolin-1 (Bowman et al., 2000; Taylor et al., 1996). To determine the aa residues in $NSP4_{113-135}$ that bind caveolin-1, nine NSP4 site-directed mutants were constructed that disrupted either the charged or hydrophobic face of the AAH in full-length NSP4 (FLNSP4) and $NSP4_{46-175}$.

Materials and Methods

Antibodies and Peptides

Synthetic peptides to NSP4 (residues 2-22, 114-135, and 150-175) and caveolin-1 (residues 2-31, 19-40, 76-101, and 161-178) were generated in our laboratory as

previously described (Huang et al. 2001). NSP4 and caveolin-1 peptide specific antibodies were generated in rabbits to NSP4 and caveolin-1 residues 2-31 as previously described (Huang et al., 2004; Swaggerty et al., 2004). Rabbit Ig anti-caveolin-1 N_{1-97} (purified polyclonal Antibody generated from human caveolin-1) was purchased from BD Biosciences (San Jose, CA). These antibodies were used as primary antibodies in Western blot assays as previously described (Fischer et al., 2007; Mir et al., 2007; Parr and Ball, 2003; Parr et al., 2006; Zhou et al., 2004). Reactive bands were visualized by the addition of goat HRPO-anti-rabbit IgG and SuperSignal West Pico or Femto chemiluminescent substrate (Pierce, Rockford, IL), and exposure and development of x-ray film.

Mammalian Cell Lines and Yeast Strains

Madin-Darby Canine Kidney (MDCK) cells were obtained from ATCC (Rockville, MD) and maintained in Dulbecco's modified Eagle medium (DMEM; Gibco, Grand Island, NY) supplemented with 10% fetal bovine serum (FBS), glutamine (2 mM), penicillin-streptomycin (100 ug/ml) and non-essential amino acid (1X) (Sigma, St. Louis, MO). *Saccharomyces cerevisiae* strain MaV203 (*MAT*α, *leu*2-3,112, *trp*1-901, *his*3Δ200, *ade*2-101, *gal*4Δ, *gal*80Δ, *SPAL*10::*URA*3, *GAL1*::*lacZ*, *HIS*$3_{UASGAL1}$:: *HIS*3@*LYS*2, can1^r, cyh2^r) was used for all yeast two-hybrid analyses (Vidal et al., 1996). A collection of yeast strains that contain plasmid pairs expressing fusion proteins with a spectrum of interaction strengths [pPC97 (*GAL4*-DB, *LEU2*), pPC97-*CYH2*^{S} and pPC86 (*GAL4*-AD, *TRP1*)] were used as controls (Invitrogen Life Technologies, 2002;

Vidal et al., 1996). The control plasmids pDBleu and pEXP-AD507 contain only the *Gal4* DNA-binding domain (BD) and the *Gal4* activating-domain (AD) respectively.

The *Saccharomyces cerevisiae* yeast strain InVSc1 (MATα*his3-Δ1, leu2, trp1-289, ura3-52*; Invitrogen) was used to express full-length FLNSP4, $FLNSP4_{Ala}$, and the eight $NSP4_{46\text{-}175}$ mutant proteins in the inducible yeast expression system.

Construction of Plasmids

Two sets of NSP4 clones were prepared for separate assays. Full-length (FL) NSP4, $NSP4_{Ala}$ and $NSP4_{HydroMut}$ (FLNSP4, $FLNSP4_{Ala}$ and $FLNSP4_{HydroMut}$) were constructed using overlapping site-directed mutagenesis and used for *in vitro* binding assays (Figure 2.1A). Because we have observed stronger positive interaction between NSP4 and caveolin-1 in yeast 2-hybrid assays using a $NSP4_{46\text{-}175}$, the N-terminal deletion mutant lacking two N-terminal hydrophobic domains (Parr et al., 2006), we utilized overlapping site-directed mutagenesis to construct the same alanine and charged amino acids substitutions in the $NSP4_{46\text{-}175}$ clone ($NSP4_{Ala}$ and $NSP4_{HydroMut}$). The primer sets for these mutants and other mutants used in this research are shown in Figure 2.1A.

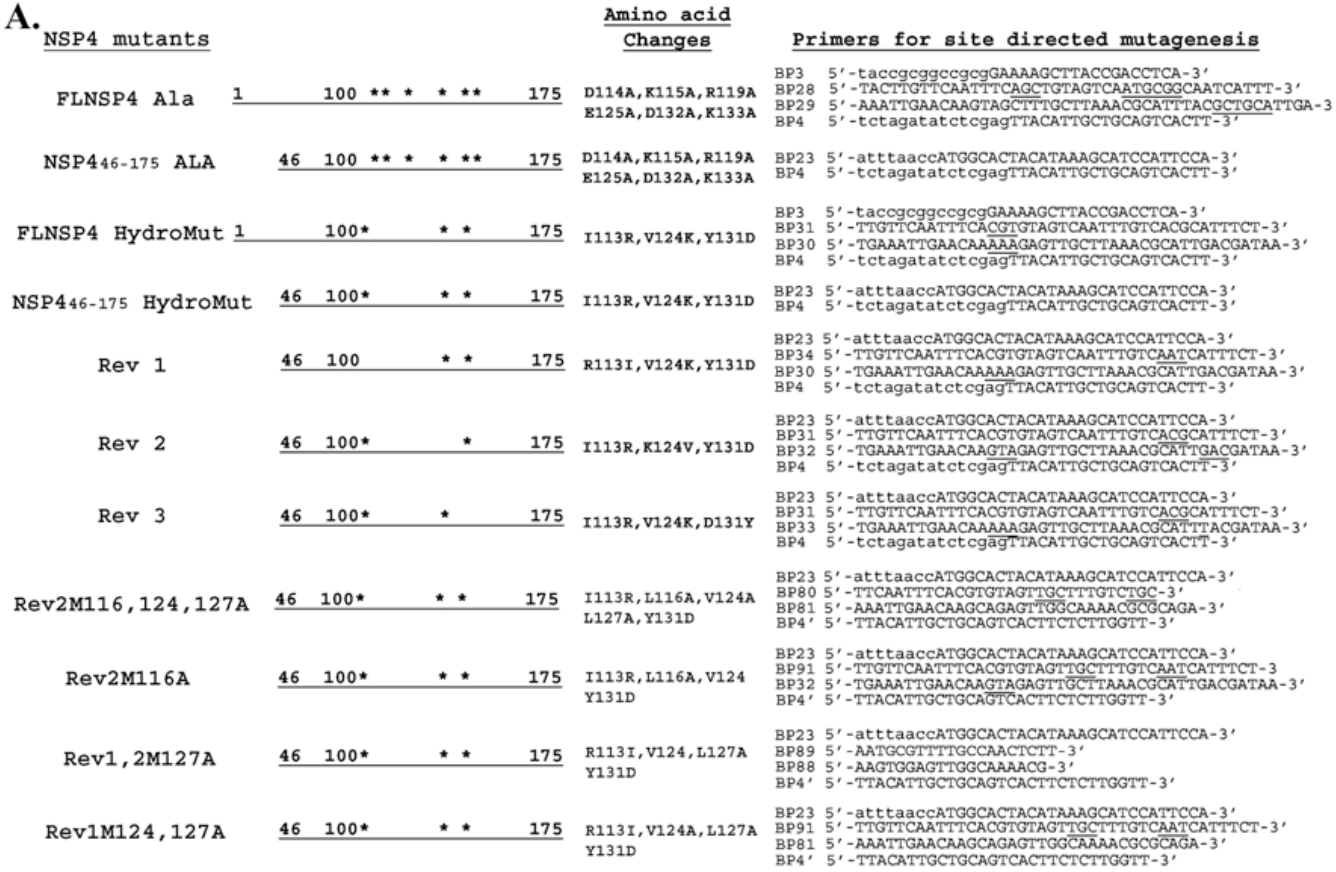

Figure 2.1. NSP4 mutants. A. Linear schematics of the NSP4 mutants used in this study are given on the left. The individual aa that were mutated are indicated by asterisks and are given to the right of each drawing as the original aa + position + new aa, i.e. D114A means aa 114 aspartic acid was mutated to alanine. The PCR fragments were produced using the forward and reverse primers listed to the right of each construct and cloned into the DNA-binding domain, pD22, the activation-domain, pD32, and pY52Dest plasmids of the Invitrogen Gateway™ System. The linear schematics include of the full-length alanine mutant ($FLNSP4_{Ala}$) and the N-terminal deletion mutant ($NSP4_{Ala}$) in which charged residues were mutated to alanine; the full-length hydromutant ($FLNSP4_{Hydromut}$) and the N-terminal deletion mutant ($NSP4_{Hydromut}$) in which hydrophobic residues were mutated to charged residues, Rev 1; Rev 2; Rev 3; Rev2 M116, 124,127A; Rev2M116A; Rev1, 2M127A; and Rev1M124, 127A.

B.

Figure 2.1. NSP4 mutants continued. B. Alignment of the FLNSP4 and the N-terminal deletion mutants.

To disrupt the charged face, six charged amino acids were changed to alanine (D114A, K115A, R119A, E125A, D132A, and K133A) in both $FLNSP4_{Ala}$ and $NSP4_{Ala}$ (Figure 2.1A). To disrupt the hydrophobic face of NSP4, three amino acids localized to the hydrophobic face of the C-terminal AAH were changed to charged residues (I113R, V124K, and Y131D) $FLNSP4_{HydroMut}$, and $NSP4_{HydroMut}$ (Figure 2.1A). The mutant PCR products were directionally cloned into the Invitrogen Gateway™ Entry vector, pENTR11 (Invitrogen, CA), sequence verified, and cloned into the Invitrogen Gateway™ Destination vectors pDEST22 and pDEST32 as previously described (Parr et al., 2006; Zhou et al., 2004).

Yeast Two-Hybrid Screening

MaV203 yeast were co-transformed with caveolin-1, -NSP4, $-NSP4_{Ala}$ or $-NSP4_{HydroMut}$ in the appropriate pD22 and pD32 vectors by a modified lithium acetate procedure as previously described (Gietz and Woods, 2002). Briefly, *S. cerevisiae* MaV203 was grown in YPAD (yeast extract, bacto-peptone, 0.01mM adenine hemifulfate, 2% dextrose), overnight at 30˚C with shaking, diluted to an OD_{600} of 0.5, and incubated at 30˚C with shaking to an OD_{600} of 2. The cells were washed with $_dH_2O$, pelleted, and washed with 2 ml of 100 mM lithium acetate (LiAc), pelleted and

resuspended in 800 μL of 100mM LiAc, divided into 50μL aliquots for individual transformations. Aliquots were pelleted and the following solutions were added in order: 240μL of 50% PEG (3350 mw); 36μL of 1M LiAc; 25μL of salmon sperm DNA (2mg/ml); 50μL of $_dH_2O$ and 100ng of each plasmid DNA. The yeast were heat shocked at 42˚C for 45 min and then incubated at 30˚C for 1h before plating onto complete synthetic medium lacking leucine and tryptophan (CSM -Leu-Trp). Transformants were grown at 30˚C for 72 hrs on CSM-Leu-Trp and replica plated onto selective media to identify colonies containing both plasmids. The interaction of candidate protein pairs was assessed by the induction of three independent reporter genes (*URA3, His3, lacZ)*, which were monitored on selective media and by β-galactosidase assays. Ninety clones of each NSP4 mutant construct (bait or prey) were screened for interaction with caveolin-1. Full length NSP4 was used as a positive control in addition to the panel of controls provided by the manufacturer.

URA3 was monitored by cell growth patterns on CSM -Leu-Trp-Ura and CSM-Leu-Trp + 0.2% 5-fluoroorotic acid (FOA). The yeast two-hybrid-dependent induction of *URA3* results in the conversion of 5-fluoroorotic acid (5FOA) to 5-fluorouracil, which is toxic and inhibits the growth of yeast. Cells with interacting proteins grow on medium lacking uracil, but are growth inhibited on medium containing 5FOA.

When *HIS3* was transcribed, the growth of the co-transformed yeast was inhibited in a dose-dependent manner by adding 3-amino-1, 2, 4-triazole (3AT: 25 mM, 50 mM, and 100 mM) to CSM- Leu-Trp-His (52). MaV203 expresses a basal level of *HIS3* that is inhibited with increasing concentrations of 3AT.

Activation of the *lacZ* promoter was detected with an assay for β-galactosidase (β-gal) expression. It was qualitatively assayed by plating the transformed yeast on YPAD medium with a nitrocellulose filter. The presence β-gal was detected by using the substrate X-gal (5-bromo-4-chloro-3-indolyl-β-D-galactopyranoside). The induction of the *lacZ* gene resulted in a blue color when assayed with X-gal. To quantitatively measure β-galactosidase activity, chlorophenol red-β-D-galactopyranoside (CPRG) was used as the substrate. Three independent isolated colonies from each positive X-gal sample and from X-gal negative samples were assayed in triplicate. Briefly, the X-gal positive yeasts were streaked onto CSM-Leu-Trp medium, grown overnight at 30°C. Individual colonies were inoculated into 2.5ml CSM-Leu-Trp, incubated overnight at 30°C with shaking. YPAD (5 mls) was inoculated with 1ml of the overnight culture, which gave an approximate OD_{600} of 0.5, then incubated 30°C with shaking until the OD_{600} = 1.0-1.5. A 1.5ml aliquot of the culture was place in a microfuge tube, centrifuged, pelleted, washed with the buffer solution sans the CPRG substrate, pelleted again, followed by addition of the buffer solution containing the CPRG substrate and incubated at 37°C and monitored for development of a rusty yellow to red-brown color. After color development, which varied from as little as 15 minutes to over 48 hours, the reaction was stopped with 6mM zinc chloride ($ZnCl_2$), the samples centrifuged, 200 μl of the supernatant transferred a well of a 96-well plate, and the optical density was determined with an ELISA reader. One β-gal unit is defined as the amount of enzyme

that hydrolyzes 1 mmol of CPRG chloramphenicol red and D-galactose per minute (Parr et al., 2006; Zhou et al., 2004).

Western Blot Assays

The co-transformed yeast were grown in liquid CSM-Leu-Trp, and yeast protein extracts were prepared using the Zymo Yeast Protein Extraction kit (Zymo Research, CA). The yeast cell pellets were resuspended in PBS (pH 7.2) containing protease inhibitors [100µM AEBSF, 80µM aprotinin, 5µM bestatin, 1.5µM E-64, 2µM leupeptin, 1µM pepstatin A, 100µM PMSF (Calbiochem-Novabiochem Corp., San Diego, CA)]. Micro bicinchoninic acid (BCA) protein assay (Pierce Biotechnology, Rockford, IL) was used to quantify protein concentrations with bovine serum albumin according to the manufacturer's protocol. All lysates were separated by 12% SDS-PAGE, electroblotted onto nitrocellulose membranes, probed with NSP4 or caveolin-1 peptide-specific antibodies, and reactive bands were visualized by the addition of HRP-conjugated IgG and SuperSignal® West Pico or Femto (for peptide binding assays only) chemiluminescent substrate (Pierce) followed by exposure to Kodak X-OMAT film as previously described (Parr and Ball, 2003; Parr et al., 2006; Zhou et al., 2004).

Expression of FLNSP4,Ful-Lengh Mutants and MSP4 Deletion Mutants

The entry level vectors encoding FLNSP4, $FLNSP4_{Ala}$, $FLNSP4_{HydroMut}$, $NSP4_{Rev1}$, $NSP4_{Rev2}$, $NSP4_{Rev3}$, $NSP4_{Rev2M116, 124, 127A}$, $NSP4_{Rev1M124, 127A}$, $NSP4_{Rev1, 2 M127A}$, $NSP4_{Rev2 116A}$ were used to shuttle the NSP4 sequences into the inducible yeast expression plasmid, pYES-DEST52 (Invitrogen) as described above. Transformants were grown on CSM-Ura and colonies were induced with YPAG medium [**y**east extract,

peptone (Difco), 0.01 mM **a**denine sulfate, 2% **g**alactose (Sigma)] to express the encoded NSP4 proteins. Cells were grown in YPAG at 30°C for 24h, washed and resuspended to an OD_{600} of 0.5 in YPAG and incubated at 30°C for 24h. Yeast lysates were prepared using the Zymo Yeast Protein Extraction kit (Zymo Research, Orange, CA) as previously described and were utilized in the peptide binding assays (Parr et al., 2006; Zhou et al., 2004). Approximately 1 x 10^6 cells were pelleted and 25µl Y-Lysis buffer and 1 µl zymolase were added to the samples and incubated at 37°C for 1 h. The cells were centrifuged at 400 x *g* for 5 min, resuspended in PBS (pH 7.2), containing protease inhibitors [100µM AEBSF, 80µM aprotinin, 5µM bestatin, 1.5µM E-64, 2µM leupeptin, 1µM pepstatin A, 100µM PMSF (Calbiochem-Novabiochem Corp., San Diego, CA)]. Micro bicinchoninic acid (BCA) protein assay (Pierce Biotechnology, Rockford, IL) was used to quantify protein concentrations with bovine serum albumin according to the manufacturer's protocol. The cell lysates were used in the *in vitro* peptide binding and Western blot assays as described below.

In Vitro Peptide Binding Assay

To confirm the protein-protein interaction of caveolin-1 with FLNSP4, FLNSP4 mutants or NSP4 deletion mutants, synthetic peptides corresponding to either N-caveolin-1 (residues 2-31 or 19-40), caveolin-1 containing only the scaffolding domain residues 76-101, or C-caveolin-1 (residues 161-178) were attached to CNBr-activated sepharose 4B beads as recommended by the manufacturer (Amersham Biosciences Corp., Piscataway, NJ). Controls included Sepharose beads alone and lysates from InVSc1without an expression plasmid insert. Cells lysates with approximately 2mg total

protein was incubated with 50ml of a 50% slurry CNBr-activated sepharose 4B beads with and without peptides overnight at 4ºC with gentle mixing. The beads were washed three times with wash buffer (10 mM Tris pH 7.5; 10 mM Tris pH 7.5 + 0.5 M NaCl) and resuspended in SDS-PAGE loading buffer. The proteins were separated on 12% SDS-PAGE, transferred to nitrocellulose membranes and probed with caveolin-1- or NSP4-specific antibodies in a Western blot assay.

EndoH Digestion of NSP4$_{HydroMut}$ Expressed in Yeast

To ensure that the lack of reactivity of FLNSP4$_{HydroMut}$ was not due to the lack of glycosylation pattern that we previously have shown with NSP4 from RV-infected MDCK cells (Parr et al., 2006), yeast expressing FLNSP4$_{HydroMut}$ were treated with endoglycosidase H (Endo H). RV-infected MDCK cells were used as a control that demonstrated normal NSP4 glycosylation pattern. Briefly, glycoprotein denaturing was completed per manufacturer's directions using the Endo H kit (New England Biolabs, Ipswich, MA). Samples were mock treated or digested with Endo H for 1 h at 37°C. The treated lysates were resolved by 12% SDS-PAGE, electrotransferred onto nitrocellulose and probed with NSP4-specific antibody in a Western blot. A shift in the NSP4 molecular weight due to glycosidase treatment was visualized by chemiluminescence (Parr et al., 2006).

Results

NSP4- and Caveolin-1-fusion Proteins Are Present in the Co-transformed Yeast

To verify the presence of the encoded NSP4 clones and caveolin-1 GAL-4 fusion proteins, the co-transformed lysates were probed with peptide specific antibodies, either anti-NSP4$_{150\text{-}175}$ or anti-caveolin-1 (Figure 2.2 A-D). Untransformed InVSc1 demonstrated a non-specific band at ~30 kD when blotted with both antisera (Figure 2.2A and B, lane 1). The fusion proteins pD22caveolin-1 (~34.9kD) were present in all co-transformed yeast and pD32NSP4$_{46\text{-}175,\ Ala,\ HydroMut,\ Rev1,\ Rev2,\ and\ Rev3}$ (Figure 2.2 Panel A). Similar results were obtained with the fusion proteins formed by the co-transformation of pD22caveolin-1 with pD32NSP4 $_{Rev1,2\ M127A}$, pD32NSP4 $_{Rev1,2\ M124,\ 127A}$, pD32NSP4$_{Rev2\ M\ 116A,\ 124A,\ 127A}$, pD32NSP4$_{Rev2\ M116A}$ (Figure 2.2 Panel C). The NSP4 fusion proteins evaluated with caveolin-1-specific antibodies (panels B and D) were expressed and were present at ~34.4kD (Figure 2.2B and D). These data confirm that the encoded sequences from both plasmids are translated as fusion proteins.

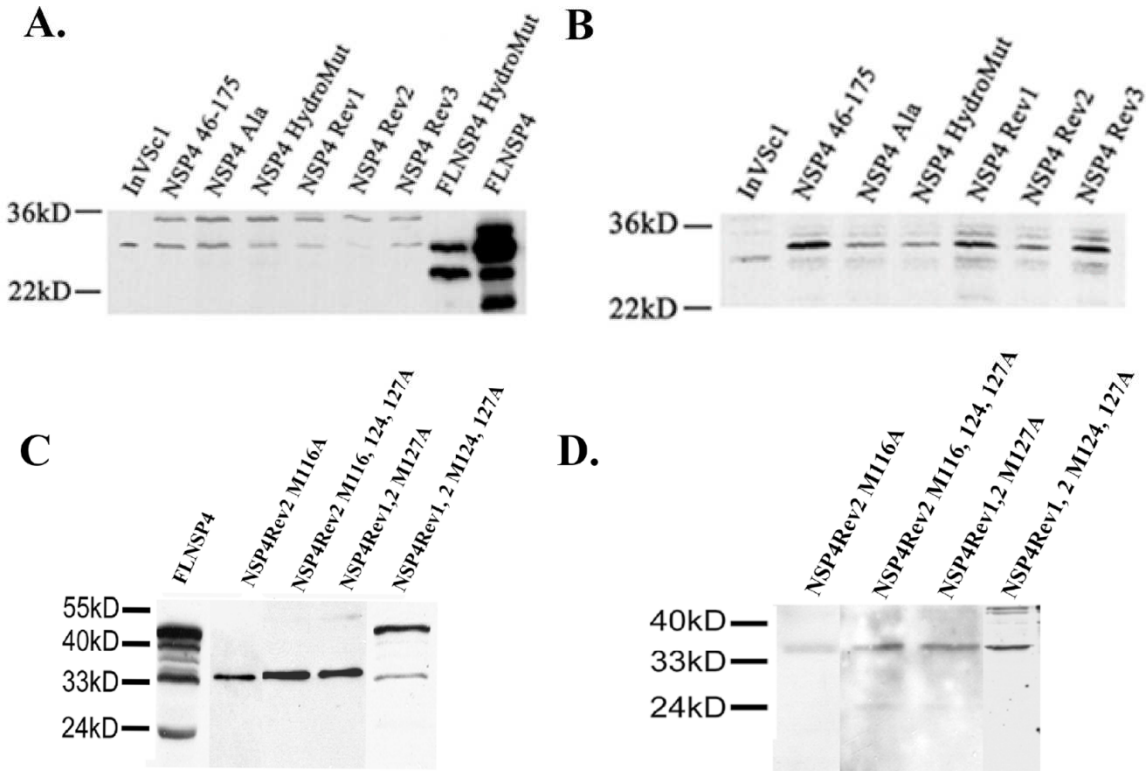

Figure 2.2. NSP4- and caveolin-fusion protein expression. To verify the presence of NSP4- and caveolin-1 fusion proteins in the yeast-two-hybrid assay, Western blot analyses of the yeast co-transformed with pD22cav-1 and each of the following: pD32NSP4$_{46\text{-}175}$, pD32NSP4$_{46\text{-}175Ala}$, pD32NSP4$_{46\text{-}175HydroMut}$, pD32NSP4$_{Rev1}$, pD32NSP4 $_{Rev2}$, pD32NSP4$_{Rev3}$, pD32NSP4$_{Rev2\ M116A}$, pD32NSP4$_{Rev2\ M\ 116A,\ 124A,\ 127A}$, pD32NSP4 $_{Rev1,2\ M127A}$, and pD32NSP4 $_{Rev1,2\ M124,\ 127A}$, were examined using (A and C) rabbit anti-NSP4150-175 or (B and D) rabbit anti-Cav2-22. A. The non-transformed yeast (InVSc1) only showed a non-specific band at ~29kD that was observed in all lanes. Lysates expressing FLNSP4 demonstrated NSP4-specific bands at ~ 28, 24, and 20kD, and FLNSP4Hydromut showed bands at ~ 28, 24kD. All of the co-transformed yeast demonstrated a NSP4-fusion protein band at ~ 34.4kD (A and C). B. The same lysates showed faint contaminating bands above and below the 34.9kDspecific caveolin-1- fusion protein bands. (B and D).

The Hydrophobic Face of the AAH of NSP4 Binds Caveolin-1

We previously have shown a protein-protein interaction between NSP4 residues 114-135 and caveolin-1 by yeast two-hybrid, in peptide binding, and coimmunoprecipitation assays (Parr et al., 2006). In this study, we observed a stronger interaction with NSP4$_{46\text{-}175}$ than with full-length protein; therefore, we performed the

two hybrid assays with the N-terminal deleted NSP4. NSP4 residues 95-137 form an amphipathic alpha helix (Bowman et al., 2000; Taylor et al., 1996), in which the putative NSP4-caveolin-1 binding site occurs. To identify the precise aa in $NSP4_{114-135}$ (Figure 2.3A) involved in binding caveolin-1, the AAH was disrupted by mutating the hydrophobic face ($NSP4_{HydroMut}$) or charged face ($NSP4_{Ala}$) as depicted in the helical wheel diagram (Figure 2.3B and C). These mutants were then introduced into the ProQuest™ Yeast Two-Hybrid System (Invitrogen). The $pD22NSP4_{46-175Ala}$ and $pD22NSP4_{46-175HydroMut}$, plasmids were co-transformed along with pD32caveolin-1 ($CSM^{-}Leu^{-}Trp$) (Table 2.1). Three independent co-transformations demonstrated transformation efficiencies of ~ 2-5 x 10^6 transformants/μg plasmid DNA (data not shown), within the range of the standard efficiencies (greater than 1 x 10^6 transformants/μg plasmid DNA) (Geitz and Woods, 2002). Similar results were obtained when the experiments were repeated in reverse using $pD32NSP4_{46-175Ala}$ and $pD32NSP4_{46-175HydroMut}$ along with pD22caveolin-1 (data not shown).

The growth patterns of the co-transformed yeast were monitored to detect the activation of transcription from three chromosomally integrated reporter genes *Ura3, His3,* and *lacZ.* Four growth phenotypes, $His^{+}(3AT^{R})$, Ura^{+}, $5FOA^{S}$ and $\beta\text{-}gal^{+}$, were used to assess transcription activation of histidine, uracil and β-galactosidase, respectively. Control yeast, supplied with the ProQuest™ ™ Two-Hybrid System, and only yeast co-transformed with pDest32 and pDest22 plasmids grew on $CSM^{-}Leu^{-}Trp$ medium.

Table 2.1. Analysis of Y2H assay of pD32-NSP4 mutants plus pD22-caveolin-1[a]

CSM Leu⁻Trp⁻	CSM Leu⁻Trp⁻His⁻ + 3AT			CSM Leu⁻ Trp⁻Ura⁻	CSM Leu⁻Trp⁻ + 0.2% 5FOA	β-gal Units[b]	Phenotypes[c]
	12.5mM	50mM	100mM				
2+ Control	+	-	-	+	-	37	Positive
1+ Control	+	+/-	-	+/-	+/-	0.334	Positive
Negative Control	+	+/-	-	-	+	0.134	Negative
NSP4 46-175	+	-	-	-	+/-	1.39	Positive
NSP4 46-175Ala	+/-	-	-	-	+/-	1.822	Positive
NSP4 46-175HydroMut	+	-	-	+/-	+	0.105	Negative
NSP4 46-175Rev1	+	-	-	-	+/-	3.941	Positive
NSP4 46-175Rev2	+	+/-	-	-	+/-	3.042	Positive
NSP4 46-175Rev3	+	+/-	-	+/-	-	3.195	Positive
NSP4 46-175Rev2M116, 124, 127A	+	+/-	-	+/-	+/-	0.056	Negative
NSP4 46-175Rev2M116A	+	-	-	-	+/-	0.165	Negative
NSP4 46-175Rev1, 2M127A	+	+/-	-	-	+/-	2.581	Positive
NSP4 46-175Rev1M124, 127A	+	-	-	-	+/-	4.044	Positive

[a] Colonies were grown on CSM Leu⁻Trp⁻ and replica plated on CSM Leu⁻Trp⁻His⁻ with 12.5, 50, or 100mM 3AT; CSM Leu⁻Trp⁻Ura⁻, and CSM Leu⁻Trp⁻ with 0.2% %FOA.

[b] Expression of β-galactosidase was qualitatively monitored by using X-gal (not shown) and β-galactosidase activity was quantitatively measured with CPRG assays. The β-gal units (BGU) were calculated using the following formula: β-gal units = 1,000 x OD_{574}/(t x V x OD_{600})
where:
t = elapsed time (in minutes) of incubation
V = volume of culture used in the assay (ml)
OD_{570} = absorbance by chloramphenicol red and light scattering by cell debris
OD_{600} = cell density at the start of the assay

[c] The phenotype was determined by combining the results from growth on the different media and β-galactosidase assays.

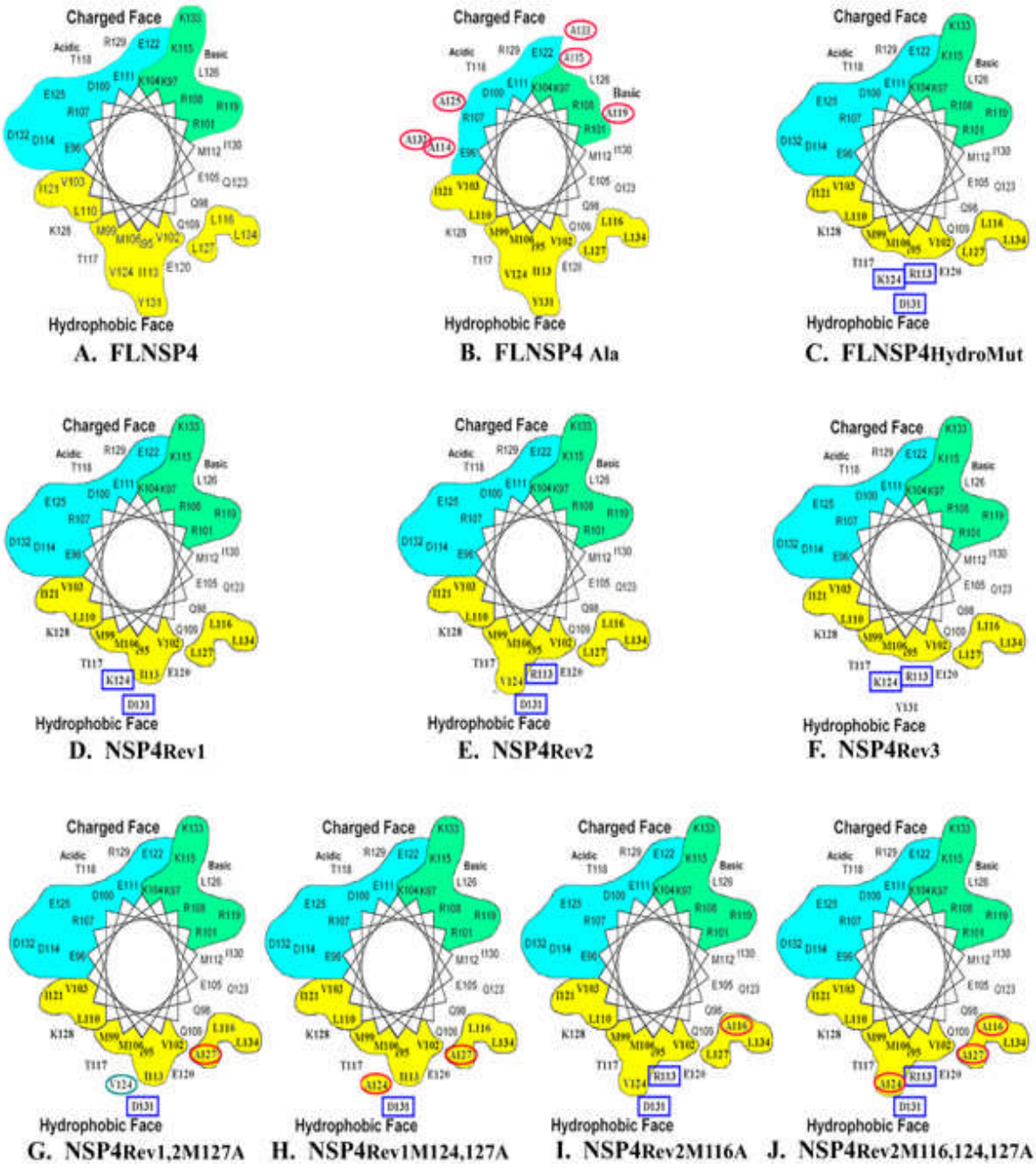

Figure 2.3. Helical wheel of the NSP4 Ampath α helix in the NSP4 mutants. Helical wheel schematics of NSP4 residues 95-135 (A. upper left), $NSP4_{ala}$ (B. upper middle), $NSP4_{HydroMut}$ (C. upper right), the three revertant (D-F, Rev1, 2, 3, middle panel) and the four other mutants (G-J, $NSP4_{Rev2M116,124,127A}$, $NSP4_{Rev2M116A}$, $NSP4_{Rev1,2M127A}$, $NSP4_{Rev1M124,127A}$). Note that the NSP4 sequence contains clearly delineated hydrophobic (yellow) and charged faces. The charged face contains both acidic (blue) and basic (green) domains. The disruption of the hydrophobic face is shown in the $NSP4_{HydroMut}$ and alterations of this face are seen the seven mutants.

The *HIS3* gene was induced as shown with a dose-dependent growth with increasing levels of 3AT (CSM Leu$^-$Trp$^-$His$^-$ + 3AT) (Table 2.1). All test and control yeast grew with 12.5mM 3AT, but growth on media with 50 and 100mM 3AT demonstrated little to no growth. The negative and 1+ positive control yeasts had a reduced amount of growth at 50mM 3AT, but the 2+ positive control showed no growth. All three clones, $NSP4_{46\text{-}175}$, $NSP4_{46\text{-}175Ala}$, and $NSP4_{46\text{-}175HydroMut,}$ failed to grow at 50 or 100mM 3AT (Table 2.1).

The *URA3* gene was induced as shown with growth on CSM$^-$Leu$^-$Trp$^-$Ura plates and with the inhibition of growth on CSM$^-$Leu$^-$Trp + 0.2% 5FOA. The *URA3* promoter, *SPO13,* previously has been shown to be a weak promoter, producing a very small amount of yeast growth. Likewise, our data agree with this report as we saw only a small amount of yeast growth. Growth on the CSM$^-$Leu$^-$Trp$^-$Ura plates demonstrated moderate and small growth patterns for the 2+ and 1+ positive controls respectively, while $NSP4_{46\text{-}175}$ and $NSP4_{46\text{-}175Ala}$ showed no growth. $NSP4_{HydroMut}$ showed a very small amount of growth on the CSM$^-$Leu$^-$Trp$^-$Ura plates. Inhibition of growth on CSM$^-$Leu$^-$Trp + 0.2% 5FOA was seen with the 2+ positive control, while both the negative control and $NSP4_{HydroMut}$ grew well. All the other test colonies, 1+ positive control, $NSP4_{46\text{-}175}$ and $NSP4_{46\text{-}175Ala}$ had a very small amount of growth on CSM Leu$^-$Trp$^-$ + 0.2% 5FOA.

The induction of *lacZ* gene was indicated with the production of β-galactosidase (β-gal) as indicated by the development of a blue color upon addition of substrate X-gal to yeast grown on nitrocellulose membranes (data not shown). All colonies that were positive for β-gal with the addition of X-gal or demonstrated phenotypes interpreted as

possible weak interactors using criteria outlined in the Y2H manual were confirmed using the quantitative chorophenol red-β-D-galactopyranoside (CPRG) assay for β-gal activity (Table 2.1). The positive controls (2+ and 1+) had 37 and 0.334 β-galactosidase units (BGU), respectively. The negative control and $NSP4_{46\text{-}175HydroMut}$ had 0.134 and 0.105 BGU, respectively, while $NSP4_{46\text{-}175}$ and $NSP4_{46\text{-}175Ala}$ had 1.39, 1.822 BGU, respectively.

FLNSP4 and FLNSP4$_{Ala}$ Associate With Caveolin-1 in an In Vitro Peptide Binding Assay

To confirm the yeast two-hybrid results, synthesized caveolin-1 peptides were bound to sepharose beads and utilized to capture full-length (FL) proteins, i.e., FLNSP4, $FLNSP4_{Ala}$, or $FLNSP4_{HydroMut}$ from yeast lysates expressing the respective proteins (Figure 2.4). Western blot analyses of cell lysates demonstrated no NSP4-specific bands with sepharose beads only (lanes 1, 2, 3, 4). NSP4-specific bands were observed at ~ 28, 24 and 20kD from FLNSP4 lysates with $Cav_{2\text{-}31}$ (lane 5), whereas $FLNSP4_{Ala}$ demonstrated only 24 and 20kD bands (lane 6). Likewise a 24kD NSP4-specific band was shown with both FLNSP4 and $FLNSP4_{Ala}$ with $Cav_{161\text{-}178}$ (lanes 9 and 10). No bands were detected from $FLNSP4_{HydroMut}$ lysates with either $Cav_{2\text{-}31}$ or $Cav_{161\text{-}178}$ (lane 7 and 11). Yeast lysates without NSP4 plasmids showed no specific binding to either $Cav_{2\text{-}31}$ or $Cav_{161\text{-}178}$ (lane 8 and 12).

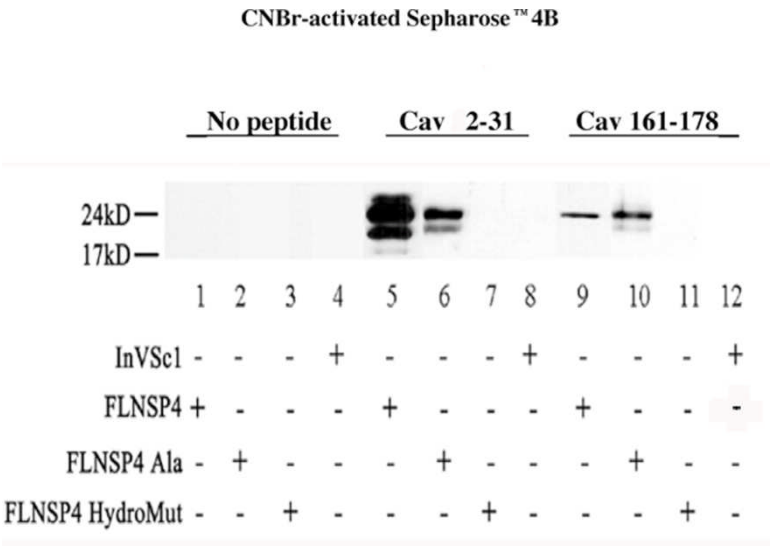

Figure 2.4. Caveolin-1 peptide binding assays with FLNSP4, FLNSP4$_{Ala}$, and FLNSP4$_{HydroMut}$. Western blot analysis of yeast lysates containing expressed full-length- NSP4, -NSP4$_{Ala}$ and -NSP4$_{HydroMut}$ (FLNSP4, FLNSP4$_{Ala}$, and FLNSP4$_{HydroMut}$) and incubated with CNBr-activated sepharose 4B beads with either N-terminal (Cav$_{2-31}$), C-terminal (Cav$_{161-178}$), or no peptide. The beads were washed and bound proteins were separated by SDS-PAGE, transferred to nitrocellulose membranes for Western blot analysis, and probed using rabbit anti-NSP4$_{150-175}$. Control lanes (1-4) show the absence of non-specific binding to the sepharose beads with all lysates tested. Lanes 5-7 show the reactivity of FLNSP4 and FLNSP4 mutants to Cav$_{2-31}$. Only the FLNSP4$_{HydroMut}$ failed to bind the N-terminal caveolin-1 peptide. The same binding pattern was observed when FLNSP4 and FLNSP4 mutant proteins where incubated with Cav$_{161-178}$ (lanes 9, 10, and 11). InVSc1 alone showed no NSP4-specific bands using either peptide (lanes 8 and 12).

NSP4 Revertants Bind to Caveolin-1 by Yeast Two-Hybrid Analyses

Since our previous data demonstrate stronger binding of NSP4 to caveolin-1 in yeast two-hybrid assays when two N-terminal hydrophobic domains are deleted (Parr et al., 2006), we PCR amplified the 46-175 portion of the full length mutants and cloned the respective deletion mutants into the entry plasmids. To map the binding of NSP4 to caveolin-1 to a single amino acid, each of the three mutated hydrophobic amino acids of NSP4$_{46-175HydroMut}$ were separately reverted to produce three additional clones, NSP4$_{Rev\ 1}$, NSP4$_{Rev2}$, and NSP4$_{Rev3}$ (Table 2.1, Figures 2.3D, E, and F). The NSP4$_{46-175Ala}$ and

$NSP4_{46\text{-}175HydroMut}$ and the three revertant clones were transformed into yeast with caveolin-1. The $NSP4_{46\text{-}175}$ $NSP4_{46\text{-}175HydroMut}$, $NSP4_{Rev1}$, $NSP4_{Rev2}$, $NSP4_{Rev3}$ clones grew on $CSM^{-}Leu^{-}Trp$, $CSM^{-}Leu^{-}Trp^{-}His$ + 12.5mM 3AT, while $NSP4_{46\text{-}175Ala}$ showed a reduced amount of growth. Only $NSP4_{Rev2}$ and $NSP4_{Rev3}$ demonstrated a reduced amount of growth on $CSM^{-}Leu^{-}Trp^{-}His$ + 50mM 3AT while $NSP4_{46\text{-}175}$, $NSP4_{46\text{-}175Ala}$, $NSP4_{46\text{-}175HydroMut}$ and $NSP4_{Rev1}$ demonstrated no growth on $CSM^{-}Leu^{-}Trp^{-}His$ + 50mM 3AT. None of the five clones grew on $CSM^{-}Leu^{-}Trp^{-}His$ +100mM 3AT (Table 2.1).

No growth was observed on the $CSM^{-}Leu^{-}Trp^{-}Ura$ plates with $NSP4_{46\text{-}175}$, $NSP4_{46\text{-}175Ala}$, $NSP4_{46\text{-}175HydroMut}$, $NSP4_{Rev1}$, $NSP4_{Rev2}$, or the negative control, whereas $NSP4_{Rev3}$ demonstrated a very small amount of growth. Inhibition of growth on $CSM^{-}Leu^{-}Trp$ + 0.2% 5FOA was observed with $NSP4_{Rev3}$, but $NSP4_{46\text{-}175}$, $NSP4_{46\text{-}175Ala}$, $NSP4_{Rev1}$ and $NSP4_{Rev2}$ had a very small amount of growth. The negative control and $NSP4_{46\text{-}175HydroMut}$ grew well.

β-galactosidase activity was measured both qualitatively and quantitatively with X-gal and CPRG assays, respectively. $NSP4_{46\text{-}175}$ and $NSP4_{46\text{-}175Ala}$ and the three revertant clones were positive in the X-gal assay, only $NSP4_{46\text{-}175HydroMut}$ was negative indicating no β-gal activity. The quantitative β-gal $NSP4_{46\text{-}175HydroMut}$ was measured as 0.105 BGU, less than that of the negative control (0.134 BGU) whereas the $NSP4_{46\text{-}175}$, $NSP4_{46\text{-}175Ala}$ β-gal activity was 4-5 times that of the positive control at 1.39 and 1.822 BGU. The quantitative β-galactosidase activity of revertants measured significantly greater than the positive control (Table 2.1). $NSP4_{Rev1}$, $NSP4_{Rev2}$, $NSP4_{Rev3}$ produced 3.941, 3.042, and 3.195 BGU, respectively, which are approximately 20-30 times that of

the negative control (0.134 BGU) and 10 times of that the 1+ positive control (0.334BGU).

Binding of NSP4 Alanine Mutants NSP4 to Caveolin-1

Four additional mutants, $NSP4_{Rev2M116, 124, 127A}$, $NSP4_{Rev2M116A}$, $NSP4_{Rev1, 2M127A}$, and $NSP4_{Rev1M124, 127A}$ (Figure 2.3G-J), were made to further delineate the amino acid sequence necessary for caveolin-1 binding. The four clones were transformed into InVSc1 with caveolin-1 and grown on CSM$^-$Leu$^-$Trp, CSM$^-$Leu$^-$Trp$^-$His + 12.5mM 3AT, however $NSP4_{Rev2M116, 124, 127A}$ and $NSP4_{Rev1, 2M127A}$, demonstrated a reduced amount of growth on CSM$^-$Leu$^-$Trp$^-$His + 50 mM 3AT while $NSP4_{Rev2M116A}$ and $NSP4_{Rev1M124, 127A}$ demonstrated no growth. None of the clones grew on CSM$^-$Leu$^-$Trp$^-$His +100mM 3AT (Table 2.1).

No growth was observed on the CSM$^-$Leu$^-$Trp$^-$Ura plates with $NSP4_{Rev2M116A}$, $NSP4_{Rev1, 2M127A}$, and $NSP4_{Rev1M124, 127A}$, while the $NSP4_{Rev2M116, 124, 127A}$ demonstrated a very small amount of growth. All four of the clone exhibited a small amount of growth on CSM Leu$^-$Trp$^-$ + 0.2% 5FOA.

β-galactosidase activity was measured both qualitatively and quantitatively with X-gal and CPRG assays, respectively. The four clones were qualitatively positive when treated with the X-gal substrate. The $NSP4_{Rev2M116, 124, 127A}$ and $NSP4_{Rev2M116A}$ had β-gal activity of 0.056 and 0.165 BGU, the former being less than half of that of the negative control and the latter only slightly greater than the negative control. $NSP4_{Rev1, 2M127A}$ and $NSP4_{Rev1M124, 127A}$ demonstrated quantitative amounts of β-gal activity greater than the positive control, 2.581 and 4.044 BGU respectively (Table 2.1). Similar to the

revertants, these β-gal activities are approximately 20-30 times that of the negative control (0.134 BGU) and 10 times of that the 1+ positive control (0.334BGU).

$NSP4_{Rev1}$, $NSP4_{Rev2}$, $NSP4_{Rev3}$, $NSP4_{Rev1,2\ M127A}$, and $NSP4_{Rev1,2\ M124,\ 127A}$ Associate With N-terminal and C-terminal Caveolin-1 Peptides In Vitro, While $NSP4_{46\text{-}175HydroMut}$, $NSP4_{Rev2\ M\ 116A,\ 124A,\ 127A}$ and $NSP4_{Rev2\ M116A}$ Do Not

To confirm the data of the yeast two-hybrid assay, caveolin-1 peptides ($Cav_{2\text{-}31}$, $Cav_{19\text{-}40}$, $Cav_{76\text{-}101}$, and $Cav_{161\text{-}178}$) were bound to sepharose beads and tested for binding to the NSP4 mutants. No bands were observed from yeast lysates that did not express NSP4 mutant proteins (InVSc1) (Figure 2.5A, lanes 8 and 12; Figure 2.5B, lane 7; and Figure 2.4C, lane 7). Western blot analyses of mutant-derived proteins that were incubated with sepharose beads only demonstrated no bands (Figure 2.5A, lanes 2-4; Figure 2.5B, lanes 2-7). No NSP4-specific bands were present when the lysates from $NSP4_{46\text{-}175}$, $NSP4_{46\text{-}175Ala}$, $NSP4_{Rev1}$, $NSP4_{Rev2}$, and $NSP4_{Rev3}$ were incubated with CSD $Cav_{76\text{-}101}$ peptide (data not shown). Similarly, no bands were evident in Western blot analyses of cell lysates from $NSP4_{Rev1}$, $NSP4_{Rev2\ M\ 116A,\ 124A,\ 127A}$, $NSP4_{Rev2\ M116A}$, $NSP4_{Rev1,2\ M127A}$, $NSP4_{Rev1,2\ M124,\ 127A}$ and $NSP4_{46\text{-}175HydroMut}$ that were incubated with Sepharose beads with bound CSD $Cav_{76\text{-}101}$ peptide (Figure 2.5B, lanes 8-13). Additionally, no NSP4 specific bands were detected by Western blot analysis of cell lysates derived from the $NSP4_{Rev2\ M\ 116A,\ 124A,\ 127A}$, $NSP4_{Rev2\ M116A}$ and $NSP4_{46\text{-}175HydroMut}$ incubated with $Cav_{19\text{-}40}$ and $Cav_{161\text{-}178}$ (Figure 2.5C, lanes 2, 3, 6; lanes 9, 10, 13).

A.

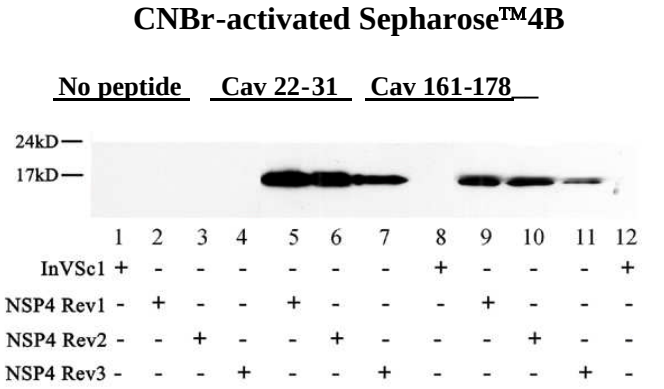

B.

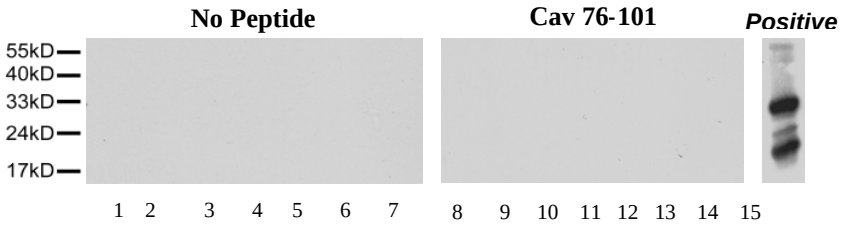

	1	2	3	4	5	6	7	8	9	10	11	12	13	14	15
InVSc1	-	-	-	-	-	-	+	-	-	-	-	-	-	+	-
Rev2	+	-	-	-	-	-	-	+	-	-	-	-	-	-	-
Rev2M116, 124, 127A	-	+	-	-	-	-	-	-	+	-	-	-	-	-	-
Rev2M116A	-	-	+	-	-	-	-	-	-	+	-	-	-	-	-
Rev1, 2M127A	-	-	-	+	-	-	-	-	-	-	+	-	-	-	-
Rev1,2M124, 127A	-	-	-	-	+	-	-	-	-	-	-	+	-	-	-
NSP4$_{46\text{-}175Hydo}$	-	-	-	-	-	+	-	-	-	-	-	-	+	-	-
RV Positive Control	-	-	-	-	-	-	-	-	-	-	-	-	-	-	+

Figure 2.5. Caveolin-1 peptide binding assays of NSP4 mutants. A. Western blot analyses of yeast lysates expressing NSP4$_{Rev1}$, NSP4$_{Rev2}$, and Rev3 and incubated with CNBr-activated sepharose 4B beads with Cav$_{2\text{-}22}$, Cav$_{161\text{-}178}$ or no peptide. The beads were washed, separated by SDS-PAGE, and the peptide-bound proteins were detected by Western blot using rabbit anti-NSP4$_{150\text{-}175}$. InVSc1 alone showed no NSP4-specific bands using either peptide (lanes 1and 8). Control lanes (1-4) show the absence of non-specific binding to the sepharose beads with revertant yeast cell lysates. Lanes 5, 6, and 7 indicate that all three revertant NSP4 proteins bound to the N-terminal peptide, Cav$_{2\text{-}32}$. The same binding pattern was observed with the C-terminal peptide, Cav$_{161\text{-}178}$ (lanes 9, 10, and 11). B. Western blot analysis of yeast lysates containing expressed NSP4$_{Rev2}$, NSP4$_{Rev2\ M\ 116A,\ 124A,\ 127A}$, NSP4$_{Rev2\ M116A}$, NSP4 $_{Rev1,2\ M127A}$,NSP4 $_{Rev1,2\ M124,\ 127A}$ and NSP4$_{46\text{-}175HydroMut}$ and incubated with CNBr-activated sepharose 4B beads with either no peptide or CSD peptide (Cav$_{76\text{-}101}$). The beads were washed and bound proteins were separated by SDS-PAGE, transferred to nitrocellulose membranes for Western blot analysis, and probed using rabbit anti-NSP4$_{150\text{-}175}$. InVSc1 alone showed no NSP4-specific bands using either the beads or the peptide (lane 7). Control lanes (1-6) show the absence of non-specific binding to the sepharose beads with all yeast cell lysates tested. Similarly, lanes 8-13 show no binding between Cav$_{76\text{-}101}$ and any of the yeast cell lysates tested.

C.

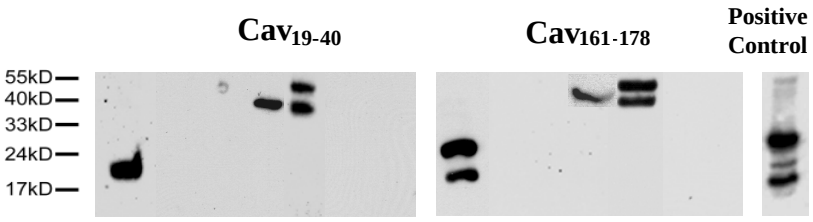

InVSc1	-	-	-	-	-	-	+	-	-	-	-	-	-	+	-
Rev2	+	-	-	-	-	-	-	+	-	-	-	-	-	-	-
Rev2M116, 124, 127A	-	+	-	-	-	-	-	-	+	-	-	-	-	-	-
Rev2M116A	-	-	+	-	-	-	-	-	-	+	-	-	-	-	-
Rev1, 2M127A	-	-	-	+	-	-	-	-	-	-	+	-	-	-	-
Rev1,2M124, 127A	-	-	-	-	+	-	-	-	-	-	-	+	-	-	-
NSP4 46-175Hydo	-	-	-	-	-	+	-	-	-	-	-	-	+	-	-
RV Positive Control	-	-	-	-	-	-	-	-	-	-	-	-	-	-	+

Figure 2.5. Caveolin-1 peptide binding assays of NSP4 mutants, continued. C. Western blot analysis of yeast lysates containing expressed $NSP4_{Rev2}$, $NSP4_{Rev2\ M\ 116A,\ 124A,\ 127A}$, $NSP4_{Rev2\ M116A}$, $NSP4_{Rev1,2\ M127A}$, $NSP4_{Rev1,2\ M124,\ 127A}$ and $NSP4_{46\text{-}175HydroMut}$ and incubated with CNBr-activated sepharose 4B beads with either N-terminal ($Cav_{19\text{-}40}$) or C-terminal ($Cav_{161\text{-}178}$). InVSc1 alone did not bind the N-terminal peptide, $Cav_{19\text{-}40}$ peptide. Lanes 1, 4, and 5 indicate that $NSP4_{Rev2}$, $NSP4_{Rev1,2\ M127A}$, $NSP4_{Rev1,2\ M124,\ 127A}$ bound to the N-terminal, $Cav_{19\text{-}40}$. The same binding pattern was observed with the C-terminal peptide, $Cav_{161\text{-}178}$ (lanes 8, 11, and 12). $NSP4_{46\text{-}175HydroMut}$, $NSP4_{Rev2\ M\ 116A,\ 124A,\ 127A}$, nor $NSP4_{Rev2\ M116A}$ bound either the N-terminal (lanes 2, 3, 6) or the C-terminal (lanes 9, 10, and 13) caveilin-1 peptides. RV-infected cell lysates were used a positive control.

Only in the Western blot analyses of $NSP4_{Rev1}$, $NSP4_{Rev2}$, $NSP4_{Rev3}$, $NSP4_{Rev1,2\ M127A}$, and $NSP4_{Rev1,2\ M124,\ 127A}$ were NSP4-specific bands was observed. The NSP4 specific band of ~17kD was observed in the three revertants with both $Cav_{2\text{-}31}$ and $Cav_{161\text{-}178}$ (Figure 2.5A lanes 5, 6, 7 and 9, 10, 11, respectively). Cell lysates derived from mutants $NSP4_{Rev1,2\ M127A}$, and $NSP4_{Rev1,2\ M124,\ 127A}$ that were incubated with $Cav_{19\text{-}40}$ and $Cav_{161\text{-}178}$ demonstrated typical NSP4 bands (Figure 2.5C, lanes 4 and 5; lanes 11, 12). When bound to $Cav_{19\text{-}40}$ both mutants exhibited a multimer ~40kD, however $NSP4_{Rev1,2\ M124,\ 127A}$ also exhibited multimers of 48kD.

FLNSP4$_{HydroMut}$ Is Glycosylated When Expressed in Yeast

To determine if the multiple NSP4-specific bands from FLNSP4$_{HydroMut}$ represented the same glycosylation pattern as that observed in RV-infected mammalian cells (Parr et al., 2006) and to ensure the lack of binding to the Cav$_{2-31}$, Cav$_{19-40}$, and Cav$_{161-178}$ was not due to an altered glycosylation pattern, yeast lysates were digested with Endo H and evaluated by Western blot analysis (Figure 2.6). The mock treated FLNSP4$_{HydroMut}$ (lane 1) demonstrated proteins ~28, 24, 20 and 17 kD, and with the addition of EndoH decreased to mostly 20kD with the same amount of a 17kD protein (lane 2). The RV-infected MDCK cell lysates showed a possible dimer ~56kD, and a monomer ~28kD that were both decreased to ~40kD and 20kD respectively with the addition of EndoH (lanes 3 and 4). These data verify that the glycosylation in the yeast was equivalent to that observed in mammalian cells and not responsible for the lack of binding.

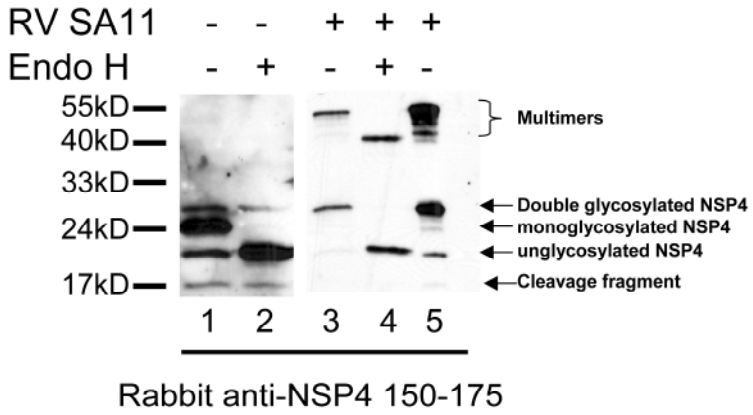

Figure 2.6. FLNSP4$_{HydroMut}$ is glycosylated when expressed in yeast. To discern if the 28 and 24kD bands correspond to the singly- and doubly-glycosylated forms seen in mammalian cells, yeast expressing FLNSP4$_{HydroMut}$ and RV-infected MDCK lysates were Endo H digested and compared by Western blot analyses using rabbit anti-NSP4$_{150-175}$. Lanes 1 and 3 correspond to the mock digested lysates, whereas lanes 2 and 4 represent the Endo H digested yeast and MDCK cell lysates, respectively. Lane 5 diaplays the glycosylation of NSP4.

Modification of the Hydrophobic Face of the NSP4 AAH Does Not Necessarily Abrogate Binding to Caveolin-1

Binding of caveolin-1 to the NSP4 enterotoxic domain is through the hydrophobic face of the AAH. Our study demonstrates NSP4 is able to bind caveolin-1 even when some of the hydrophobic residues are mutated. By using the remaining hydrophobic residues putative hydrophobic binding faces are able to form. Table 2.2 shows the mutation in the hydrophobic aa residues in the hydrophobic face and the hydrophobic aa residues available to form potential putative hydrophobic binding faces. Two hydrophobic planes can be defined using multiples of 3.5 turns on the AAH that bring individual hydrophobic/aromatic aa into alignment and include (a) Plane A I113-V124-Y131D and (b) Plane B L116-L127-L134 (Table 2.2).

Five possible hydrophobic binding faces have been identified from the hydrophobic planes NSP4 mutants: (a) Rev1: Plane A--I113 and Plane B--L116, L127, L134; (b) Rev 2: Plane A--V124 and Plane B--L116, L127, L134; (c) Rev 3: Plane A--Y131 and Plane B--L116, L127, L134; (d) Rev1, 2 M127A: Plane A--I113, V124 and Plane B--L116, L134; and (e) Rev1 M124, 127 A: Plane A--I113 and Plane B--L116, L134.

Table 2.2 Hydrophobic plane mutations and intact hydrophobic aa residue available to form a modified hydrophobic face that binds caveolin-1

Mutant	Binding	Hydrophobic Planes Mutations A (left) I113 V124 Y131		B (right) L116 L127 L134		Hydrophobic/Aromatic aa Available for Binding Each Plane	
		Charged aa	Alanine	Charged aa	Alanine	A	B
Rev 1	Positive	2[1] V124K Y131D	--	--	-- --	1[3] I113	3[4] I116 L127 L134
Rev 2	Positive	2 I113R Y131D	--	--	--	1 V124	3 I116 L127 L134
Rev 3	Positive	2 1113K V124K	--	--	--	1 1131	3 I116 LI27 L 134
Rev 1, 2 M127A	Positive	1 Y131D	--	--	1 127A	2 L113 V124	2 1116 L134
Rev 1 M124, 127A	Positive	1 Y131D	1[2] L124A	--	1 1127A	1 I113	2 1116 1.134
Rev 2 M116A	Negative	2 I113R Y131D	--	--	1 L116A	1 V124	2 LI27 L134
Rev 2 M116, 124, 127A	Negative	2 I113R Y131D	1 V124A	--	2 L116A L127A	0	1 L134
HydroMut	Negative	3 I116R V124K Y131D	--	--	--	0	3 1116 L127 L134

[1] Orange indicates charged aa (R, K, or D.)
[2] Green indicates alanine.
[3] Blue denotes the hydrophobic plane on the left side of the 3-D image of the AAH of NSP4.
[4] Red denotes the hydrophobic plane on the right side of the 4-D image of the AAH of NSP4.

Discussion

We have previously shown the enterotoxic domain of NSP4, residues 114-135, binds to caveolin-1, the defining structural protein of caveolae (Thomas and Smart,

2008; Parr et al., 2006; Spisni et al., 2005). To dissect the precise NSP4 binding domain, six charged amino acids (aas) in the polar face of the AAH of FLNSP4 (Figure 2.7A) were changed to alanine by site-directed mutagenesis ($FLNSP4_{Ala}$, Figure 2.7B). Three specific hydrophobic residues within the hydrophobic face of FLNSP4 were replaced with charged aas in the AAH ($FLNSP4_{HydroMut}$, Figure 2.7C). $FLNSP4_{Ala}$ bound caveolin-1 in the Y2H, CPRG and peptide binding assays equivalent to wild type, but disruption of hydrophobic in $FLNSP4_{HydroMut}$ abrogated the binding to caveolin-1. These data strongly suggest the protein-protein interaction between NSP4 and caveolin-1 occurs through the hydrophobic face of the AAH.

In this study, we further mapped the hydrophobic residues of NSP4 responsible for caveolin-1 binding by reverting the individual charged residues of $NSP4_{HydroMut}$ (Figure 2.8A) back to the original hydrophobic aa. The three revertant mutants (Rev 1, 2, and 3; Figure 2.8B-D), regained caveolin-1 binding. Further analysis of the three revertants reveled residues that could form hydrophobic binding sites (Figure 2.3D-F and Figure 2.8B-D). The hydrophobic face of each revertant is disrupted by two charged aa residues not 3 as in $NSP4_{HydroMut}$.

The putative hydrophobic binding site for Rev1 contains aa residues I113, L116, L127, and L134. Whereas, caveolin-1 binding to Rev2 appears to depend on aa L116, V124, L127, and L134, while Rev 3 binding to caveolin-1 seems to be contingent on aa L116, L127, and Y131 or L134. All three revertants have three aas, L116, L127, and L134 in common in the theoretical binding sites (Figure 2.8B-D). Protein-protein interactions not only rely on the recognition of specific aa motifs, but also may depend

upon their exposure at the surface of the protein, the environment of the aa residues, or may bind conformationally-dependent epitopes (Couet et al., 1997a). For example, the putative hydrophobic face of L116, L127, and L134 is present in $NSP4_{HydroMut}$ (Figure 2.8A); however, it does not bind caveolin-1 either because of conformational constraints or possibility due to repulsion by charged aas. This specificity of conformation is demonstrated by transmembrane envelope glycoprotein of some HIV-1 viruses that interact with caveolin-1. For example, the highly conserved CBD1 but not CBD2 in the transmembrane envelope glycoprotein of some HIV-1 viruses can adopt a defined secondary structure and bind the CSD of caveolin-1 (Benferhat et al., 2008).

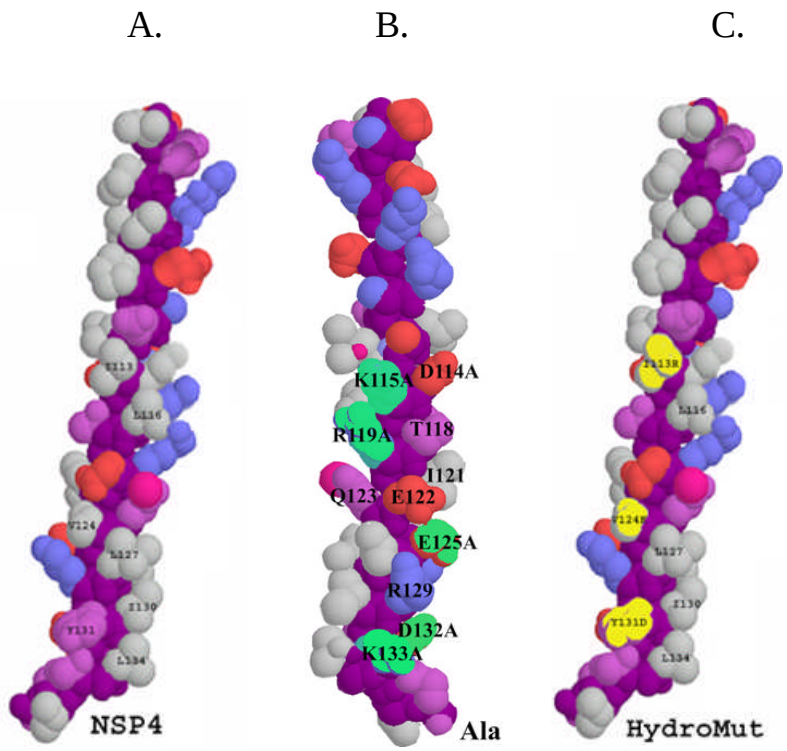

Figure 2.7. Three-dimensional of the NSP4 alanine and hydrophobic mutants of the AAH. A. NSP4, **B**. $NSP4_{Ala}$ generated by replacing charged aa with alanine: D114A, K115A, R119A, E125A, D132A, and K133A, and C. $NSP4_{HydroMut}$ was generated by site-directed mutagenesis to replace three specific hydrophobic residues with charged aas: I113R, V124K, and Y131D.

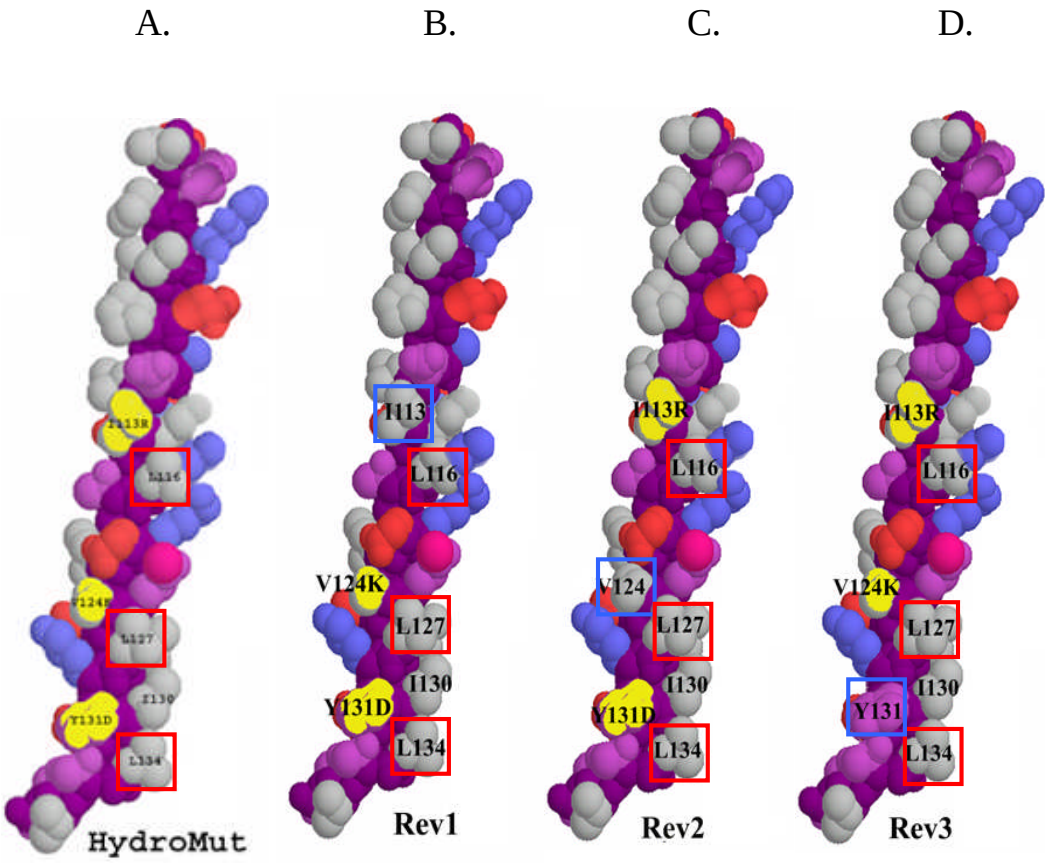

Figure 2.8. Three-dimensional of the NSP4 Rev 1, Rev, 2, and Rev 3. A: HydroMut. B. In Rev1 the I113R was reverted to I113. C: In Rev2 the V124K was reverted to V124. D: In Rev 3 the Y131D was reverted to Y131. In each case the Rev mutants contain one hydrophobic or aromatic aa in the left plane (blue boxes) and three hydrophobic aa in the right plane (red boxes).

A panel of four alanine NSP4 hydrophobic mutants was constructed to further localize the specific NSP4-caveolin-1 binding site. Alanine was used to minimize conformational and structural disruption of the hydrophobic face of the AAH allowing for the identification of specific aas that are required for binding caveolin-1. In Rev1, 2 M127A and Rev1 M124, 127A the hydrophobic face was altered by a charged residue and one or two alanine residues; however, binding to caveolin-1 is retained (Figure 2.9A and B). Both mutants bind caveolin-1 and 3D analyses demonstrate a potential hydrophobic binding site that includes aa residues I113, L116, and L134 (Figure 2.9C and D) that is present in Rev1 as describe above.

Rev2 M116, 124, 127A (Figure 2.9D) does not bind caveolin-1, indicating that there are insufficient hydrophobic residues to form a hydrophobic face. Likewise, Rev2M116A (Figure 2.9C), does not bind caveolin-1. The only difference between this mutant and Rev2, which does bind caveolin-1, is the replacement of L116 by an alanine residue. Additionally, neither of these two non-binding mutants appear to retain one of the above described putative hydrophobic faces present in the Rev mutants. These data strongly suggest that L116 is pivotal to binding NSP4 to caveolin-1.

Additionally, peptides to both the N- and C-terminus of caveolin-1, residues 2-31 or 19-40 and 161-178, respectively, bind NSP4, $NSP4_{Ala}$, the three revertant clones, $NSP4_{Rev1,2M127}$, $NSP4_{Rev1M124,\ 127A}$, but not $NSP4_{HydroMut}$, $NSP4_{Rev2M116,\ 124,\ 127A}$, or $NSP4_{Rev2M116A}$ supporting the yeast two-hybrid results. There was no binding between any of the tested wild type and mutant NSP4 proteins and the caveolin-1 peptide residues 76-101. These results complement the results shown by Mir et al. (2007), which

mapped the NSP4 binding site to both the N- and C-terminus of caveolin-1. Taken together, these data strongly suggest that NSP4 binds the N- and C-termini of caveolin-1via the hydrophobic face, and that conformation and structure of both molecules are important for binding.

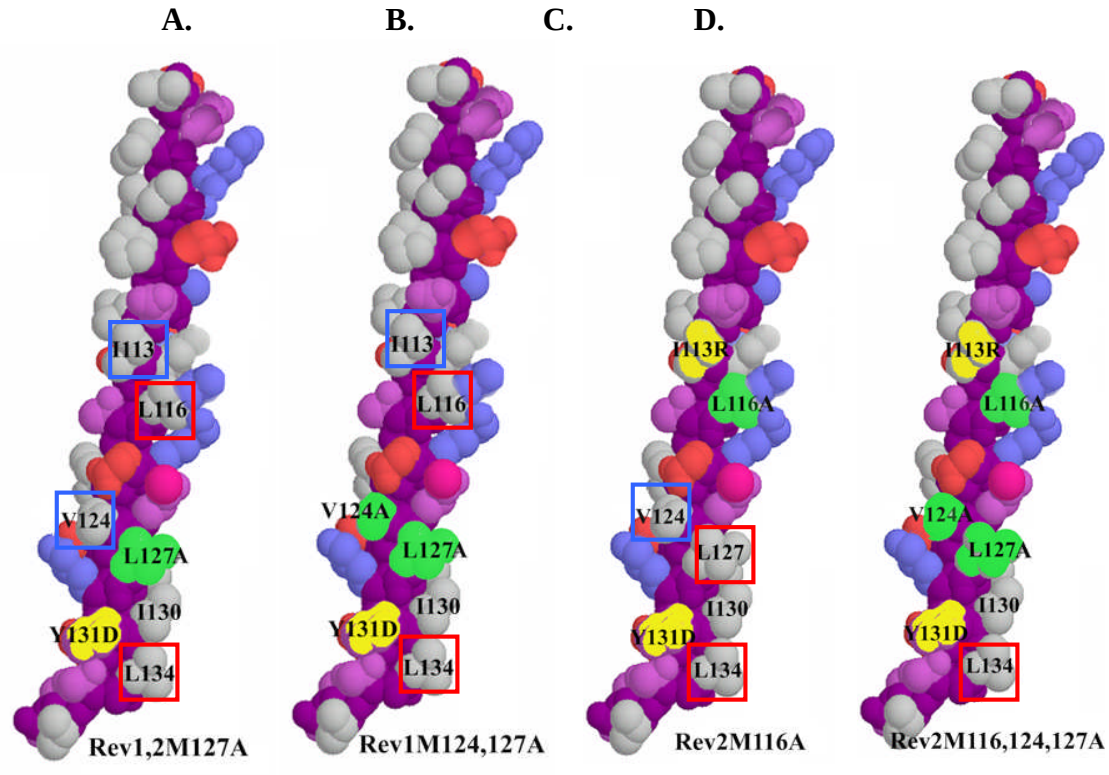

Figure 2.9. Three-dimensional of the NSP4 alanine mutants. A: In Rev1, 2 M127A, I113R was reverted to I113, V124D was reverted to V124, and L127 was replaced with alanine. B: In Rev1 M124, 127 A, I113R was reverted to I113, V124K and L127A were replaced with alanines. Both A and B bound caveolin-1. C: In Rev2 M116A, V124D was reverted to V124 and l116 was replaced with alanine. D. In Rev 2 M116, 127, 127A, V124D, L116, and L127 were replaced with alanines. Both C and D failed to bind caveolin-1. Blue boxes indicate hydrophobic aa in the left plane and red boxes indicate hydrophobic aa in the right plane.

These data indicated that the NSP4 binding face includes hydrophobic aa residues I113, L116, V124, L127, L134 and the possibly aromatic residue Y131 as shown in the helical wheel depiction (Figure 2.3A and 2.7A). The tyrosine residue at position 131 is located in the face as the assumed NSP4-caveolin-1 binding face and functions diarrhea induction. The tyrosine appears not to be required for caveolin-1 binding as both Rev 1 and Rev 2 bind caveolin-1 in the absence of Y131. Reverting the charged Y131D to Y131 in Rev 3 does reconstitute its caveolin-1 binding. It is possible that in the absence of the charged aa at the position 131, the mutant assumes a conformation more like wild type NSP4 making the hydrophobic aas more available to bind caveolin-1.

Peptide binding assays have indicated that the caveolin-1 binding domain in NSP4 is localized the aa residues 114-135 (Parr et al., 2006), that is I113 is not part of the binding domain. However, the binding domain defined by Y2H does include I113. It may be that I113 is recruited to reinforce and stabilize the binding between the mutants and caveolin-1.

From these data, we can identify a NSP4-caveolin-1 binding motif of $\theta_{113}L_{116}\theta_{124}\theta_{127}\phi_{131}\theta_{134}$ where $\theta$is hydrophobic, ϕ is aromatic, and L is leucine. The five potential hydrophobic binding configurations that are contained in this binding motif can be generated: (1) I113, L116, L127; (2) L116, V124, L127; (3) L116, L127, Y131; (4) I113, L116, V124; and (5) I113, L116, L134. Our data indicate L116 is critical for NSP4-caveolin-1 binding as it occurs in all hydrophobic faces; however, it is unclear if L134 is

required for binding. Rev 1, Rev 2, Rev 3, R1,2 M127A, and Rev1 M124, 127A bind caveolin-1 and contain both L116 and L134.

The specificity of NSP4-caveolin-1 interaction with short binding motifs is not unique. A 20-amino acid region of the cytosolic amino terminus of the caveolin-1 scaffolding domain (CSD) has been shown to mediate interactions with signaling molecules such as G-proteins, Src-like kinases, Ras, and others (Couet et al., 1997b; Dubroca et al., 2007; Li et al., 1995, 1996; Razani et al., 2001; Song et al., 1996; Stahlhut and van Deurs, 2000). Couet et al. (1997a) used random peptide ligands from phage display libraries to examine the nature of the interaction between G-proteins α subunits and $G_{i2\alpha}$, a known caveolin-1 interacting protein and caveolin-1. They showed that the interaction was strictly dependent a short peptide sequence ($\phi X\phi XXXX\phi$ or $\phi XXXX\phi XX\phi$, where ϕ is an aromatic residues W, F, or Y) containing aromatic residues as replacement of critical phenylalanine residues with glycine or alanine abrogated the interaction. A sequence of four aa residues (^{92}FTVT^{95}) within the CSD are strictly required for $G_{i2\alpha}$ binding to caveolin-1. Numerous other caveolae-associated proteins (intracellular signal transducers, e.g., Src-like kinases, eNOS, MAP kinase, growth factors, and others) contain cytoplasmically accessible sequences that are reminiscent of the $G_{i2\alpha}$ binding sequence (Lisanti et al., 1994; Sargiacomo et al., 1993; 1996; Smart et al., 1995). These data suggest that short aa sequences do facilitate protein-caveolin-1 binding. In fact, Song et al. (1996) found that a single amino acid change prevents the interaction between Ras and caveolin-1.

Viral proteins are known to mimic cellular functions to take over cellular processes. The possible use of caveolin-1 by RV NSP4 to traffic within the cell is not unique. The HIV-1 gp41 has been shown to contain a putative caveolin-1 binding motif (ϕXXXXϕXϕ) that is like that of $G_{i2\alpha}$ (Huang et al., 2007) and may be involved endocytosis of this virus. Additionally, caveolin-1 has been shown to function in locating the matrix protein (MA) of Gag precursor of murine leukemia virus to the PM via a caveolin-1 binding domain (CBD) within the N-terminus of the MA. This CBD is highly conserved among other γ-retroviruses suggesting that this class of viruses may use the MA-caveolin-1 interaction to traffic to the PM similar to that of the RV NSP4-caveolin-1 interaction (Yu et al., 2006).

Our data show that three hydrophobic aa are needed for NSP4 to bind to caveolin-1 and at least one hydrophobic mutant must reside in Plane A and at least two must reside in Plane B one of which must be L116 (Table 2.3). For example, Rev 1M 124, 127A demonstrates this minimum binding requirement. Rev 1, Rev 2, Rev 3, and Rev 1,2 M127A exceed the minimum requirement by having 4 aa available for binding. Rev2 M116A possesses 3 hydrophobic aas available for binding, but not L116, whereas Rev 2 M116, 124, 127 A only has one hydrophobic aa available for binding; therefore, these mutants do not bind caveolin-1. HydroMut has the requisite 3 hydrophobic and the L116, but does not have a hydrophobic aa in Plane A available for binding; hence, it does not bind caveolin-1.

Table 2.3. Hydrophobic plane mutations and modified hydrophobic faces

Mutant	Hydrophobic Planes	
	A	*B*
Rev 1	I113	L116 L127 L134
Rev 2	V124	L116 L127 L134
Rev 3	Y131	L116 L127 L134
Rev 1, 2 M127A	I113 V124	L116 L134
Rev 1M 124, 127A	I113	L116 L134
Rev 2 M116A	V124	L127 L134
Rev 2 M116, 124, 127 A	--	L134
HydroMut	--	L116 L127 L134

Our data suggest: (a) NSP4 binds caveolin-1 via an interaction with hydrophobic face of the NSP4 AAH; (b) the NSP4-caveolin-1 interaction is specific in that it requires one hydrophobic aa in the left plane and two hydrophobic aas in the right plane, one of which must be L116; (c) both the N- or the C-terminus of caveolin-1 can function as the accepting substrate for the NSP4, which may result in different biological outcomes; (d) the presence of the binding motif is not sufficient to facilitate binding, binding of NSP4 to caveolin-1 may be conformational specific, as the HydroMut contains the critical aa and surrounding hydrophobic residues but does not bind caveolin-1, maybe due to

apparent conformational changes caused by the presence of the charged residues; (e) NSP4 may use the caveolin-1 interaction to traffic to the PM, analogous to γ-retroviruses. The requisite for hydrophobic aa in each plane of the NSP4 AAH might play a role in NSP4 binding both the C- and N-termini. Since both NSP4 and caveolin-1 form multimers, different NSP4 planes could be exposed for binding. The caveolin-1 termini may fold around the NSP4 such that each terminus binds a different face of a different monomer of the multimer.

CHAPTER III

ROTAVIRUS NSP4 EXPRESSION AND TRANSPORT IN THE ABSENCE OF OTHER VIRAL PROTEINS

Overview

In RV-infected cells, NSP4 was shown to transport from the ER to the PM by a Golgi-bypassing pathway (Gibbons, 2007). The focus of this study was to determine if transfected NSP4, in the absence of other viral proteins, traffics similarly to NSP4 expressed in infected cells. We showed that full-length, endoH-sensitive NSP4 was exposed on the exofacial surface of intact kidney-derived MDCK epithelial cells at 7 hours post infection. To begin to dissect those residues that contribute to NSP4 transport and exposure on the cell surface, Baby Hamster Kidney (BHK) cells were transfected with full-length NSP4 FLNSP4$_{1\text{-}175\text{Alanine}}$ NSP4$_{1\text{-}175\text{Hydrophobic}}$ (FLNSP4$_{\text{Hydro}}$) plasmid DNA, surface biotinylated, and examined by IFA or Western blot at 20 h post transfection. Our results revealed FLNSP4 and FLNSP4$_{\text{Ala}}$ were expressed and exposed on the surface of BHK cells in the absence of other viral proteins, whereas FLNSP4$_{\text{Hydro}}$ was not observed at the cell surface. The expression of NSP4 in the absence of other viral proteins does not appear to interfere with ability to traffic in the cell.

NSP4-transfected cells also were used to determine if additional viral proteins were required for the intracellular NSP4-caveolin-1 association by epifluorescence. In the absence of other viral proteins, transfected NSP4 colocalized with caveolin-1 similar to that observed in RV-infected cells. These results confirmed that the NSP4 protein is sufficient in and of itself to associate with the key caveolar structural protein caveolin-1

in two different cell types. NSP4 expression was sufficient for redistribution and colocalization of the caveolin-1 chaperone complex proteins, cyclophilin A, cyclophilin 40, and HSP56 as seen in RV-infected cells. The data presented here suggest NSP4 expression alone does not hinder its intracellular transport or its interaction with caveolin-1. The toxin traffics to the PM, binds and co-localizes with caveolin-1, and redistributes the caveolin-1 chaperone complex proteins in the absence of any other viral proteins.

Introduction

Rotavirus (RV) NSP4 viral enterotoxin and the enterotoxic peptide, amino acids (aa) 114-135, have been shown to induce diarrhea in young mice by promoting Cl^- secretory currents via a calcium-mediated pathway in the absence of histological alterations (Ball et al., 1996; Mebus, 1989; Osborne et al., 1988). NSP4, initially identified as an endoplasmic reticulum (ER) resident glycoprotein, plays a critical role in viral morphogenesis and performs an important regulatory role in the morphogenesis of the transcriptionally active double-layered particles to triple-layered particles (Au et al., 1989; Bergmann et al., 1989; Pesavento et al., 2006; Taylor et al., 1992, 1996).

A C-terminal fragment of NSP4 (residues 112-175) has been identified in the culture media RV-infected epithelial cells (Zhang et al. 2000). Additionally, a 32 kD, partially endo-H resistant NSP4 species has been identified in culture media of RV-infected Caco-2 cells (Bugarcic and Taylor, 2006). These data indicate at least a portion of NSP4 leaves the ER. Subsequent studies confirm the presence of NSP4 at multiple locations in RV-infected cells (Berkova et al., 2006; Boshuizen et al., 2004; Cuadras and

Greenberg, 2003; Parr et al., 2006; Xu et al., 2000). In addition, co-localization with caveolin-1 places NSP4 in the cytosol and at the cell periphery (Parr et al., 2006). These data confirm NSP4 is found throughout the cell and is released from the cell.

Similarly, caveolin-1 exists in a number of pools within the cell and occurs as an integral membrane protein as well as a soluble protein. Caveolin-1 is found in the intestine, interacts with cholesterol, and functions to transport *de novo* synthesized cholesterol to and from the ER and PM caveolae. It functions in organizing signaling of the cell surface molecules, including those involved in calcium homeostasis (Cheng et al., 2006; Field et al., 1998; Hailstones et al., 1998). The integral membrane pool of caveolin-1 traffics via the secretory pathway, which travels through the Golgi complex in the classical secretory pathway (Bergmann et al., 1989; Bugarcic and Taylor, 2006). The cytosolic pool of caveolin-1 has been reported to associate with cyclophilin 40, cyclophilin A, and heat shock protein 56 (Uittenbogaard et al., 1998); however, a separate laboratory has not confirmed these studies.

Both caveolin-1 and NSP4 function as integral membrane proteins and as soluble proteins, occur at multiple sites within the cell, and are multifunctional. Caveolin-1 is a likely candidate to facilitate the trafficking of NSP4 within the cell.

Using a novel raft isolation technique, FLNSP4 has been shown to traffic to the PM (Storey et al., 2007) and has been shown to be exposed on the exofacial leaflet of the PM by surface biotinylation followed by western blot analyses or by FRET analyses (Gibbons, 2007). The NSP4-caveolin-1 association as well as the association of NSP4

with the caveolin-1 chaperone complex (CCC) proteins was resolved to 10-nm radius by FRET analyses (Gibbons, 2007; Storey et al., 2007).

The goal of this study was to determine if FLNSP4, FL $NSP4_{Ala}$, and $FLNSP4_{Hydro}$) transfected into mammalian cells traffic similarly to NSP4 in RV-infected mammalian cells in the absence of other viral proteins. We used surface biotinylation and epifluorescence microscopy techniques to determine the exofacial expression of transfected NSP4 and NSP4 mutants, as well as their association with caveolin-1 and caveolin-1 chaperone complex proteins.

Materials and Methods

Antibodies and Reagents

Antibodies were generated in rabbits and mice to NSP4 residues 150-175 and used as primary antibodies in Western blot assays as previously described (Parr and Ball, 2003; Parr et al., 2006; Zhou et al., 2004). Antibodies directed against Sodium/Potassium ATPase (mouse anti-Na/KATPase, Affinity BioReagents, Golden, CO), horseradish peroxidase (HRP: goat anti-rabbit immunoglobulin G, Pierce Biotechnology, Rockford, IL) and Immunofluorescence Assay (IFA) reagents (goat anti-rabbit Cy2, Streptavidin Cy5, and goat anti-mouse IgG Texas Red (Rockland Immunochem, Inc., Gilbertsville, PA) were purchased commercially. Hoechst 33342 was used to visualize the nuclei to verify the presence of cells.

Micro bicinchoninic acid (BCA) protein assay (Pierce Biotechnology, Rockford, IL) was used to quantify protein concentrations with bovine serum albumin standards according to the manufacturer's protocol. Lipofectamine 2000™ transfection reagent

(Invitrogen, Carlsbad, CA) and Amaxa Nucleofection Solution L were used for transient transfection of the baby hamster kidney-21 (BHK-21) cells with NSP4 or mutant NSP4 plasmid DNA. To distinguish cell surface proteins, surface biotinylation was accomplished using 0.5mg/ml of membrane impermeable Sulfo-NHS-SS Biotin (Pierce Biotechnology, Rockford, IL).

Cultured Cells

BHK-21 cells were obtained from ATCC (Rockville, MD) and were maintained in Minimal Essential Medium (MEM; Mediatech, Inc., Herndon, VA) supplemented with 5% fetal bovine serum, and 5% Serum Supreme, (Cambrex, East Rutherford, NJ), 10% tryptose phosphate broth, 2 mM L-glutamine (Biowhittaker/Cambrex), 1mM sodium pyruvate (Cambrex, East Rutherford, NJ), 0.1 mM non-essential amino acids (Mediatech, Inc., Herndon, VA); 100 U/L penicillin, 100 μg/L streptomycin, 0.25 μg/L amphotericin (10,000 U p enicillin- 10,000 U of streptomycin- 25 μg/liter amphotericin B; Cambrex, East Rutherford, NJ), 26.1 mM sodium bicarbonate (GIBCO, Grand Island, NY), and 10mM HEPES (Amresco, Solon, OH), pH adjusted to 7.3 ± 0.1, and incubated at 37^{o}C in 5% CO_2. Madin-Darby Canine Kidney cells (MDCK, American Type Culture Collection, Manassas, VA) were grown in Dulbecco's Modification of Eagle's media (DMEM) supplemented as above and incubated at 37^{o}C in 5% CO_2. The transient transfections were performed according to the manufacturer's protocol in OptiMeM® Reduced Serum Medium modification of MEM (Gibco, Grand Island, NY) supplemented as above without FBS, serum supreme, or antibiotics, the pH adjusted to

7.3 ± 0.1, and hereafter called transfection media. Transfected cells were maintained in OptiMeM® supplemented as above without antibiotics at 37°C in 5% CO_2.

Transfection

Lipofectamine 2000™

The day before transfection, the BHK cells were washed with PBS three times, trypsinized for 5 minutes with trypsin-versine at 37°C in 5% CO_2. The cells were diluted in 5 mls of MEM, transferred to a 15 ml conical tube, and pelleted for 10 minutes at 1000 rpm. The supernatant was discarded and the cells re-suspended in 5 mls maintenance media and counted with a hemacytometer. The cells were plated in 6-well culture plates at a density of 1.0×10^5 cells per well in 2 mls of their normal growth medium without antibiotics such that they were ~70% confluent on the day of transfection. For each well of the 6-well plate that was transfected, 8 µg of pcDNA3.2Dest $NSP4_{1\text{-}175}$, pcDNA3.2Dest $NSP4_{1\text{-}175Alanine}$, or pcDNA3.2Dest $NSP4_{1\text{-}175Hydrophobic}$ plasmid DNA were diluted in 250 µl of transfection media, added to 10 µl of Lipofectamine 2000™ transfection reagent in 240 µl transfection media, and incubated for 20 minutes (to allow DNA-LF2000™ Reagent complexes to form). The growth media was removed from the cells, the cells were washed two times with 0.5 ml of the transfection media, and the DNA-LF2000 Reagent complexes (500 µl) were added directly to each well of cells. The samples were mixed gently by continuous and incubated at 37°C in 5 % CO_2 for 4 hours after which 1.5 mls of MEM growth media without antibiotics were added, and incubated at 37°C in 5 % CO_2 for 20 hours.

Nucleofection

BHK-21 cells were transiently transfected with pcDNA3.2Dest $NSP4_{1-175}$ plasmid DNA using nucleofection, which delivers the DNA directly into the nuclei of the cells. The Amaxa Nucleofector II® and Nucleofector I® kits were used following the protocols designed by Amaxa Biosystems (Cologne, Germany). The cells were grown to 60-70 % confluency (~2 x $10^6/cm^2$), harvested, and counted. BHK-21 (1 x 10^6 cells) in 100 μl transfection media were mixed with 100 μl of cell-type specific Nucleofector solution L and 2 μg $NSP4_{1-175}$ plasmid DNA, nucleofected using Nucleofector program A-031 and plated on 10 mm cover slips and incubated at 37°C in 5 % CO_2 for 20 hours.

Western Blot Analyses

Equal amounts of total protein as assessed by BCA were resolved on 12% polyacrylamide minigels and transferred to nitrocellulose filters (0.45 μ pure nitrocellulose; GE Osmonics) according to the manufacturer protocol (Mini-PROTEAN II and Trans-Blot respectively; BioRad). The filters were blocked in 10% Blotto (wt/vol non-fat dry milk in PBS) for 2 hours at room temperature (RT) with rocking and then reacted with the primary antibody in 2.5% Blotto overnight (~14 hours) at 4°C with rocking. The filters were incubated an additional 1 hour at RT with the primary antibody, then washed once in PBS, twice in PBS with 0.05% Tween-20, and once in PBS with rocking (10 min per wash). Secondary antibodies were diluted in 2.5% Blotto and incubated with the filters for 30 minutes at RT with rocking. The nitrocellulose filters were washed as above, and reacted with Immobilon Western chemiluminescent

substrates as per the manufacturer's protocols (Millipore, Billerica MA). The marker-specific bands were visualized by exposure to and development of x-ray film.

Surface Biotinylation for Isolation of Cell Surface Proteins

Mock and transfected cells were grown in 12-well culture plates for 20 hours, rinsed with ice cold filter sterilized PBS with 0.1mM $CaCl_2$ and 1mM $MgCl_2$ (PBS-CM), and then reacted with 0.5mg/ml of membrane impermeable Sulfo-NHS-SS-Biotin (PIERCE #21331) for 20 minutes at 4°C. Excess biotin was quenched with cold cell culture media (MEM with serum) and washed 4 times (ice cold PBS-CM). Then the cells were lysed with RIPA buffer (150 mM NaCl, 50 mM Tris-base, 1% SDS, 0.5% DOC, pH 8.0) containing protease inhibitors (0.2 μM PMSF and 1 μl/ml protease inhibitor cocktail set III) for 20 minutes at 4°C. To extract the biotin-labeled cell surface proteins, 50 μl of streptavidin-agarose slurry (10%) (Pierce #20347D) per 1 ml of cell lysates were incubated overnight at 4°C with continuous rotation. The streptavidin-agarose-bound proteins were pelleted, washed 3 times with 1 ml of RIPA buffer, the supernatants removed, and the remaining pellet suspended in sample reducing buffer. The proteins were separated by SDS-PAGE and transferred to nitrocellulose membranes. Mock biotinylated samples were used to control for non-specific binding of proteins to the streptavidin beads.

Indirect Fluorescence Analysis (IFA) With Digital Imaging

Biotinylated Samples

The nucleofected BHK-21 cells plated on 10 mm cover slips were used for IFA analyses in biotinylation or co-localization experiments. After removal of the growth media and washing with PBS, the cells were biotinylated as indicated above, after which they were fixed and permeabilized with ice-cold methanol:acetone (1:1), incubated at -20°C for 10 minutes, washed with PBS and blocked with 2% Blotto with rocking overnight. After blocking, the samples were stained with affinity purified rabbit anti-$NSP4_{150-175}$ (1:1000) diluted in 1% blotto for 30 minutes. Following four 10-minute washes with PBS, the monolayers were treated with goat anti-rabbit Cy2 (1:200 in 1% blotto) and Steptavidin Cy5 (1:1000 in 1% blotto) to detect the primary antibodies, and incubated in the dark at RT for 30 minutes with rocking. The cell monolayers were washed once with PBS (5 minutes), counter stained with Hoechst stain, and washed 4 times with PBS (10 minutes each) in the dark. After washing, the cover slips were air-dried, mounted inverted on slides using fluorescent mounting media (KPL Inc.) and sealed with enamel.

NaKATPase Plasma Membrane Marker Samples

To determine the extent to which NSP4 trafficed to the PM, cover slips of BHK cells prepared as above were probed with rabbit anti-$NSP4_{150-175}$ (1:1000 in 1% blotto) and mouse anti-Na/KATPase, a PM marker (1:100 in 1% blotto). The cell monolayers were washed 4 times (10 minutes each) with PBS, followed by treatment with goat anti-rabbit IgG-Cy2 (1:250 in 1% blotto)to detect NSP4 antibodies, and goat anti-mouse IgG

Texas Red (1:100 in 1% blotto) to detect the antibody to the PM, incubated in the dark at RT for 30 minutes with rocking. The cell monolayers were counter stained Hoechst and mounted as above.

Epifluorescence

Epifluorescence was used to detect the presence of biotinylated $NSP4_{1-175}$ on the exofacial leaflet of the PM and colocalization of NSP4 or NSP4 mutants with NaKATPase. Cells were visualized using a Stallion Digital Imaging Workstation (Carl Zeiss MicroImaging, Inc., Thornwood, NY) equipped with 300W xenon fluorescent light source with rapid switching (<2msec) between excitation wavelengths. Images were collected using a 63X objective 0.75 N.A. a ROPER CoolSnap HQ camera (Ottobrunn, Germany) and Slidebook 4.2 software (Intelligent Imaging Innovations (Denver, CO). The Stallion system filter set includes excitation/emission wavelengths suitable for the color combinations utilized: DAPI and Hoechst (365:445/50 nm), FITC and Cy2 (470/20:505-530 nm), TX Red and Cy3 (560/40:590 nm) and Cy5 (575-625/660-710 nm). The images were processed using Image J, which is a public domain, Java-based image-processing program developed at the National Institutes of Health.

Results

NSP4 Was Exposed on the Exofacial Surface of MDCK Cells Early Post Infection as Shown by Surface Biotinylation and Western Blot

In our study, the surface expression of NSP4 in RV-infected MDCK cells was examined at several time points early post infection to determine when NSP4 was first

exposed on the cell surface. Initial experiments were completed to establish the presence of NSP4 on the surface of MDCKs at 8 hpi (data not shown). The surface biotinylated fraction was pulled down with streptavidin coated agarose beads and was examined by Western blot. In RV-infected MDCK cells, NSP4 was detected on the exofacial surface only at one time point (7 hpi, Figure 3.1, Panel B, lane 1) prior to 8 hpi with the 4 hpi time point showing a lack of NSP4 on the exofacial surface (Figure 3.1, Panel A, lane 1). These data indicate NSP4 reached the cell surface between 4 and 7 hpi in MDCK cells. We only detected the doubly-glycosylated, 28 kD NSP4 indicating only the fully glycosylated protein is exposed on the cell surface of these cells (Figure 3.1, Panel B-1).

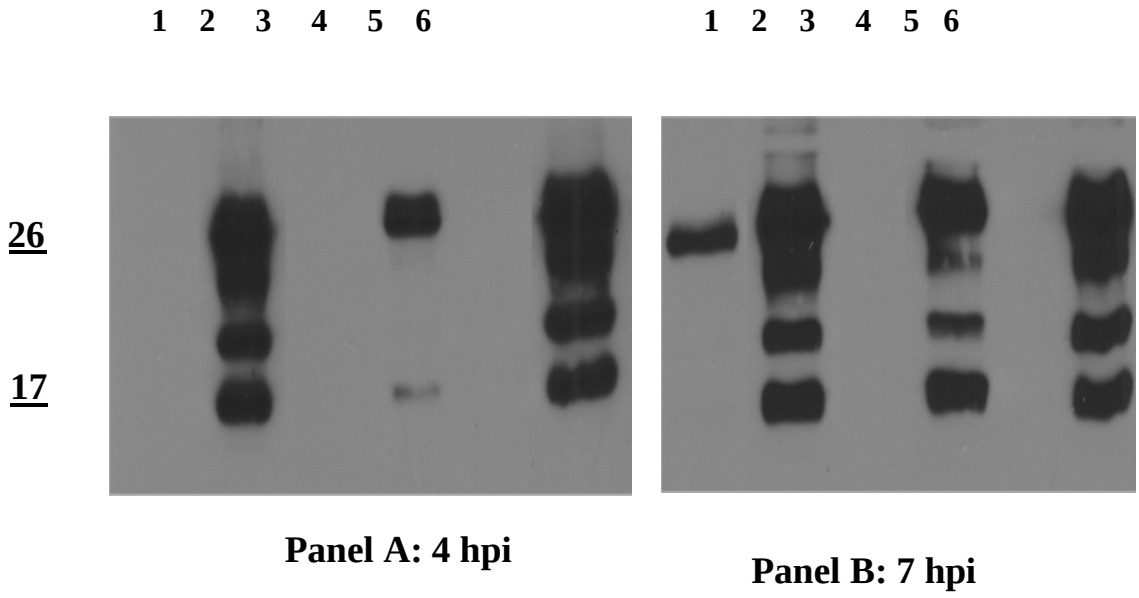

Figure 3.1. Western blot analyses of surface biotinylated proteins (Panels A and B). MDCK cells were infected with RV SA11.4F at a moi of 2 for 4 and 7 hours, surface biotinylated and precipitated with streptavidin agarose. The cell lysates and precipitated surface proteins were separated by SDS-PAGE and analyzed by Western blot using anit-NSP4$_{150\text{-}175}$. For the two blots 1 = streptavidin pull down of biotinylated exofacial proteins, 2 = lysates from biotinylated cells, 3 = streptavidin pull down of mock biotinylated exofacial proteins, 4 = lysates from no biotin control, 5 = lysates from no RV cell control, 6 = lysates from RV cell control.

FLNSP4 Was Exposed on the Exofacial Surface of Transfected BHK Cells as Shown by Biotinylation Analysis

BHK cells were transfected with FLNSP4 plasmid DNA and examined the transfected BHK cells at 20 h post transfection for surface expression of FLNSP4 using surface biotinylation. Our results showed that NSP4 is expressed on the surface of the BHK cells that have been transfected with FLNSP4. In Figure 3.2, Panel A shows results for the FLNSP4 transfected cells, panel B shows mock transfected cells, and panel C shows positive viral (RV SA11.4F) controls. As in RV-infected cells, we only detected the doubly-glycosylated, 28 kD NSP4 indicating only the fully glycosylated protein was exposed on the cell surface of these cells. Panel A, lane 2 results verified that FLNSP4 traffics to the PM in the absence of other viral proteins and doubly-glycosylated NSP4 is exposed on the exofacial surface.

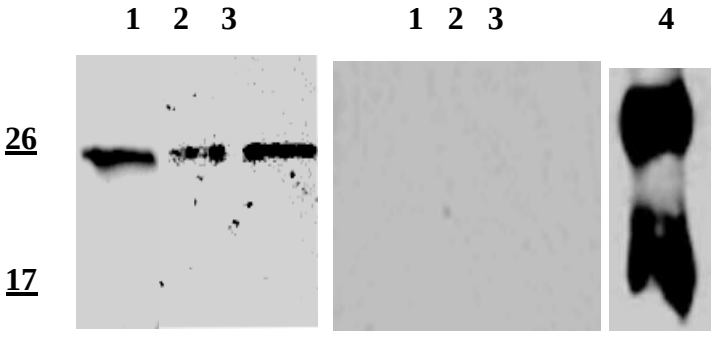

Figure 3.2. Western blot analyses of surface biotinylated proteins (Panels A, B, and C). BHK cells were mock transfected or transfected with NSP4-FL, surface biotinylated and precipitated with streptavidin agarose. The cell lysates and precipitated surface proteins were separated by SDS-PAGE and analyzed by Western blot using anit-NSP4$_{150\text{-}175}$. For the blots 1 = lysates from no biotin control, 2 = streptavidin pull down of biotinylated exofacial proteins, 3 = lysates from biotinylated cells, 4 = lysates from RV SA11.4F infected cells.

$FLNSP4_{Ala}$ Was Exposed on the Exofacial Surface of Transfected BHK Cells While $FLNSP4_{Hydro}$ Lacked Exposure as Shown by Biotinylation Analysis

To expand this finding, BHK cells were transfected the NSP4 mutant plasmid DNA ($FLNSP4_{Ala}$ and $FLNSP4_{Hydro}$) and examined at 20 h post transfection. In $FLNSP4_{Ala}$ the charged face of the AAH is disrupted with six alanine residues (D114A, K115A, R119A, E125A, D132A, and K133A), while the hydrophobic face $FLNSP4_{Hydro}$ was independently disrupted with point mutations at I113R, V124K, and Y131D. As shown in Figure 3.3, $FLNSP4_{Ala}$ was exposed on the surface of the BHK cells (Panel B, lane 2), while $FLNSP4_{Hydro}$ was not seen on the cell surface (Panel A, lane2). Taken together these results indicate that $FLNSP4_{Ala}$ traffics to the cell membrane in the absence of any other viral proteins. Additionally, the lack of the NSP4-Hydro proteins at the surface supports the argument that the hydrophobic face of the amphipathic alpha helix of NSP4 plays a key role in NSP4 trafficing to the cell surface.

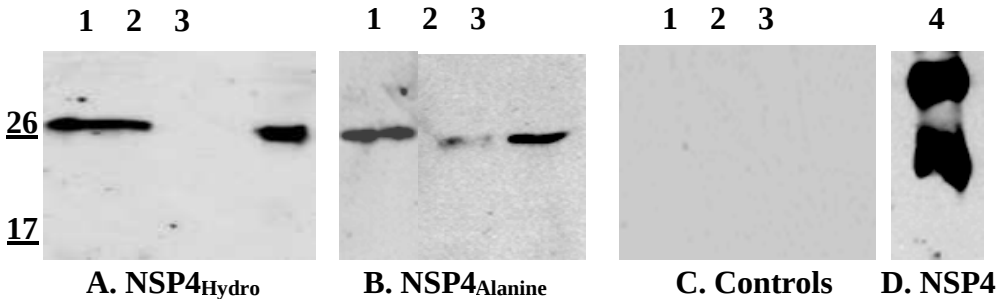

Figure 3.3. Western blot analyses of surface biotinylated proteins (Panels A, B, C, and D). BHK cells were mock transfected or transfected with $FLNSP4_{Ala}$ or $FLNSP4_{Hydro}$ for 20 hrs, surface biotinylated and precipitated with streptavidin agarose. The cell lysates and precipitated surface proteins were separated by SDS-PAGE and analyzed by Western blot using anit-$NSP4_{150\text{-}175}$. For the blots 1 = lysates from no biotin control, 2 = streptavidin pull down of biotinylated exofacial proteins, 3 = lysates from biotinylated cells, 4 = lysates from RV SA11.4F infected cells.

IFA Analysis Confirms That FLNSP4 and FLNSP4$_{Ala}$ Were Exposed on the Exofacial Surface of Transfected BHK Cells While NSP4$_{Hydro}$ Failed to Traffic to the Cell Surface

Transfected BHK cells were surface biotinylated, or simply fixed and permerablized and examined by IFA at 20 h post transfection to verify the biotinylation/Western blot data showing FLNSP4 and FLNSP4$_{Ala}$ localize to the PM and are exposed on the cell surface, while NSP4$_{1\text{-}175Hydro}$ does not. The cells were probed with RbαNSP4$_{150\text{-}175}$ followed by gtαRb-Cy2 and Streptavidin Cy5 to detect the biotinylated cell surface proteins or MαNa/K-ATPase followed by GtαMTXRed to evaluate colocalization at the PM. As seen in Figures 3.4-3.6, FLNSP4 and FLNSP4$_{Ala}$ were expressed and exposed on the surface of BHK cells in the absence of viral proteins, whereas FLNSP4$_{Hydro}$ was not observed at the cell surface.

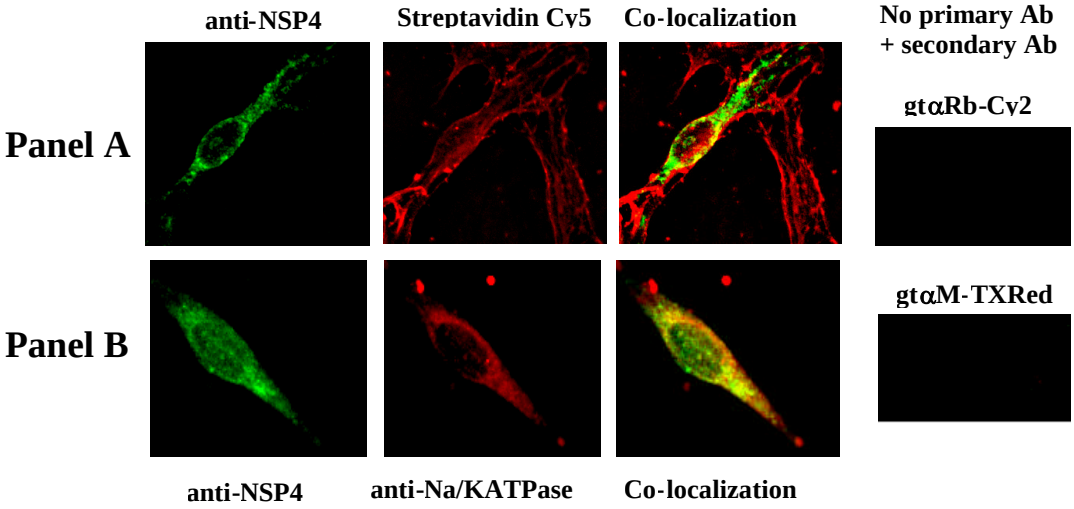

Figure 3.4. IFA of NSP4-FL biotinylated surface proteins and NSP4-Na/K-ATPase co-localization. BHK cells were transfected with pcDNA3.2D NSP4$_{1\text{-}175}$ plasmid DNA and probed with the indicated antibodies. Fluorescently tagged secondary antibodies were imaged with 480-nm and then 625-nm wavelength excitation source to capture Cy2, Texas Red or Cy5 signal. NSP4 (left panels), biotinylated surface proteins (Panel A, center), Na/K-ATPase (Panel B, center) distributions are shown. The FLNSP4 colocalizes with biotin at the cell surface (yellow, Panel A, right) and Na/K-ATPase (yellow, Panel B, right) indicating that it traffics to the cell membrane in the absence of any other viral proteins.

These data support the surface biotinylation-western blot analyses. The biotinylated surface proteins were pseudo-colored red (Figure 3.4, Panel A, center) and the secondary antibody to NSP4-FL green (Figure 3.4, Panels A and B, left). The images were merged and co-localized pixels were assessed (yellow, Figure 3.4, Panel A, right). The presence of co-localized pixels (yellow) indicate that NSP4 is exposed on the cell surface in the surface-biotinylated samples. This finding is supported by the colocalization (Figure 3.4, Panel B, right) of NSP4 (green, Figure 3.4, Panel B, left) with NaKATPase (pseudo-colored red, Figure 3.4, Panel B, center), a plasma membrane marker.

Figure 3.5 shows FLNSP4$_{Ala}$-transfected BHK cells (pseudo-colored green, Panel A, left) as well as total biotinylated surface proteins (pseudo-colored red, Panel A, center), and the merged image (yellow, Panel A, right), which shows colocalization of FLNSP4$_{Ala}$ with the surface biotin. These data confirming that FLNSP4$_{Ala}$ had trafficked to the cell surface in FLNSP4$_{Ala}$-transfected BHK cells (Figure 3.5, Panel A, left). This finding is supported by the colocalization of FLNSP4$_{Ala}$ with NaKATPase (Figure 3.5, Panel B, left), a plasma membrane marker. Hence, FLNSP4$_{Ala}$ trafficked to the PM and was exposed on the cell surface akin to the WT FLNSP4.

In contrast to the cells transfected with FLNSP4 and FLNSP4$_{Ala}$, FLNSP4$_{Hydro}$ failed to traffic to the cell surface (Figure 3.6) as there was no colocalization with the biotin (Panel A) or with the PM marker (Panel B). Again, these data support the Western blot analyses.

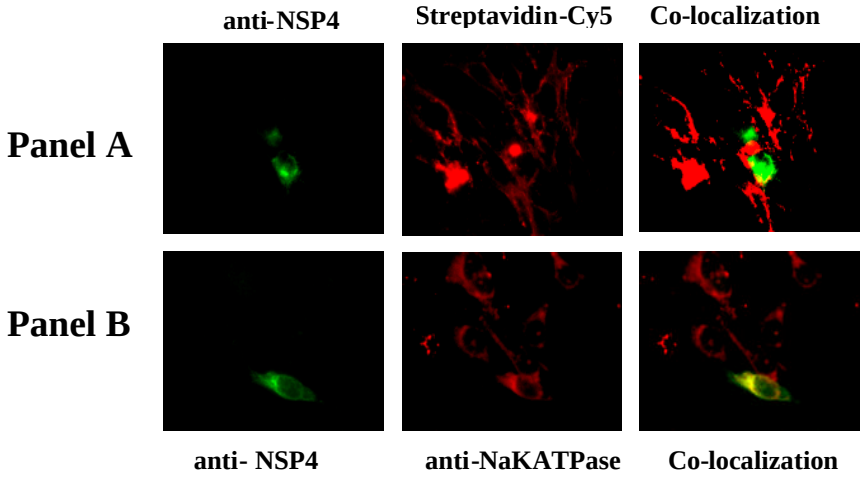

Figure 3.5. IFA of biotinylated surface proteins in BKS cells transfected with FLNSP4$_{Ala}$ and FLNSP4$_{Ala}$ -Na/K-ATPase colocalization. BHK cells were transfected with pcDNA3.2D NSP4$_{1\text{-}175Ala}$ plasmid DNA and probed with the indicated antibodies. Fluorescently tagged secondary antibodies were imaged with 480-nm and then 625-nm wavelength excitation source to capture Cy2, Texas Red or Cy5 signal. NSP4$_{1\text{-}175Ala}$ (left panels), biotinylated surface proteins (Panel A, center), Na/K-ATPase (Panel B, center) distributions are shown. The FLNSP4$_{1\text{-}175Ala}$ (green) (Panels A and B) colocalizes with biotin at the cell surface (Panel A, right) and Na/K-ATPase (Panel B, right) indicating that it traffics to the cell membrane in the absence of any other viral proteins.

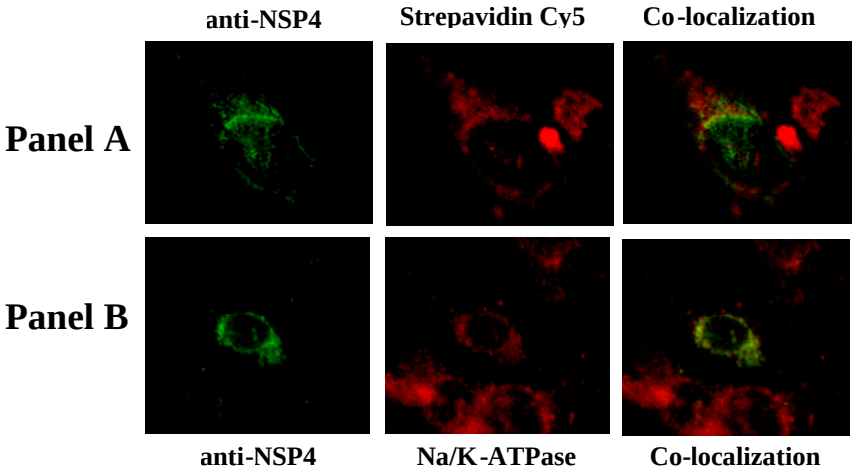

Figure 3.6. IFA of FLNSP4$_{Hydro}$ biotinylated surface proteins, and FLNSP4$_{Hydro}$-Na/KATPase. BHK cells were transfected with pcDNA3.2D NSP4$_{1\text{-}175Hydro}$ plasmid DNA and probed with the indicated antibodies. Fluorescently tagged secondary antibodies were imaged with 480-nm and then 560-nm or 625-nm wavelength excitation source to capture Cy2, Texas Red or Cy5 signal. NSP4$_{1\text{-}175Ala}$ (left panels), biotinylated surface proteins (Panel A, center), Na/K-ATPase (Panel B, center) distributions are shown. The FLNSP4$_{Hydro}$ does not traffic to the cell surface as indicated by the lack of colocalization with biotin at the cell surface (Panel A, right) or Na/K-ATPase (Panel B, right). These findings support the argument that the hydrophobic face of the amphipathic alpha helix of NSP4 plays a key role in trafficking NSP4 to the cell surface.

NSP4 Expression Was Sufficient for Colocalization With Caveolin-1

To determine if viral proteins were required for the intracellular NSP4-caveolin-1 association, epifluorescence was utilized with NSP4-transfected cells. In the absence of other proteins, transfected NSP4 had similar subcellular distribution patterns in MDCK and HT29.f8 cells as those observed during RV infection (Figure 3.7, central panels) (Storey et al., 2007). Both cell lines stained for caveolin-1, whereas only one of the HT29.f8 cells (of the two shown) was transfected, as indicated by the presence of NSP4 (Figure 3.7, upper panels). Additionally, the NSP4 and caveolin-1 proteins in the transfected cells colocalized (Figure 3.7, far-right panels) at intracellular sites similar to those observed in RV-infected cells (Storey et al., 2007), i.e. perinuclear sites, in the cytosol and at the cell periphery. These results suggest that the NSP4 protein is sufficient in and of itself to associate with the key caveolar structural protein caveolin-1 in two different cell types.

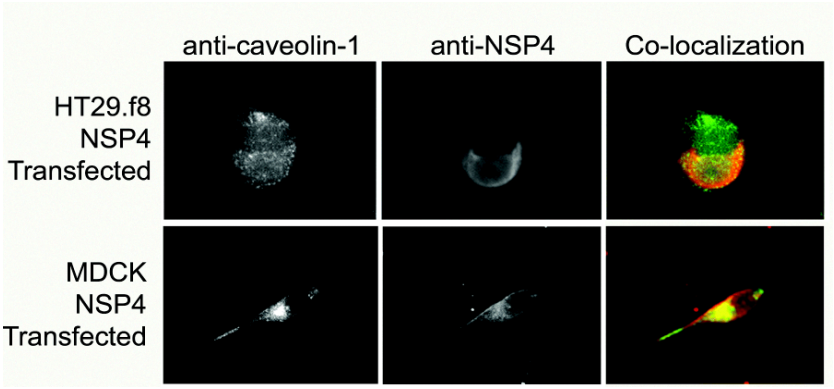

Figure 3.7. Colocalization of NSP4 with caveolin-1 in transfected cells. HT29.f8 (top panels) and MDCK (bottom panels) cells were transfected with pcDNA3.2D $_{NSP4150\text{-}175}$ plasmid DNA and probed with the indicated primary antibodies. Fluorescently tagged secondary antibodies were imaged with 470-nm and then 560-nm wavelength excitation source to capture Cy2 and Texas Red signals, respectively (n = 4). Caveolin-1 (left panels) and NSP4 (center panels) distributions are shown. Note that only one of the two HT29.f8 cells shown was transfected (NSP4 signal). The panels on the far right are merged images showing the colocalization of NSP4 (red) and caveolin-1 (green).

NSP4 Expression Was Sufficient for Redistribution and Colocalization of the Caveolin-1 Chaperone Complex Proteins, Cyclophilin A, Cyclophilin 40, and HSP56 Similar to RV-infected Cells

Epifluorescence was utilized with NSP4-transfected BHK cells to determine if RV viral proteins were necessary for the association of NSP4 with the proteins of the Caveolin-1 Chaperone Complex (CCC). Previously, it had been shown that cyclophilin A, cyclophilin 40, and heat shock protein 56 were redistributed similarly to caveolin-1 in RV infected cells and the association of these CCC proteins with NSP4 were resolved to within 10 nm (Gibbons, 2007). Here we use indirect fluorescence analysis (IFA) with digital imaging to determine if cyclophilin A, cyclophilin 40, and heat shock protein redistribution is similar to caveolin-1 in transfected cells. BHK cells were transfected with FLNSP4, fixed, and permerablized and examined by IFA at 20 h post transfection. The transfected cells were probed with RbαCyclophilin A, RbαCyclophilin 40, or RbαHSP56, then RbαNSP4$_{150\text{-}175}$Cy3 followed by gtαRb-Cy2 and Hoechst stain. Figure 3.8 shows the expression of NSP4 (pseudo-colored red, Panels A-C, lane 1) and the redistribution of the CCC proteins in pseudo-colored green (cyclophilin A, Panel A, lane 2; cyclophilin 40, Panel B lane 2; HSP56, Panel C lane 2). In lane 3 (Figure 3.8, Panels A-C) the cells have been counter stained with Hoechst stain. Observation of the non-transfected cells demonstrated that in the absence of t ransfected NSP4, the CCC proteins were not redistributed. The images from lanes 1 and 2 were merged and co-localized pixels were assessed (yellow, Figure 3.8, Panels A-C, lane 4). The presence of co-localized pixels (yellow) indicated NSP4 was colocalized with each CCC protein.

With each CCC protein the patterns and distributions were similar to the caveolin-1 pattern in the transfected NSP4. IFA results indicate that expression of NSP4 was sufficient for redistribution of and co-localization with cyclophilin A, cyclophilin 40, and HSP56 in a similar fashion as in RV-infected cells.

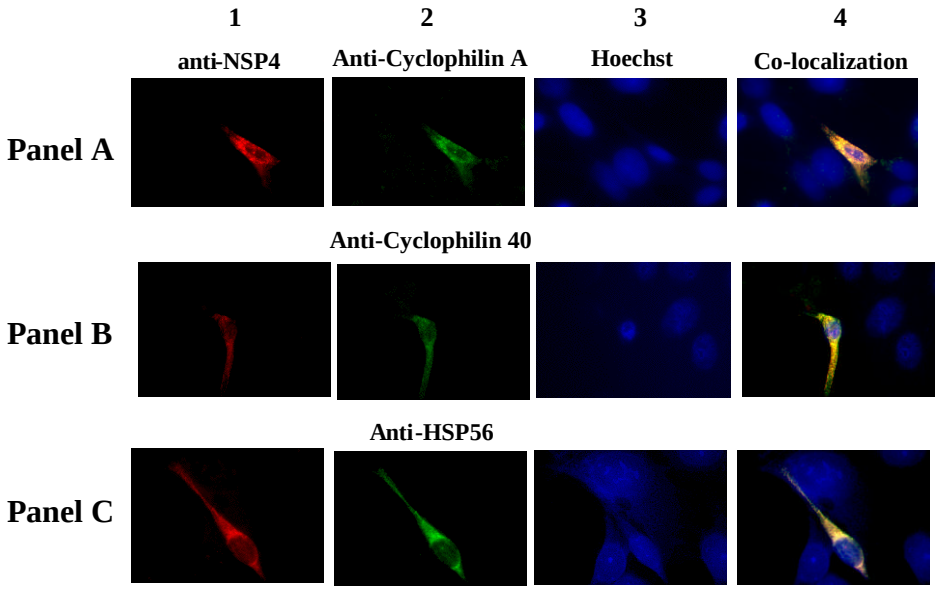

Figure 3.8. NSP4 expression was sufficient for redistribution and colocalization of cyclophilin A, cyclophilin 40, and HSP56. The proteins of the caveolin-1 chaperone complex redistribute and co-localized with transfected NSP4in transfect BHK cells. Each of the proteins of the caveolin-1 chaperone complex were probed with anti-NSP4 and either anti-cyclophilin A (Panel A), anti-cylcophilin40 (Panel B), or HSP 56 (Panel C). Redistribution of these proteins occurs in the absence of any other viral proteins.

Discussion

This study examined transfected FLNSP4 and its association with the PM, with caveolin-1 and the CCC proteins. Additionally, we evaluated whether $FLNSP4_{Ala}$ and $FLNSP4_{Hydro}$ traffic to the PM and were exposed on the cell surface.

We first examined RV-infected MDCK cells to determine if, when, and what form of NSP4 is exposed on the exofacial surface of the PM. The results of this study showed a full-length, endoH-sensitive NSP4 pool was exposed on the exofacial surface of intact kidney-derived MDCK epithelial cells (7hpi). Several recent reports have indicated that the NSP4 enterotoxin is secreted from infected cells; however, the form of NSP4 reported varied. Bugarcic and Taylor (2006) observed secretion of NSP4 by 16 hpi in Caco-2 cells infected with the UK strain of bovine RV at a moi of 10, however the NSP4 appears post-translationally processed to approximately 32kD with endo H-resistance. This study reported the 32 kD as predominant form of NSP4 secreted between 16 and 42 hours post infection. Additionally, the C-terminal NSP4 fragment (aa 112-175) has been isolated from culture medium of baculovirus-gene 10 recombinant infected *Spodoptera frugiperda* (SF9) insect cells and RV-infected mammalian cells (Zhang et al., 2000). Storey et al. (2007) reported that NSP4 traffics to the PM caveolae of MDCK cells as the doubly glycosylated, endoH-sensitive mature form of the enterotoxin and is found at the PM at 24 hpi (MOI of 2).

Additionally, caveolae isolated from PM-rich material from RV-infected MDCK cells yield full-length, high mannose glycosylated NSP4 (Storey et al., 2007). Here we report that in RV-infected MDCK cells, the same 28kD ‘mature’ form of NSP4 reached the cell surface between 4 and 7 hpi. Similarly Gibbons (2007) reports PM exofacial expression of NSP4 at 2-3 hpi in HT29.f8 cells. The detection of NSP4 at early time post infection is likely prior to release of progeny virus from the cell suggesting that NSP4 does not need infective progeny virus to traffic to from the ER to the PM. These data

indicate that NSP4 is released from an infected cell well prior to the maturation of the viral progeny and likely functions in attachment to non-infected cells making them susceptible to RV-infection.

Our biotinylation data on transfected cells showed that FLNSP4 and $FLNSP4_{Ala}$ were expressed, localized to the PM, and exposed on the surface of BHK cells in the absence of other viral proteins, whereas NSP4-Hydro was expressed, but not observed at the cell surface. The lack of cell surface exposure of transfected $FLNSP4_{Hydro}$ is likely not related to the absence of other viral proteins, but could be due to the lack of ability of $FLNSP4_{Hydro}$ to bind caveolin-1. In $FLNSP4_{Ala}$ the charged face of the amphipathic alpha helical (AAH) is altered with six alanine residues (D114A, K115A, R119A, E125A, D132A, and K133A), while the hydrophobic face was unaltered. $FLNSP4_{Hydro}$ was disrupted with point mutations at I113R, V124K, and Y131D in the hydrophobic face and the charged face was unaltered (Figure 2.3). Previously, we have shown by yeast two-hybrid that the NSP4-caveolin-1 binding domain was localized to one critical hydrophobic aa (L116) and one or two additional aa (I113, L127, and/or L134) on the hydrophobic face. $FLNSP4_{Ala}$ retained binding to caveolin-1, while $FLNSP4_{Hydro}$ lacked binding with caveolin-1. Taken together the failure of $FLNSP4_{Hydro}$ to traffic to the cell surface or co-localization with the PM marker and its lack caveolin-1 binding suggest the interaction of NSP4 and caveolin-1 contribute to the transport of the enterotoxin to the cell surface. This supports the argument that the hydrophobic face of the AAh of NSP4 plays a key role in trafficking NSP4 to the cell surface and supports the thesis of Parr et

al. (2006) suggesting the NSP4-caveolin-1 association contributes to NSP4 intracellular trafficking from the ER to the cell surface.

Epifluorescence was utilized with NSP4-transfected cells to determine if other viral proteins were required for the intracellular NSP4-caveolin-1 association, NSP4 and caveolin-1 have been shown to co-localize at multiple sites within RV-infected cells (Berkova et al., 2006; Parr et al., 2006; Storey et al., 2007). A comparison of the NSP4 transfected MDCK and HT29.f8 in the absence of other viral proteins with RV-infected NSP4 localization (Storey et al., 2007) shows a similar subcellular distribution pattern. Additionally, compared with RV-infected cells, the NSP4 and caveolin-1 proteins in the transfected cells colocalized at intracellular sites similar to those observed in RV-infected cells (Storey et al., 1007).

NSP4 expression was sufficient for redistribution and colocalization of the CCC proteins, cyclophilin A, cyclophilin 40, and HSP56 similar to caveolin-1 as shown by IFA. These data suggest that in the absence of viral other proteins, some portion of NSP4 associates with the CCC. Additionally, these data support the findings that CCC proteins are redistributed during RV infection by NSP4 and the association of these CCC proteins with NSP4 has been resolved to within 10 nm (Gibbons, 2007). However, neither PCR nor western blot data showed an increase in messenger RNA for the CCC proteins (Gibbons, 2007) suggesting the CCC proteins are only redistributed and not upregulated. Silencing NSP4 has shown no marked effect on the expression of other viral proteins or on the replication of the dsRNA genome segments (Silvestri et al., 2005); however, blocking the synthesis of NSP4 suppressed viroplasm maturation and affected the

intracellular accumulation and the cellular distribution of several viral proteins (Lopez et al., 2005b). These data plus the fact that NSP4 bypasses the Golgi apparatus (Storey et al., 2007) and our data on NSP4-caveolin-1 and the CCC suggest that NSP4 may preferentially traffic using the soluble complex pathway.

The data presented here suggests NSP4 expression alone is sufficient to carry out its functions. It traffics from the ER to PM, co-localizes with caveolin-1, and redistributes the CCC protrins in the absence of other viral proteins. NSP4 may use the CCC and the soluble complex pathway for the trafficking to various regions of the cell including the viroplasm and the PM. Additional studies are needed to fully understand the pathway of NSP4 to the PM.

CHAPTER IV

CONCLUSION AND FUTURE DIRECTIONS

Overview

The purpose of this research was to identify the region or regions of the NSP4 C-terminal amphipathic alpha helix (AAH) that are sufficient for binding caveolin-1. Using the WT NSP4 and a panel of nine NSP4 mutants in yeast two hybrid (Y2H) assays, the NSP4 caveolin-1 binding domain was localized to one critical hydrophobic aa (L116) and two additional aa on the hydrophobic face. Those mutants that bound caveolin-1 bound both the N- and C-terminal caveolin-1 peptides in peptide binding assays, but lacked binding to a centrally located peptide, which verifies earlier results that WT NSP4 binds to both the N- and C- termini of caveolin-1 (Mir et al., 2007).

Additional studies determined that in the absence of other viral proteins, transfected FLNSP4 colocalized with caveolin-1, trafficked similarly to NSP4 in RV-infected cells, and appeared to redistribute and colocalize with the caveolin-1 chaperone complex proteins (Figure 3.8) as seen in RV-infected cells. These results confirm similar results from RV-infected cells and that the expression of the toxin is sufficient in and of itself to cause these effects.

Rotavirus NSP4 Binds Caveolin-1 on the Hydrophobic Face of the Extended Amphipathic Alpha Helix

To dissect the precise NSP4 binding domain to caveolin-1, NSP4 mutants were prepared by altering either the charged ($FLNSP4_{Ala}$) or hydrophobic face ($FLNSP4_{Hydromut}$) of the NSP4 C-terminal AAH and examined for binding to caveolin-1.

Initially, we demonstrated that the hydrophobic face of the NSP4 AAH binds caveolin-1 since binding was abolished with the $FLNSP4_{Hydromut}$ in which three hydrophobic residues were replaced with charged amino acids (aa). This suggested that the hydrophobic face of the NSP4 AAH binds caveolin-1 via a hydrophobic interaction. Mutants of $FLNSP4_{Hydromut}$ in which one of the three mutated aa residues was reverted to the original hydrophobic residue regained binding to caveolin-1, which led to our hypothesis that a minimum of three hydrophobic residues in the C-terminal hydrophobic face of the NSP4 AAH are required for binding caveolin-1. Additional alanine mutants were used to support our hypothesis, indicating that L116 and at least two additional hydrophobic residues were sufficient to facilitate NSP4 binding to caveolin-1. A potential binding motif of $\theta_{113}L_{116}\theta_{124}\theta_{127}\phi_{131}\theta_{134}$ (θ is hydrophobic, ϕ is aromatic, and L is leucine) has been identified, which lies in two distinct planes of the NSP4 hydrophobic face of the AAH. From our data we propose that three hydrophobic aa are needed for NSP4 to bind to caveolin-1 and at least two hydrophobic residue must reside in the plane containing L116 and at least one hydrophobic residue must reside in the other plane.

Rotavirus NSP4 Is Expressed and Trafficked in the Absence of Other Viral Proteins

The purpose of this research was to determine the effect of the absence of RV replication and other RV proteins on the expression and transport of NSP4 in transfected cells. We utilized FLNSP4, $FLNSP4_{Ala}$ and $FLNSP4_{Hydro}$ to transfect BHK cells. Our results revealed only FLNSP4 and $FLNSP4_{Ala}$ were expressed and exposed on the surface of BHK cells (by surface biotinylation) in the absence of other viral proteins.

While $FLNSP4_{Hydro}$ is expressed in transfected BKK cells, it was not exposed on the surface of BHK cells. In light of our previous finding that $FLNSP4_{Hydro}$ does not bind caveolin-1 and NSP4 has been shown in PM caveolae (Storey et al., 2007), the association NSP4 with caveolin-1 may contribute to the toxin's intracellular trafficking (Parr et al., 2006). Additional data are needed to confirm these observations.

In addition, epifluorescence was used to demonstrate that in transfected cells, FLNSP4 colocalizes with caveolin-1 similar to that observed in RV-infected cells. The data suggested that expression of NSP4 without other RV proteins does not hinder its intracellular transport or its interaction with caveolin-1. Moreover, NSP4 expression was sufficient for an apparent redistribution and the colocalization with the caveolin-1 chaperone complex proteins, cyclophilin A, cyclophilin 40, and HSP56 similar to that seen in RV-infected cells.

Advances and Significance

This research adds to the body of knowledge on RV NSP4 in that it specifically (a) verified that the NSP4 to caveolin-1 binding domain is in the hydrophobic face of the AAH and that the interaction is hydrophobic in nature; (b) established the NSP4-caveolin-1 interaction is specific in requiring L116 and two additional hydrophobic residues that possibly form a 'pocket' through which the caveolin-1 binding occurs; (c) determined that at least one hydrophobic residue must be present in each of two planes of the hydrophobic face in addition to the L116 for NSP4-caveolin-1 interaction to occur; (d) transfection of NSP4 showed that it interacts with caveolin-1 in the absence of other viral proteins; (e) supported the hypothesis that NSP4 may use the caveolin-1 interaction

to traffic to the PM as the both FLNSP4 and FLNSP4$_{Ala}$ were found on the exofacial of BHK cells; and (vi) showed an apparent redistribution of the CCC complex proteins by NSP4 in the absence of RV viral proteins similar to that observed in RV-infected cells.

The data on the NSP4-caveolin-1 interaction of the hydrophobic mutants suggest that not only are hydrophobic constraints, but also conformational constraints, may play a role in the NSP4-caveolin-1 association. For example, the Rev2 M116A mutant has hydrophobic residues in both planes of the hydrophobic face of the AAH, but lacks L116, thus fails to bind, supporting the requirement specific hydrophobic residue at the aa position116. Also, the binding NSP4 may be conformational specific as the Hydromut mutant, which does not bind caveolin-1, contains the critical aa L116 and hydrophobic residues L_{127} and L_{134}, but lacks a hydrophobic residue in one plane of the hydrophobic AAH. This suggests the hydrophobic face of the AAH is more severely disrupted than in the revertants, which differ from Hydromut only by possessing hydrophobic residues in both planes. This disruption may be due to conformational changes caused by the presence of the charged residues (Couet et al., 1997a). The hydrophobic face appears to be able accommodate for the absence of some of the aas and continues to bind caveolin-1. Another possible outcome of the two planes hypothesis may be that the N-terminus binds one plane, while the C-terminus binds the other plane. This remains to be determined.

The definitive results of the Y2H analyses led to follow-on transfection studies to verify the association of NSP4 with caveolin-1 in absence of other viral proteins. The results of the transfections studies showed that FLNSP4 and FLNSP4$_{Ala}$, but not

$FLNSP4_{Hydro}$ were expressed and exposed on the surface of BHK cells in the absence of other viral proteins. Additionally, IFA studies showed the NSP4 protein is sufficient in and of itself to associate with the key caveolar structural protein caveolin-1 and is apparently sufficient for redistribution and colocalization of the CCC proteins, cyclophilin A, cyclophilin 40, and HSP56 similar to caveolin-1. These results confirm similar results from RV-infected cells. The expression of the toxin is sufficient to cause these effects. These data coupled with the Y2H binding data suggest that NSP4 uses caveolin-1 to traffic within the cell and adds support to the thesis that the toxin may use the CCC to transport from the ER to the PM allowing NSP4 to avoid Golgi glycosylases (Parr et al., 2006).

The data on the lack of association $FLNSP4_{Hydro}$ with caveolin-1 and its lack of transport to the PM might be useful in the development of a RV vaccine and/or drug therapy. A structure-function study could be conducted to determine if a RV mutant containing $FLNSP4_{Hydro}$ has a different or less severe pathology than wild type RV. This mutant could be used to generate a vaccine that does not have the potential side effect of causing diarrhea. Alternatively, drug therapy to treat RV infection could be developed that specifically targets the hydrophobic region of the AAH of NSP4. The drug treatment would have to out compete caveolin-1 for the hydrophobic AAH binding site.

Strengths, Weaknesses, and Resolutions

Yeast-Two-Hybrid

The Proquest yeast two-hybrid system (Invitrogen, Carlsbad, CA) is a well-tested technology for detecting protein-protein interactions in vivo and adds strength and validity to this study. Proquest system uses three reporter genes to minimize false positives. Additionally, a panel of five controls that display a spectrum of protein interactions allow for assessment of test colony phenotypes resulting from the interaction of the proteins of interest. However the expression of NSP4 and caveolin-1 as the GAL4 fusion proteins may present some difficulties. The fusion proteins may not fold in a manner similar to the wt protein, which might result in steric hindrance of the binding domain and thus abrogating binding. We resolved this weakness by assaying a large number of colonies (90+) and confirming our Y2H results with peptide binding and western blot assays.

Yeast systems use different glycosylation enzymes that may result in different glycosylation patterns in the proteins of interest. In yeast N-linked glycosylation consists of as many as 50 mannose residues. This is a concern with NSP4 as it contains two N-linked glycosylation sites (Estes and Cohen, 1989). Alternative glycosylation or hyperglycosylation could affect protein folding and stabilization, and consequently binding. This issue was resolved by determining the glycosylation pattern on NSP4 mutants expressed in yeast by Endo H digestion. The glycosylation of $FLNSP4_{Hydromut}$ in yeast was equivalent to that observed in mammalian cells.

Transfection Studies

Toxic effects of NSP4 on cells made this protein difficult to transfect. The use of electroporation or chemical transfection (Lipofectamine™2000) was difficult and inconsistent. The numbers of transfected cells was extremely low (e.g., one or two cells in a field of view at 600X). Use of nucleofection did improve transfection efficiency. The use of an inducible system (e.g., Clontech's Tet-On Advanced and Tet-Off Advanced Inducible Gene Expression Systems) could be used to increase transfection efficiency. Also, transfection of intestinal cell lines (HT29.f8) proved to be especially difficult. As a result, BHK cells were used in transfection studies, which may lead to questions of validity of extrapolating results to intestinal cells. However, we did show that in the absence of other proteins, transfected NSP4 had similar subcellular distribution patterns in HT29.f8 cells as those observed during RV infection.

NSP4-Caveolin-1 Binding Site

A weakness of the current study is that NSP4-caveolin-1 binding site was not unequivocally identified. While this study has localized the NSP4-caveolin-1 binding site to L116 and two additional hydrophobic residues in each of two planes of the hydrophobic face, it did not establish: (a) if aa leucine at the 116 position is required or if any hydrophobic aa is sufficient for binding or (b) if L116/116 position alone is the binding 'site.' Also, the study did not determine whether the N- and the C-termini of caveolin bind at the same binding site.

Colocalization Does Not Mean Interaction

The colocalization of transfected NSP4 and caveolin-1 or PM markers resolved the proteins to about 200 nm. Moreover, since the PM is about 5 nm in width, colocalizing NSP4 with the PM only locates to within a 200 nm region of the PM. This only indicates that the proteins closely approach each other and may not in fact interact.

Fluorescent Resonance Energy Transfer (FRET) is a more definitive technique to verify protein-protein interaction. FRET is a process in which nonradiative energy transfer occurs from one fluorophore to another when the two fluorophores (e.g., fluorescently tagged proteins) are within 10 nm of each other (Kenworthy, 2001). The use of acceptor photobleaching, a process in which the acceptor fluorophore is bleached and an increase in fluorescence of the donor fluorophore is monitored, is useful to determine if the two proteins interact (Karpova et al., 2003). The purpose of the colocalization studies was to determine if transfected NSP4, in the absence of other viral proteins, traffics similarly to NSP4 expressed in infected cells. FRET analyses established that NSP4-caveolin-1 and the immunophilin proteins associate to within 10 nm in RV-infected cells and that the toxin is expressed on the exofacial leaflet of the PM. A future aim will be to evaluate the NSP4 mutants association with caveolin-1 and the immunophilin proteins.

Future Research

Unequivocal Delineation of the NSP4 Caveolin-1 Binding Site

Since the NSP4 binding domain was not precisely delineated, additional mutated NSP4 peptides of the AAH region, could specifically map the aa residues required for binding. The peptides would be used in direct fluorescence binding assays and/or peptide binding assays with N- and C-caveolin-1 peptides to assess NSP4-caveolin-1 interaction. Both the N- and C-caveolin-1 peptides would be used in these studies to determine if both termini bind to the same NSP4 binding site. The $NSP4_{113\text{-}135}$ used as a positive control and the $NSP4_{HydroMut}$ peptide would be used as a negative control. Peptides $NSP4_{113\text{-}135,\ L116A}$ and $NSP4_{113\text{-}135,\ L134A}$ would determine if L116 is required for binding and resolve the importance of L134 in binding. A peptide mutating I113, V124, L127, Y131, and L134 to alanine residues and retaining only the L116 would definitively resolve its importance in caveolin-1 binding. If this peptide binds caveolin-1, the L116 could be replaced with another hydrophobic molecule to determine if leucine is specifically required for binding.

Peptide $NSP4_{113\text{-}135,\ I113A,\ V127A,\ Y131A}$, the alanine analog of $NSP4_{Hydromut}$, would be used to establish the importance of conformation in the binding to caveolin-1. Recall that $NSP4_{Hydromut}$ contains one of the possible hydrophobic binding face (L116, L127, L134) identified in this study, but does not bind. Binding of alanine analog of mutant of $NSP4_{Hydromut}$ would confirm the importance of conformation, as well as support that L116, L127, L134 is a possible hydrophobic binding face.

Structural analyses using Circular Dichroism (CD) spectroscopy could be conducted to determine the structural consequences of the mutations. Yeast-two-hybrid would be used to verify positive interaction *in vivo.*

Role of the Immunophilins in NSP4 Trafficking to the PM

The focus of our research group is on the intracellular transport of NSP4 and the mechanism(s) by which it occurs. Not only have we shown that NSP4 traffics to the PM (Gibbons, 2007), but we also have shown that NSP4 associates with caveolin-1 and apparently redistributes the cytosolic immunophilin proteins, cyclophilin A, cyclophilin 40, and HSP 56 (Gibbons, 2007; Chapter III this work). The caveolin-1 and the immumophilins deliver newly synthesized cholesterol to PM caveolae. Given that NSP4 localizes to the PM caveolae, binds caveolin-1, and redistributes the immumophilin proteins, the immumophilins may function to deliver NSP4 to the PM as well. The following approach could be used to investigate the immumophilin's role in NSP4 trafficking to the PM: (a) screen for individual immunophilin protein interaction with NSP4 mutants using fluorescence binding assays; (b) map the NSP4 binding site of immunophilin proteins with positive fluorescence binding assays using yeast two-hybrid; and (c) determine structure-function impact of immunophilin protein deficiency. A brief description of the studies is given below.

Determine if Immunophilin Proteins Interact With NSP4 Mutants Peptides Using Fluorescence Binding Assays

Direct fluorescent binding assays could be used to screen for direct binding of the NSP4 mutants with each immunophilin protein (Hostetler et al., 2005) to FLNSP4 would be expressed in yeast and affinity purified, peptides NSP4 $_{113\text{-}135\text{Alanine}}$, NSP4$_{113\text{-}135\text{Hydromut}}$, and other selected NSP4 peptides can be made in our laboratory, while the immunophilin proteins are commercially available. The immunophilin proteins would be directly labeled with a Cy3 fluorescent dye and titrated with the NSP4 protein to demonstrate a direct protein-protein interaction. Initially the Cy3-labeled immunophilin protein is in a hydrophilic environment and the fluorescence is quenched, however upon titration with a binding protein/peptide, such as FLNSP4, places the Cy3 molecule in a hydrophobic environment abrogating the quenching of the Cy3 fluorescence. This results in an increase in fluorescence intensity suggesting that the two proteins or protein/peptide interact. If the titrating protein/peptide does not bind the Cy3-labeled immunophilin protein, no change in fluorescence intensity is detected. Binding to FLNSP4 only or binding FLNSP4, FLNSP4$_{\text{Alanine}}$, and FLNSP4$_{\text{Hydromut}}$ suggests that the binding is not in the AAH region. Binding to FLNSP4 and either FLNSP4$_{\text{Alanine}}$ or FLNSP4$_{\text{Hydromut}}$ indicates that binding is in the AAH region. If binding is not in the AAH region, a series NSP4 deletion peptides (e.g. NSP4$_{1\text{-}107}$, NSP4$_{45\text{-}175}$, NSP4$_{112\text{-}175}$, NSP4$_{135\text{-}175}$, and NSP4$_{90\text{-}150}$) could be made localize the binding site(s) of the immunophilins.

Confirm the NSP4 Binding Site of Each of the Immunophilin Proteins Using Our Panel of NSP4 Mutants in Yeast-two-Hybrid

Using the immunophilin proteins that have been shown to interact with NSP4 mutant peptides, we would use yeast two-hybrid as above to map the binding domains within NSP4 *in vivo*. We have both the $NSP4_{46\text{-}175}$ activating domain (AD, pDest22 AD-$NSP4_{46\text{-}175}$) and binding domain (BD, pDest 32 BD- $NSP4_{46\text{-}175}$) fusion proteins. The AD and BD fusion proteins for the immunophilin proteins could be prepared using commercially available clones (Ultimate™ ORF, Invitrogen) and subcloned into the Invitrogen Gateway™ Destination vectors pDEST22 and pDEST32 as previously described (Parr et al., 2006; Zhou et al., 2004) Expression of fusion proteins will be verified with Western blot and appropriate antibodies. A series of yeast transformation (forward and reverse) as describe earlier would be conducted to detect protein-protein associations between NSP4 and the individual immunophilins proteins. Transcription activation will be restored only if the AD fusion protein and BD fusion protein interact, resulting in the expression of the reporter genes. Interaction of caveolin-1 with $NSP4_{46\text{-}175}$ will be used as a positive control and the lack interaction between caveolin-1 with $NSP4_{Hydromut}$ will be used as a negative control. Our first screen would be with $NSP4_{Ala}$, $NSP4_{HydroMut}$, and a new mutant $NSP4_{Ala\text{-}HydroMut}$ (alanine analog of Hydromut) with each immunophilin protein. Follow-on testing would depend upon the binding pattern. If the interaction is with the hydrophobic face (binds $NSP4_{Ala}$, but not $NSP4_{HydroMut}$ or $NSP4_{Ala\text{-}HydroMut}$), we would use our existing panel of hydrophobic mutants to map the binding domains of the immunophilin proteins. If the interactions occur with the polar face (binds

$NSP4_{HydroMut}$ and $NSP4_{Ala\text{-}HydroMut}$, but not $NSP4_{Ala}$) a new set of polar face mutants will have to be designed, generated and used to map binding site(s). If the immunophilin proteins bind $NSP4_{Ala}$, $NSP4_{HydroMut}$, and $NSP4_{Ala\text{-}HydroMut}$, this would indicate that the binding site is outside the AAH, consequently we would used our panel of NSP4 deletion mutants to map the binding domains.

Verify NSP4 Interaction With Immunophilin Proteins by Peptide Binding Assays

Once the putative binding domains have been identified, peptide binding assays could be used to verify direct binding of the NSP4 peptide with each immunophilin. The NSP4 peptides containing the putative immunophilin protein binding domains would be prepared and attached to CNBr-activated sepharose 4B beads and incubated overnight at 4ºC with the commercially obtained immunophilin. The beads were washed as previously described and resuspended in SDS-PAGE loading buffer. The proteins would be separated on 12% SDS-PAGE, transferred to nitrocellulose membranes and probed with immunophilin- or NSP4-specific antibodies in a Western blot assay.

Determine Structure-Function Impact of Cyclophilin A Protein Deficiency

A Cyclophilin A negative cell line has been developed by homologous recombination (Braaten and Luban, 2001) and used to study its function in regulation HIV-1 infectivity. This cell line could be similarly used to assess the impact of the lack of cyclophilin A on the transport of NSP4 via the caveolin-1 and the immunophin.

Cyclophilin A deficient mice (Colgan et al., 2004) could be used in structure-function studies to determine if NSP4 produces diarrhea in the absence of this immunophilin. A DD50 response curve using RV SA11 would be determined in non-

deficient mice (Ball et al., 1996), which would be used to infect the cyclophilin A deficient mice. Production of diarrhea would indicate that the lack of cyclophilin A does not impair ability of NSP4 to produce its toxic effect, while the lack of diarrhea production would indicate a functional role for cyclophilin A.

Use of Quantum Dots

A quantum dot (QD) is a semiconductor whose excitons (electron-hole pair) are confined in three spatial directions. The bound electron-hole pairs provide a means to transport energy without transporting net charge. QDs have an interesting optical property that results in QDs of the same material, but different sizes emitting light of different colors. QDs are typically 5-15 nm in size. The larger QDs contain more energy levels more closely spaced, therefore can absorb photons of lower energy (longer wavelength) resulting in emission in the red region. Conversely, the smaller the QD the higher the energy of the photons absorbed resulting in blue emission. This "tenability" has allowed for the development of QDs with a common excitation profile, but different fluorescent emission maxima. QD antibody conjugation kits are available in seven (7) different fluorescent colors.

Develop a Methodology to Create a "Model Caveolin-1 CCC"

Similar Model Membranes

Apparently, the work of Uittenbogaard et al. (1998) and Uittenbogaard and Smart (2000) on the "caveolin-1 chaperone complex" has not been duplicated. They suggest that the CCC does not form in the absence of caveolin-1. It might be possible to fabricate "model CCC" using techniques similar to those used to make model membranes in the

presence and absence of caveolin-1. The commercially available components could be (CCC proteins, caveolin-1, and cholesterol) could be fluorescently tagged (possibly with Quantum dots) for use in hyperspectral imaging confocal microscopy (capable of separation of up to eight flurophores) to confirm the model caveolin-1 CCC. If it is possible to make the model Caveolin-1 CCC it would be used to verify NSP4 interaction.

Use of Quantum Dots to Determine the Formation of the Caveolin-1 Chaperone Complex (CCC) In Vivo

The CCC does not form in caveolin-1 negative cells (i.e. L1210-JF). This cell line could be then transfected with YFP-labeled caveolin-1 followed by treatment with the CCC protein QD-labeled antibodies to demonstrate the formation of the CCC. Treatment of the caveolin-1 null cells with the CCC protein QD-labeled antibodies would demonstrate the lack of formation of the CCC. The QDs could be visualized with hyperspectral imaging confocal microscopy (capable of separation of up to eight flurophores).

Use of Quantum Dots to Determine Interaction of NSP4 With CCC

If the CCC can be demonstrated, follow-on research could be conducted using L1210-JF transfected with GFP-labeled NSP4 and YFP-labeled caveolin-1 followed by treatment with the CCC protein QD-labeled antibodies to demonstrate the colocalization of NSP4 with caveolin-1 and the CCC. The samples could be visualized with hyperspectral imaging confocal microscopy.

Use of Quantum Dots to Track Externally Added NSP4 Attachment and Internalization

Seo et al. (2008) have demonstrated that integrin $\alpha1\beta1$ and $\alpha2\beta1$ are receptors for NSP4. Observation of the attachment of NSP4 to these receptors and its internalization cold be monitored in lives cells using quantum dots (QDs). A cell line (BHK) could be QD-labeled $\alpha1\beta1$ and $\alpha2\beta1$ (Invitrogen Qdot ITK™) followed by treatment with GFP-NSP4 enterotoxic peptide. Confocal and Total internal reflection fluorescence (TIRF) microscopy could be used to monitor in real-time the attachment and possible internalization of the labeled NSP4 (or NSP4 enterotoxic peptide).

Verification of Model NSP4 Binding Caveolin-1 and Caveolae Lipids

We have proposed a model whereby NSP4 binds to caveolin-1 protein and caveolae lipids on opposite faces of the C-terminal AAH, which facilitates its crossing the PM. It has been shown that NSP4 binds unilamellar vesicles (SUVs), but the binding site has not been delinated. We know NSP4 binds caveolin-1 on the hydrophobic face of the NSP4 AAH and suggest that it binds unilamellar vesicles (SUVs) on the polar face. This model could be verified by fluorescence binding assays with small unilamellar vesicles (SUVs) with $NSP4_{113\text{-}135\ Alanine}$ and $NSP4_{113\text{-}135\ HydroMut}$ mutant peptides. A positive fluorescence binding assay with $NSP4_{113\text{-}135\ HydroMut}$ and a negative fluorescence binding assay with $NSP4_{113\text{-}135Alanine}$ would support binding of NSP4 to the SUVs on the polar face of the NSP4 AAH. *In vivo* mammalian cell studies in which the cells have been treated with fluorescently tagged phospholipids (e.g., Cy5) and infected with RV or transfected with NSP4 could be used to verify the model. The NSP4 and caveolin-1 are

visualized with fluorescent antibodies (Cy 2 and Cy3). If colocalization occurs among the lipids and the two proteins, FRET analyses could be conducted to confirm possible interaction. A caveolin-1 deficient cell line (L1210-JF) could be used to determine if NSP4 binds other caveolae lipids in the absence of caveolin-1.

REFERENCES

Anderson, R. G., 1998. The caveolae membrane system. Annu. Rev. Biochem. 67, 199-225.

Arias, C. F., Romero, P., Alvarez, V., Lopez, S., 1996. Trypsin activation pathway of rotavirus infectivity. J. Virol. 70(9), 5832-5839.

Au, K. S., Chan, W. K., Burns, J. W., Estes, M. K., 1989. Receptor activity of rotavirus nonstructural glycoprotein NS28. J. Virol. 63(11), 4553-4562.

Ball, J. M., Mitchell, D. M., Gibbons, T. F., Parr, R. D., 2005. Rotavirus NSP4: A multifunctional viral enterotoxin. Viral Immunol. 18(1), 27-40.

Ball, J. M., Tian, P., Zeng, C. Q. Y., Morris, A. P., Estes, M. K., 1996. Age-dependent diarrhea induced by a rotaviral nonstructural glycoprotein. Science 272(5258), 101-104.

Barro, M., Patton, J. T., 2005. Rotavirus nonstructural protein 1 subverts innate immune response by inducing degradation of IFN regulatory factor 3. Proc. Natl. Acad. Sci. USA 102(11), 4114-4119.

Benferhat, R., Sanchez-Martinez, S., Nieva, J. L., Briand, J. P., Hovanessian, A. G., 2008. The immunogenic CBD1 peptide corresponding to the caveolin-1 binding domain in HIV-1 envelope GP41 has the capacity to penetrate the cell membrane and bind caveolin-1. Mol. Immunol. 45(7), 1963-1975.

Bergmann, C. C., Maass, D., Poruchynsky, M. S., Atkinson, P. H., Bellamy, A. R., 1989. Topology of the non-structural rotavirus receptor glycoprotein NS28 in the rough endoplasmic reticulum. Embo. J. 8(6), 1695-1703.

Berkova, Z., Crawford, S. E., Trugnan, G., Yoshimori, T., Morris, A. P., Estes, M. K., 2006. Rotavirus NSP4 induces a novel vesicular compartment regulated by calcium and associated with viroplasms. J. Virol. 80(12), 6061-6071.

Berkova, Z., Morris, A. P., Estes, M. K., 2003. Cytoplasmic calcium measurement in rotavirus enterotoxin-enhanced green fluorescent protein (NSP4-EGFP) expressing cells loaded with fura-2. Cell Calcium 34(1), 55-68.

Bist, A., Fielding, P. E., Fielding, C. J., 1997. Two sterol regulatory element-like sequences mediate up-regulation of caveolin gene transcription in response to low density lipoprotein free cholesterol. Proc. Natl. Acad. Sci. USA 94(20), 10693-10698.

Boshuizen, J. A., Rossen, J. W. A., Sitaram, C. K., Kimenai, F. F. P., Simons-Oosterhuis, Y., Laffeber, C., Buller, H. A., Einerhand, A. W. C., 2004. Rotavirus enterotoxin NSP4 binds to the extracellular matrix proteins laminin-3 and fibronectin. J. Virol. 78(18), 10045-10053.

Bowman, G. D., Nodelman, I. M., Levy, O., Lin, S. L., Tian, P., Zamb, T. J., Udem, S. A., Venkataraghavan, B., Schutt, C. E., 2000. Crystal structure of the oligomerization domain of NSP4 from rotavirus reveals a core metal-binding site. J. Mol. Biol. 304, 861-891.

Braaten, D., Luban, J., 2001. Cyclophilin A regulates HIV-1 infectivity, as demonstated by gene targeting in human T cells. Embo. J. 20(6), 1300-1309.

Brunet, J. P., Cotte-Laffitte, J., Linxe, C., Quero, A. M., Geniteau-Legendre, M., Servin, A., 2000. Rotavirus infection induces an increase in intracellular calcium concentration in human intestinal epithelial cells: Role in microvillar actin alteration. J. Virol. 74(5), 2323-2332.

Bugarcic, A., Taylor, J. A., 2006. Rotavirus nonstructural glycoprotein NSP4 is secreted from the apical surfaces of polarized epithelial cells. J. Virol. 80, 12343-12349.

Chan, W. K., Au, K. S., Estes, M. K., 1988. Topography of the simian rotavirus nonstructural glycoprotein (NS28) in the endoplasmic reticulum membrane. Virology 164(2), 435-442.

Cheng, Z. J., Singh, R. D., Marks, D. L., Pagano, R. E., 2006. Membrane microdomains, caveolae, and caveolar endocytosis of sphingolipids (review). Mol. Mem. Biol. 23(1), 101-110.

Chun, M., Liyanage, U. K., Lisanti, M. P., Lodish, H. F., 1994. Signal transduction of a G protein-coupled receptor in caveolae: Colocalization of endothelin and its receptor with caveolin. Proc. Natl. Acad. Sci. USA 91(24), 11728-11732.

Chwetzoff, S., Trugnan, G., 2006. Rotavirus assembly: An alternative model that utilizes an atypical trafficking pathway. Curr. Top Microbiol. Immunol. 309, 245-261.

Colgan, J., Asmal, M., Neagu, M., Yu, B,. Schneidkraut, J., Lee, Y., Sokolskaja, E., Andreotti, A., Luban, J., 2004. Cyclophilin A regulates TCR signal strength in CD4+ T cells via a proline-directed conformational switch in Itk. Immunity 21(2), 189-201.

Coombs, K. M., 2006. Reovirus structure and morphogenesis. Current Topics in Microbiology and Immunology: Entry, Assembly and Morphogenesis 309, 117-168.

Couet, J., Belanger, M. M., Roussel, E., Drolet, M. C., 2001. Cell biology of caveolae and caveolin. Adv. Drug Deliv. Rev. 49(3), 223-235.

Couet, J., Li, S., Okamoto, T., Ikezu, T., Lisanti, M. P., 1997a. Identification of peptide and protein ligands for the caveolin-scaffolding domain. Implications for the interaction of caveolin with caveolae-associated proteins. J. Biol. Chem. 272(10), 6525-6533.

Couet, J., Sargiacomo, M., Lisanti, M. P., 1997b. Interaction of a receptor tyrosine kinase, EGF-R, with caveolins. Caveolin binding negatively regulates tyrosine and serine/threonine kinase activities. J. Biol. Chem. 272(48), 30429-30438.

Cuadras, M. A., Feigelstock, D. A., An, S., Greenberg, H. B., 2002. Gene expression pattern in Caco-2 cells following rotavirus infection. J. Virol. 76(9), 4467-4482.

Cuadras, M. A., Greenberg, H. B., 2003. Rotavirus infectious particles use lipid rafts during replication for transport to the cell surface in vitro and in vivo. Virology 313(1), 308-321.

Cuadras, M. A., Bordier, B. B., Zambrano, J. L., Ludert, J. E., Greenberg, H. B., 2006. Dissecting rotavirus particle-raft interaction with small interfering RANa: Insights into rotavirus transit through the secretory pathway. J. Virol. 80(8), 3935-3946.

Das, K., Lewis, R. Y., Scherer, P. E., Lisanti, M. P., 1999. The membrane-spanning domains of caveolins-1 and -2 mediate the formation of caveolin hetero-oligomers. Implications for the assembly of caveolae membranes in vivo. J. Biol. Chem. 274(26), 18721-18728.

Davidson, G. P., Gall, D. G., Petric, M., Butler, D. G., Hamilton, J. R., 1977. Human rotavirus enteritis induced in conventional piglets. Intestinal structure and transport. J. Clin. Invest. 60(6), 1402-1409.

Delmas, O., Durand-Schneider, A. M., Cohen, J., Colard, O., Trugnan, G., 2004. Spike protein VP4 assembly with maturing rotavirus requires a postendoplasmic reticulum event in polarized Caco-2 cells. J. Virol. 78(20), 10987-10994.

Desselberger, U., Iturriza-Gomara, M., Gray, J. J., 2001. Rotavirus epidemiology and surveillance. Novartis Found. Symp. 238, 125-47.

Devaux, P. F., Morris, R., 2004. Transmembrane asymmetry and lateral domains in biological membranes. Traffic 5(4), 241-246.

Dietzen, D. J., Hastings, W. R., Lublin, D. M., 1995. Caveolin is palmitoylated on multiple cysteine residues. Palmitoylation is not necessary for localization of caveolin to caveolae. J. Biol. Chem. 270(12), 6838-6842.

Dong, Y., Zeng, C. Q. Y., Ball, J. M., Estes, M. K., Morris, A. P., 1997. The rotavirus enterotoxin NSP4 mobilizes intracellular calcium in human intestinal cells by stimulating phospholipase C-mediated inositol 1,4,5-trisphosphate production. PNAS 94(8), 3960-3965.

Dormitzer, P. R., Sun, Z. Y., Wagner, G., Harrison, S. C., 2002. The rhesus rotavirus VP4 sialic acid binding domain has a galectin fold with a novel carbohydrate binding site. EMBO J. 21(5), 885-897.

Dubroca, C., Loyer, X., Retailleau, K., Loirand, G., Pacaud, P., Feron, O., Balligand, J. L., Levy, B. I., Heymes, C., Henrion, D., 2007. RhoA activation and interaction with caveolin-1 are critical for pressure-induced myogenic tone in rat mesenteric resistance arteries. Cardiovasc. Res. 73(1), 190-197.

Dupuis, P., Beby, A., Bourgoin, A., Lussier-Bonneau, M. D., Agius, G., 1995. Epidemic of viral gastroenteritis in an elderly community. Presse. Med. 24(7), 356-358.

Ericson, B. L., Graham, D. Y., Mason, B. B., Hanssen, H. H., Estes, M. K., 1983a. Two types of glycoprotein precursors are produced by the simian rotavirus SA11. Virology 127(2), 320-332.

Ericson, B. L., Petrie, B. L., Graham, D. Y., Mason, B. B., Estes, M. K., 1983b. Rotaviruses code for two types of glycoprotein precursors. J. Cell Biochem. 22(3), 151-160.

Estes, M. K., 2001. Rotaviruses and their replication. Field's Virology, 1747-1785.

Estes, M. K., Cohen, J., 1989. Rotavirus gene structure and function. Microbiol Rev. 53(4), 410-449.

Estes, M. K., Kang, G., Zeng, C. Q., Crawford, S. E., Ciarlet, M., 2001. Pathogenesis of rotavirus gastroenteritis. Novartis Found. Symp. 238, 82-96; discussion 96-100.

Fabbretti, E., Afrikanova, I., Vascotto, F., Burrone, O. R., 1999. Two non-structural rotavirus proteins, NSP2 and NSP5, form viroplasm-like structures in vivo. J. Gen. Virol. 80 (Pt 2), 333-339.

Fang, Z. Y., Ye, Q., Ho, M. S., Dong, H., Qing, S., Penaranda, M. E., Hung, T., Wen, L., Glass, R. I., 1989. Investigation of an outbreak of adult diarrhea rotavirus in China. J. Infect. Dis. 160(6), 948-953.

Field, F. J., Born, E., Murthy, S., Mathur, S. N., 1998. Caveolin is present in intestinal cells: Role in cholesterol trafficking? J. Lipid Res. 39(10), 1938-1950.

Fielding, C. J., Bist, A., Fielding, P. E., 1997. Caveolin mRNA levels are up-regulated by free cholesterol and down-regulated by oxysterols in fibroblast monolayers. Proc. Natl. Acad. Sci. USA 94(8), 3753-3758.

Fischer, T. K., Viboud, C., Parashar, U., Malek, M., Steiner, C., Glass, R., Simonsen, L., 2007. Hospitalizations and deaths from diarrhea and rotavirus among children <5 years of age in the United States, 1993-2003. J. Infect. Dis. 195(8), 1117-1125.

Fujimoto, T., 1993. Calcium pump of the plasma membrane is localized in caveolae. J. Cell Biol. 120(5), 1147-1157.

Fujimoto, T., Kogo, H., Nomura, R., Une, T., 2000. Isoforms of caveolin-1 and caveolar structure. J. Cell Sci. 113 Pt 19, 3509-3517.

Gallegos, C. O., Patton, J. T., 1989. Characterization of rotavirus replication intermediates: A model for the assembly of single-shelled particles. Virology 172(2), 616-627.

Gibbons, T. F., 2007. Rotavirus NSP4 in extrareticular sites: Support for its pathogenic role as an enterotoxin. Unpublished doctoral dissertation, Texas A&M University, College Station.

Gietz, R. D., Woods, R. A., 2002. Transformation of yeast by lithium acetate/single-stranded carrier DNA/polyethylene glycol method. Methods Enzymol. 350, 87-96.

Glass, R. I., Kilgore, P. E., Holman, R. C., Jin, S., Smith, J. C., Woods, P. A., Clarke, M. J., Ho, M. S., Gentsch, J. R., 1996. The epidemiology of rotavirus diarrhea in the United States: Surveillance and estimates of disease burden. J. Infect. Dis. 174 Suppl 1, S5-11.

Golantsova, N. E., Gorbunova, E. E., Mackow, E. R., 2004. Discrete domains within the rotavirus VP5* direct peripheral membrane association and membrane permeability. J. Virol. 78(4), 2037-2044.

Gonzalez, R. A., Espinosa, R., Romero, P., Lopez, S., Arias, C. F., 2000. Relative localization of viroplasmic and endoplasmic reticulum-resident rotavirus proteins in infected cells. Arch. Virol. 145(9), 1963-1973.

Graf, G. A., Connell, P. M., van der Westhuyzen, D. R., Smart, E. J., 1999. The class B, type I scavenger receptor promotes the selective uptake of high density lipoprotein cholesterol ethers into caveolae. J. Biol. Chem. 274(17), 12043-12048.

Guerrero, C. A., Zarate, S., Corkidi, G., Lopez, S., Arias, C. F., 2000. Biochemical characterization of rotavirus receptors in MA104 cells. J. Virol. 74(20), 9362-9371.

Hailstones, D., Sleer, L. S., Parton, R. G., Stanley, K. K., 1998. Regulation of caveolin and caveolae by cholesterol in MDCK cells. J. Lipid Res. 39(2), 369-379.

Halaihel, N., Lievin, V., Ball, J. M., Estes, M. K., Alvarado, F., Vasseur, M., 2000. Direct inhibitory effect of rotavirus NSP4 (114-135) peptide on the Na^{+}-D-glucose symporter of rabbit intestinal brush border membrane. J. Virol. 74(20), 9464-9470.

Hostetler, H. A., Petrescu, A. D., Kier, A. B., Schroeder, F., 2005. Peroxisome proliferator-activated receptor alphs interactions with high affinity and is conformationally responsive to endogenous ligands. J. Biol. Chem. 280(19), 18667-18687.

Huang, H., Schroeder, F., Estes, M. K., McPherson, T., Ball, J. M., 2004. Interaction(s) of rotavirus non-structural protein 4 (NSP4) C-terminal peptides with model membranes. Biochem. J. 380, 723-733.

Huang, H., Schroeder, F., Zeng, C., Estes, M. K., Schoer, J. K., Ball, J. M., 2001. Membrane interactions of a novel viral enterotoxin: Rotavirus nonstructural glycoprotein NSP4. Biochemistry 40(13), 4169-4180.

Huang, J. H., Lu, L., Lu, H., Chen, X., Jaing, S., Chen, Y. H., 2007. Identification of the HIV-1 GP41 core-binding motif in the scaffolding domain of caveolin-1. J. Biol. Chem. 282(9), 6143-6152.

Invitrogen Life Technologies, 2002. Proquest two-hybrid system with gateway technology manual. Carlsbad, CA: Author.

Isa, P., Realpe, M., Romero, P., Lopez, S., Arias, C. F., 2004. Rotavirus RRV associates with lipid membrane microdomains during cell entry. Virology 322(2), 370-381.

Jayaram, H., Estes, M. K., Prasad, B. V., 2004. Emerging themes in rotavirus cell entry, genome organization, transcription and replication. Virus Res. 101(1), 67-81.

Jourdan, N., Maurice, M., Delautier, D., Quero, A. M., Servin, A. L., Trugnan, G., 1997. Rotavirus is released from the apical surface of cultured human intestinal cells through nonconventional vesicular transport that bypasses the Golgi apparatus. J. Virol. 71(11), 8268-8278.

Kaljot, K. T., Shaw, R. D., Rubin, D. H., Greenberg, H. B., 1988. Infectious rotavirus enters cells by direct cell membrane penetration, not by endocytosis. J. Virol. 62(4), 1136-1144.

Karpova, T. S., Baumann, C. T., He, L., Wu, X., Grammer, A., Lipsky, P., Hager, G. L., McNally, J. G., 2003. Fluorescence resonance energy transfer from cyan to yellow fluorescent protein detected by acceptor photobleaching using confocal microscopy and a single laser. J. Microsc. 209(Pt 1), 56-70.

Kenworthy, A. K., 2001. Imaging protein-protein interactions using fluorescence resonance eneergy transfer microscopy. Methods 24(3), 289-296.

Krishnan, T., Sen, A., Choudhury, J. S., Das, S., Naik, T. N., Bhattacharya, S. K., 1999. Emergence of adult diarrhoea rotavirus in Calcutta, India. Lancet 353(9150), 380-381.

Kurzchalia, T. V., Dupree, P., Parton, R. G., Kellner, R., Virta, H., Lehnert, M., Simons, K., 1992. VIP21, a 21-kD membrane protein is an integral component of trans-Golgi-network-derived transport vesicles. J. Cell Biol. 118(5), 1003-1014.

Lawton, J. A., Estes, M. K., Prasad, B. V., 2000. Mechanism of genome transcription in segmented dsRNA viruses. Adv. Virus Res. 55, 185-229.

Li, S., Couet, J., Lisanti, M. P., 1996. Src tyrosine kinases, G_{α} subunits, and H-Ras share a common membrane-anchored scaffolding protein, caveolin. Caveolin binding negatively regulates the auto-activation of Src tyrosine kinases. J. Biol. Chem. 271(46), 29182-29190.

Li, S., Galbiati, F., Volonte, D., Sargiacomo, M., Engelman, J. A., Das, K., Scherer, P. E., Lisanti, M. P., 1998. Mutational analysis of caveolin-induced vesicle formation. Expression of caveolin-1 recruits caveolin-2 to caveolae membranes. FEBS Lett. 434(1-2), 127-134.

Li, S., Okamoto, T., Chun, M., Sargiacomo, M., Casanova, J. E., Hansen, S. H., Nishimoto, I., Lisanti, M. P., 1995. Evidence for a regulated interaction between heterotrimeric G proteins and caveolin. J. Biol. Chem. 270(26), 15693-15701.

Lisanti, M. P., Scherer, P. E., Vidugiriene, J., Tang, Z., Hermanowski-Vosatka, A., Tu, Y. H., Cook, R. F., Sargiacomo, M., 1994. Characterization of caveolin-rich membrane domains isolated from an endothelial-rich source: Implications for human disease. J. Cell. Biol. 126(1) 111-126.

Liu, P., Rudick, M., Anderson, R. G., 2002. Multiple functions of caveolin-1. J. Biol. Chem. 277(44), 41295-41298.

Lopez, S., Arias, C. F., 2004. Multistep entry of rotavirus into cells: A versaillesque dance. Trends Microbiol. 12(6), 271-278.

Lopez, S., Arias, C. F., 2006. Early steps in rotavirus cell entry. Current Topics in Microbiology and Immunology: Entry, Assembly and Morphogenesis 309, 39-66.

Lopez, T., Camacho, M., Zayas, M., Najera, R., Sanchez, R., Arias, C. F., Lopez, S., 2005b. Silencing the morphogenesis of rotavirus. J. Virol. 79(1), 184-192.

Lopez, T., Rojas, M., Ayala-Breton, C., Lopez, S., Arias, C. F., 2005a. Reduced expression of the rotavirus NSP5 gene has a pleiotropic effect on virus replication. J. Gen. Virol. 86 (Pt 6), 1609-1617.

Marrie, T. J., Lee, S. H., Faulkner, R. S., Ethier, J., Young, C. H., 1982. Rotavirus infection in a geriatric population. Arch. Intern. Med. 142(2), 313-316.

Mattion, N. M., Cohen, J., Estes, M. K., 1994. The rotavirus proteins. Viral Infectios of the Gastrointestinal Tract, 169-248.

Mebus, J. C., 1989. Reovirus-like calf enteritis. Am. Digest. Dis. 21, 592-599.

Mendez, E., Lopez, S., Cuadras, M. A., Romero, P., Arias, C. F., 1999. Entry of rotaviruses is a multistep process. Virology 263(2), 450-459.

Michelangeli, F., Liprandi, F., Chemello, M. E., Ciarlet, M., Ruiz, M. C., 1995. Selective depletion of stored calcium by thapsigargin blocks rotavirus maturation but not the cytopathic effect. J. Virol. 69(6), 3838-3847.

Mir, K. D., Parr, R. D., Schroeder, F., Ball, J. M., 2007. Rotavirus NSP4 interacts with both the amino- and carboxyl-termini of caveolin-1. Virus Res. 126(1-2), 106-115.

Morris, A. P., Estes, M. K., 2001. Microbes and microbial toxins: Paradigms for microbial-mucosal interactions: VIII. Pathological consequences of rotavirus infection and its enterotoxin. Am. J. Physiol. Gastrointest. Liver Physiol. 281(2), G303-310.

Morris, A. P., Scott, J. K., Ball, J. M., Zeng, C. Q., O'Neal. W. K., Estes, M. K., 1999. NSP4 elicits age-dependent diarrhea and Ca(2+)mediated I(-) influx into intestinal crypts of CF mice. Am. J. Physiol. 277(2 Pt1), G431-444.

Nichols, B. J., 2002. A distinct class of endosome mediates clathrin-independent endocytosis to the Golgi complex. Nat. Cell Biol. 4(5), 374-378.

Osborne, M. P., Haddon, S. J., Spencer, A. J., Collins, J., Starkey, W. G., Wallis, T. S., Clarke, G. J., Worton, K. J., Candy, D. C., Stephen, J., 1988. An electron microscopic investigation of time-related changes in the intestine of neonatal mice infected with murine rotavirus. J. Pediatr. Gastroenterol. Nutr. 7(2), 236-248.

Padilla-Noriega, L., Paniagua, O., Guzman-Leon, S., 2002. Rotavirus protein NSP3 shuts off host cell protein synthesis. Virology 298(1), 1-7.

Palade, G. E., 1953. Fine structure of blood capillaries. J. Appl. Phys. 24, 1424-1435.

Parashar, U. D., Hummelman, E. G., Bresee, J. S., Miller, M. A., Grass, R. I., 2003. Global illness and deaths caused by rotavirus disease in children. Emerg. Infect. Dis. 9, 565-572.

Parr, R. D., Ball, J. M., 2003. New donor vector for generation of histidine-tagged fusion proteins using the gateway cloning system. Plasmid. 49(2), 179-183.

Parr, R. D., Storey, S. M., Mitchell, D. M., McIntosh, A. L., Zhou, M., Mir, K. D., Ball, J. M., 2006. The rotavirus enterotoxin NSP4 directly interacts with the caveolar structural protein caveolin-1. J. Virol. 80(6), 2842-2854.

Pelkmans, L., Kartenbeck, J., and Helenius, A., 2001. Caveolar endocytosis of simian virus 40 reveals a new two-step vesicular-transport pathway to the ER. Nat Cel Biol. 3(5), 473-483.

Pesavento, J. B., Crawford, S. E., Estes, M. K., Prasad, B. V., 2006. Rotavirus proteins: Structure and assembly. Curr. Top Microbiol. Immunol. 309, 189-219.

Pizarro, J. L., Sandino, A. M., Pizarro, J. M., Fernandez, J., Spencer, E., 1991. Characterization of rotavirus guanylyltransferase activity associated with polypeptide VP3. J. Gen. Virol. 72 (Pt 2), 325-332.

Ramig, R. F., 1994. Rotaviruses, Springer-Velag, Berlin, p. 380.

Ramig, R. F., 1997. Genetics of the rotaviruses. Annu. Rev. Microbiol. 51, 225-255.

Ramig, R. F., 2004. Pathogenesis of intestinal and systemic rotavirus infection. J. Virol. 78(19), 10213-10220.

Razani, B., Zhang, X. L., Bitzer, M., von Gersdorff, G., Bottinger, E. P., Lisanti, M. P., 2001. Caveolin-1 regulates transforming growth factor (TGF)-beta/SMADsignaling through an interaction with the TGF-betatype I receptor. J. Biol. Chem. 276(9), 6727-6738.

Robbins, S. M., Quintrell, N. A., Bishop, J. M., 1995. Myristoylation and differential palmitoylation of the HCK protein-tyrosine kinases govern their attachment to membranes and association with caveolae. Mol. Cell. Biol. 15(7), 3507-3515.

Rothberg, K. G., Heuser, J. E., Donzell, W. C., Ying, Y. S., Glenney, J. R., Anderson, R. G., 1992. Caveolin, a protein component of caveolae membrane coats. Cell 68(4), 673-682.

Ruiz, M. C., Cohen, J., Michelangeli, F., 2000. Role of Ca^{2+} in the replication and pathogenesis of rotavirus and other viral infections. Cell Calcium 28(3), 137-149.

Sapin, C., Colard, O., Delmas, O., Tessier, C., Breton, M., Enouf, V., Chwetzoff, S., Ouanich, J., Cohen, J., Wolf, C., Trugnan, G., 2002. Rafts promote assembly and atypical targeting of a nonenveloped virus, rotavirus, in Caco-2 cells. J. Virol. 76(9), 4591-4602.

Sargiacomo, M., Sudol. M., Tang, Z., Lisanti, M. P., 1993. Signal tranducing molecules and glycosyl-phosphatidylinositol-linked protein form a caveilon-rich insoluble complex in MDCk cells. J. Cell Biol. 122(4) 789-807.

Scheiffele, P., Verkade, P., Fra, A. M., Virta, H., Simons, K., Ikonen, E., 1998. Caveolin-1 and -2 in the exocytic pathway of MDCK cells. J. Cell Biol. 140(4), 795-806.

Schlegel, A., Lisanti, M. P., 2000. A molecular dissection of caveolin-1 membrane attachment and oligomerization. Two separate regions of the caveolin-1 C-terminal domain mediate membrane binding and oligomer/oligomer interactions in vivo. J. Biol. Chem. 275(28), 21605-21617.

Schroeder, F., Gallegos, A. M., Atshaves, B. P., Storey, S. M., McIntosh, A. L., Petrescu, A. D., Huang, H., Starodub, O., Chao, H., Yang, H., Frolov, A., Kier, A. B., 2001. Recent advances in membrane microdomains: Rafts, caveolae, and intracellular cholesterol trafficking. Exp. Biol. Med., 226(10),873-890.

Seo, N. S., Zeng, C. Q., Hyser, J. M., Utama, B., Crawford, S. E., Kim, K. J., Hook, M., Estes, M. K., 2008. Inaugural article: Integrins $\alpha 1\beta 1$ and $\alpha 2\beta 1$ are receptors for the rotavirus enretotoxin. Proc. Natl. Acad. Sci. 105(26) 8811-8818.

Shenoy-Scaria, A. M., Dietzen, D. J., Kwong, J., Link, D. C., Lublin, D. M., 1994. Cysteine3 of Src family protein tyrosine kinase determines palmitoylation and localization in caveolae. J. Cell. Biol. 126(2), 353-363.

Silvestri, L. S., Taraporewala, Z. F., Patton, J. T., 2004. Rotavirus replication: Plus-sense templates for double-stranded RNA synthesis are made in viroplasms. J. Virol. 78(14), 7763-7774.

Silvestri, L. S., Tortorici, M. A., Vasquez-Del Carpio, R., Patton, J. T., 2005. Rotavirus glycoprotein NSP4 is a modulator of viral transcription in the infected cell. J. Virol. 79(24), 15165-15174.

Simionescu, N., 1983. Cellular aspects of transcapillary exchange. Physiol. Rev. 63(4), 1536-1579.

Simionescu, N., Lupu, F., Simionescu, M., 1983. Rings of membrane sterols surround the openings of vesicles and fenestrae, in capillary endothelium. J. Cell Biol. 97(5 Pt 1), 1592-1600.

Smart, E. J., Ying, Y. S., Conrad, P. A., Anderson, R. G., 1994. Caveolin moves from caveolae to the Golgi apparatus in response to cholesterol oxidation. J. Cell Biol. 127(5), 1185-1197.

Smart, E. J., Ying, Y. S., Donzell, W. C., Anderson, R. G., 1996. A role for caveolin in transport of cholesterol from endoplasmic reticulum to plasma membrane. J. Biol. Chem. 271(46), 29427-29435.

Smart, E. J., Ying, Y. S., Mineo, C., Anderson, R. G., 1995. A detergent-free method for purifying caveolae membrane from tissue cultured cells. Proc. Natl. Acad. Sci. USA. 92(22), 10104-10108.

Song, K. S., Li, S., Okamoto, T., Quilliam, L. A., Sargiacomo, M., Lisanti, M. P., 1996. Co-purification and direct interaction of Ras with caveolin, an integral membrane protein of caveolae microdomains. Detergent-free purification of caveolae microdomains. J. Biol. Chem. 271(16), 9690-9697.

Spisni, E., Tomasi, V., Cestaro, A., Tosatto, S. C., 2005. Structural insights into the function of human caveolin. J. Biochem Biophys Res Commun. 338(3), 1393-1390.

Stahlhut, M., van Deurs, B., 2000. Identification of filamin as a novel ligand for caveolin-1: Evidence for the organization of caveolin-1-associated membrane domains by the actin cytoskeleton. Mol. Biol. Cell 11(1), 325-337.

Storey, S. M., Gallegos, A. M., Atshaves, B. P., McIntosh, A. L., Martin, G. G., Parr, R. D., Landrock, K. K., Kier, A. B., Ball, J. M., Schroeder, F., 2007. Selective cholesterol dynamics between lipoproteins and caveolae/lipid rafts. Biochemistry 46(48), 13891-13906.

Swaggerty, C. L., Huang, H., Lim, W. S., Schroeder, F., Ball, J. M., 2004. Comparison of SIVmac239$_{352-382}$ and SIVsmmPBj41$_{360-390}$ enterotoxic synthetic peptides. Virology 320(2), 243-257.

Tafazoli, F., Zeng, C. Q., Estes, M. K., Magnusson, K. E., Svensson, L., 2001. NSP4 enterotoxin of rotavirus induces paracellular leakage in polarized epithelial cells. J. Virol. 75(3), 1540-1546.

Tang, Z., Scherer, P. E., Okamoto, T., Song, K., Chu, C., Kohtz, D. S., Nishimoto, I., Lodish, H. F., Lisanti, M. P., 1996. Molecular cloning of caveolin-3, a novel member of the caveolin gene family expressed predominantly in muscle. J. Biol. Chem. 271(4), 2255-2261.

Taylor, J. A., Meyer, J. C., Legge, M. A., O'Brian, J. A., Street, J. E., Bergmann, C. C., Bellamy, A. R., 1992. Transient expression and mutational analysis of the rotavirus intracellular receptor; the C-terminal methionine residue is essential for ligand binding. J. Virol. 66(6), 3566-3572.

Taylor, J. A., O'Brien, J. A., Yeager, M., 1996. The cytoplasmic tail of NSP4, the endoplasmic reticulum-localized non-structural glycoprotein of rotavirus, contains distinct virus binding and coiled coil domains. EMBO J. 15(17), 4469-4476.

Thomas, C. M., Smart, E. J., 2008. Caveolae structure and function. J Cell Mol Med. 12(3), 796-809.

Tian, P., Ball, J. M., Zeng, C. Q., Estes, M. K., 1996. The rotavirus nonstructural glycoprotein NSP4 possesses membrane destabilization activity. J. Virol. 70(10), 6973-6981.

Tian, P., Estes, M. K., Hu, Y., Ball, J. M., Zeng, C. Q., Schilling, W. P., 1995. The rotavirus nonstructural glycoprotein NSP4 mobilizes Ca^{2+} from the endoplasmic reticulum. J. Virol. 69(9), 5763-5772.

Tian, P., Hu, Y., Schilling, W. P., Lindsay, D. A., Eiden, J., Estes, M. K., 1994. The nonstructural glycoprotein of rotavirus affects intracellular calcium levels. J. Virol. 68(1), 251-257.

Uittenbogaard, A., Smart, E. J., 2000. Palmitoylation of caveolin-1 is required for cholesterol binding, chaperone complex formation, and rapid transport of cholesterol to caveolae. J. Biol. Chem. 275(33), 25595-25599.

Uittenbogaard, A., Ying, Y., Smart, E. J., 1998. Characterization of a cytosolic heat-shock protein-caveolin chaperone complex. Involvement in cholesterol trafficking. J. Biol. Chem. 273(11), 6525-6532.

Valenzuela, S., Pizarro, J., Sandino, A. M., Vasquez, M., Fernandez, J., Hernandez, O., Patton, J., Spencer, E., 1991. Photoaffinity labeling of rotavirus VP1 with 8-azido-ATP: Identification of the viral RNA polymerase. J. Virol. 65(7), 3964-3967.

Varani, G., Allain, F. H., 2002. How a rotavirus hijacks the human protein synthesis machinery. Nat. Struct. Biol. 9(3), 158-160.

Vidal, M., Brachmann, R. K., Fattaey, A., Harlow. E., Boeke, J. D., 1996. Reverse two-hybrid and one-hybrid systems to detect dissociation of protein-protein and DNA-protein interactions. Proc. Natl. Acad. Sci. USA. 93 (19), 10315-10320.

Widdowson, M. A., Bresee, J. S., Gentsch, J. R., Glass, R. I., 2005. Rotavirus disease and its prevention. Curr. Opin. Gastroenterol. 21(1), 26-31.

Xu, A., Bellamy, A. R., Taylor, J. A., 2000. Immobilization of the early secretory pathway by a virus glycoprotein that binds to microtubules. EMBO J. 19(23), 6465-6474.

Yu, Z., Beer, C., Koester, M., Wirth, M., 2006. Caveolin-1 interacts with the Gag precursor of murine leukaemia virus and modulates virus production. Virol. J. 3, 73.

Zarate, S., Espinosa, R., Romero, P., Guerrero, C. A., Arias, C. F., Lopez, S., 2000. Integrin $\alpha 2\beta 1$ mediates the cell attachment of the rotavirus neuraminidase-resistant variant nar3. Virology 278(1), 50-54.

Zhang, M., Zeng, C. Q., Morris, A. P., Estes, M. K. , 2000. A functional NSP4 entertoxin peptide secreted from rotavirus-infected cells. J. Virol. 74(24), 11663-11670.

Zhou, M., Parr, R. D., Petrescu, A. D., Payne, H. R., Atshaves, B. P., Kier, A. B., Ball, J. M., Schroeder, F., 2004. Sterol carrier protein-2 directly interacts with Caveolin-1 in vitro and in vivo. Biochemistry 43(23), 7288-7306.

VITA

Cecelia Victoria Williams
P. O. Box 5800 MS779
Sandia National Laboratories
Albuquerque, New Mexico 87185-0779
cvwilli@sandia.gov

Cecelia Victoria Williams is a Principal Member of the Technical Staff at Sandia National Laboratories. Currently, Ms. Williams is leading the Integrated Bioenergy Processing project to produce biofuels from algae. Also, she is part of a team that is developing an agriculture and food vulnerability assessment tool for USDA and FDA. Prior to her current work, Ms. Williams worked on Chemical Biological Warfare (CBW) agent decontamination and led a DARPA project that was part of the Immune Building Program. Prior to the CBW work, Ms. Williams worked in the Underground Storage Technology Department supporting the Strategic Petroleum Reserve. She has been a principal investigator on a variety of technology development projects for the Office of Science and Technology. She has also worked in Polymer Science R&D.

She obtained a Bachelor of Arts degree in 1969, a Master of Science degree in chemistry (polymer science) in 1975, and a Master of Science degree in geology (meteoritics) in 1990 from the University of New Mexico. She earned her Ph.D. at Texas A&M in December 2008. She is also certified in Hazardous Waste Management. Ms. Williams has been at Sandia for 25 years. Ms. Williams has taught analytical and organic chemistry, physical geology, and mineralogy at the University of New Mexico and worked at The Catholic University of America Vitreous State Laboratory.